University of Bologna
School of Engineering and Architecture
Civil, Chemical, Environmental and Materials Engineering (DICAM)
Subject of Thermodynamic of Energy and Materials

ENHANCING PREDICTIVE CAPABILITY OF MODELS FOR SOLUBILITY AND PERMEABILITY IN POLYMERS AND COMPOSITES

Abdullah Abdulmohsen A Albahrani, Ph.D
The University of Bologna, 2023

Keywords
Gas Solubility - Polymer Composite - Permeability– Thermodynamic Modelling – Glass Transition

Academic Year
2022-2023

ABSTRACT

The interpretation of phase equilibrium and mass transport phenomena in gas/solvent - polymer system at molten or glassy state is relevant in many industrial applications. Among tools available for the prediction of thermodynamics properties in these systems, at molten/rubbery state, is the group contribution lattice-fluid equation of state (GCLF-EoS), developed by Lee and Danner and ultimately based on Panayiotou and Vera LF theory. On the other side, a thermodynamic approach namely non-equilibrium lattice-fluid (NELF) was proposed by Doghieri and Sarti to consistently extend the description of thermodynamic properties of solute polymer systems obtained through a suitable equilibrium model to the case of non-equilibrium conditions below the glass transition temperature. The first objective of this work is to investigate the phase behaviour in solvent/polymer at glassy state by using NELF model and to develop a predictive tool for gas or vapor solubility that could be applied in several different applications: membrane gas separation, barrier materials for food packaging, polymer-based gas sensors and drug delivery devices. Within the efforts to develop a predictive tool of this kind, a revision of the group contribution method developed by High and Danner for the application of LF model by Panayiotou and Vera is considered, with reference to possible alternatives for the mixing rule for characteristic interaction energy between segments. The work also devotes efforts to the analysis of gas permeability in polymer composite materials as formed by a polymer matrix in which domains are dispersed of a second phase and attention is focused on relation for deviation from Maxwell law as function of arrangement, shape of dispersed domains and loading.

TABLE OF CONTENTS

LIST OF TABLES. vii

LIST OF FIGURES. viii

LIST OF SYMBOLS. xi

LIST OF ABBREVIATIONS. xvi

ACKNOWLEDGEMENTS. xvii

Chapter 1. INTRODUCTION. 1

Chapter 2. MOTIVATION. 6

Chapter 3. EARLY LATTICE MODEL THEORIES. 8

3.1.1. Flory and Huggins Lattice Fluid Theory. 8

3.1.2. Flory Equation of State. 14

3.2. Sanchez and Lacombe Lattice Fluid Theory. 17

3.2.1. Pure Lattice Fluid. 17

3.2.2. Mixed Lattice Fluid. 19

3.2.3. Alternative Mixing Rules for Sanchez and Lacombe LF model. . . . . …22

3.2.3.1. Modified mixing rule which uses two fitting parameters k_{ij} and l_{ij} 22

3.2.3.2. Mixing rule proposed by West et al. 23

3.2.3.3. Mixing rule proposed by Sanchez and Panayiotou. 24

Chapter 4. PANAYIOTOU AND VERA EQUATION OF STATE [EOS]. 25

4.1. Statistical Mechanics of the Lattice-Fluid Equation of State for a Pure Component. . . 25

4.2. Statistical Mechanics of the Lattice-Fluid Equation of State for a Mixture. 27

Chapter 5. GROUP CONTRIBUTION METHOD. 30

5.1. Introduction to Group Contribution Method [GCM]. 30

5.2. Group Contribution Methods [GCMs] 30

5.2.1. UNIFAC model. 30

5.2.2. GC-Flory EoS. 30

TABLE OF CONTENTS (continued)

5.2.3. Developed GC-Flory EoS. 35

5.2.4. GC-Sanchez and Lacombe EoS. 36

5.3. Calculation of the Molecular Parameters through Group Contributions for a Pure Component. 38

5.4. Calculation of the Molecular Parameters through Group Contributions for Mixture.42

Chapter 6. NONEQUILIBIRUM LATTICE FLUID [NELF] 44

6. NELF Model for Gas Solubility in Glassy Polymers. 44

6.1. Early Version. 44

6.2. Recent version. 45

Chapter 7. NELF & GCLF COMBINATION [NEGCLF-EOS] 47

7.1. Introduction to NEGCLF-EOS. 47

7.2. Solubility Prediction in Solvent-Polymer Systems. 50

7.3. Results of NE-GCLF-EoS. 52

7.3.1. Solubility Prediction in Poly (methyl methacrylate) - CO2 system. 52

7.3.2. Solubility Prediction in Poly (ethyl methacrylate) - CO2 system. 54

7.3.3. Solubility Prediction in Polycarbonate + CO2 system. 57

7.3.4. Solubility Prediction in Poly(2,6-dimethyl phenylene oxide) - CO2 system. 58

7.3.5. Solubility Prediction in Polycarbonate - EtOH system. 59

7.3.6. Solubility Prediction in Polystyrene – m-xylene system. 60

7.4. Conclusions of Solubility Part I. 61

Chapter 8. DEVELOPMENT OF A GROUP CONTRIBUTION MIXING RULE. 62

8.1. Introduction to the developed GCLF-EoS. 62

8.1.1. Mixing Rule for Pure Component. 62

8.1.2. Mixing Rule for Mixture. 62

8.2. Prediction the Molecular Reference Volume, Interaction Energy and Entropy Parameters and Results. 63

TABLE OF CONTENTS (continued)

8.2.1. Prediction of the Molecular Reference Volume, Enthalpic Interaction Energy and Entropic Interaction Energy Parameters of CH3 CH3 Using the Properties of Vapor Pressure and Liquid Density of Ethane. 66

8.2.2. Prediction of the Molecular Reference Volume, Enthalpic Interaction Energy and Entropic Interaction Energy Parameters of CH2 CH2 Using the Properties of Vapor Pressure and Liquid Density of Cyclohexane. 67

8.2.3. Prediction of the Molecular Enthalpic Interaction Energy and Entropic Interaction Energy Parameters of CH2 CH3 Using the Properties of Vapor Pressure and Liquid Density of Pentane. 68

8.2.4. Prediction of the Molecular Reference Volume, Enthalpic Interaction Energy and Entropic Interaction Energy Parameters of CO2 CO2 Using the Properties of Vapor Pressure and Liquid Density of Carbon Dioxide. 69

8.2.5. Prediction of the Molecular Enthalpic Interaction Energy and Entropic Interaction Energy Parameters of CO2 CH3 Using the Properties of Vapor/Liquid Equilibria of CO2/Ethane. 70

8.2.6. Prediction of the Molecular Enthalpic Interaction Energy and Entropic Interaction Energy Parameters of CO2 CH2 Using the Properties of Vapor/Liquid Equilibria of CO2/Propane. 72

8.2.7. Prediction of the Molecular Reference Volume of CH3COO, Enthalpic Interaction Energy and Entropic Interaction Energy Parameters of CH3COO CH3COO, CH3 CH3COO Using the Properties of Vapor/Liquid Equilibria of Ethane/Methyl Acetate. 74

8.2.8. Prediction of the Molecular Enthalpic Interaction Energy and Entropic Interaction Energy Parameters of CH2 CH3COO Using the Properties of Vapor/Liquid Equilibria of Methyl Acetate/Dodecane. 76

8.3. Solubility Prediction in Poly (methyl methacrylate) + CO2 system. 81

8.4. Test and Consistency of the Developed GCLF-EoS. 82

8.5. Conclusions of Solubility Part II. 84

Chapter 9. ANALYSIS OF PERMEABILITY IN COMPOSITE MATERIALS. 85

9.1. Introduction and Aim. 85

9.2. Methods. 89

9.2.1. Laplace Equation for Fugacity. 89

9.2.2. Discretization Method. 90

9.2.3. Control-Volume Formulation Method. 90

9.2.4. Control-Volume-based Finite-Element Method. 91

TABLE OF CONTENTS (continued)

9.3. Prediction of the Effective Permeability along Principal Axis for the Case of Isotropic Composite Geometries. 92

9.3.1. Prediction of the Effective Thermal Conductivity of Simple Cubic (SC) Octahedron. 95

9.3.2. Prediction of the Effective Thermal Conductivity of Face Centered Cubic (FCC) Rhombic Dodecahedron. 102

9.3.3. Prediction of the Effective Thermal Conductivity of Body Centered Cubic (BCC) Truncated Octahedron. 104

9.3.4. Prediction of the Effective Thermal Conductivity of Simple Cubic (SC) Cube. 105

9.3.5. Prediction of the Effective Thermal Conductivity of Body Centered Cubic (BCC) Sphere. 106

9.3.6. Prediction of the Effective Thermal Conductivity of Face Centered Cubic (FCC) Sphere. 107

9.3.7. Prediction of the Effective Thermal Conductivity of Simple Cubic (SC) Sphere. 108

9.4. Results. 109

BIBLIOGRAPHY. 116

APPENDIX A – ALGORITHM LOOP FOR SOLVING PURE COMPONENT EOS. 122

APPENDIX B – ALGORITHM LOOP FOR SEARCHING PURE COMPONENT REDUCED VOLUME OF LIQUID OR VAPOR IN EOS. 123

APPENDIX C – CALCULATION OF THE EQUILIBRIUM CONCENTRATION ω_1^{Eq}. 124

APPENDIX D – CALCULATION OF THE NON-EQUILIBRIUM CONCENTRATION ω_1^{NE} 125

LIST OF TABLES

Table

5.1. Group Interaction Energy and Reference Volume Parameters [Linear] 41

5.2. Group Interaction Energy and Reference Volume Parameters [Quadratic]. 41

5.3. Group Binary Interaction Parameters (α_{mn}) [Quadratic]. 43

7.1. The Properties of Polymers. 51

8.1. Group Binary of the Molecular Enthalpic Interaction Energy Parameters (e_{mn_h}). 64

8.2. Group Binary of the Molecular Entropic Interaction Energy Parameters (e_{mn_s}). 64

8.3. Group Reference Volume, Rm and Surface Area Parameters of Developed GCLF – EoS. 65

8.4. Interaction Energy between Group m and n. 82

8.5. Interaction Energy Parameter between Group m and n. 83

9.1. Types of Lattices and Dispersed Shapes. 94

LIST OF FIGURES

Figure

7.1.A. Solubility isotherm of CO2 in PMMA at 35, 55 and 80°C: experimental data from ref 44 and predictions given by GCLF EOS and NELF model. 53

7.1.B. Solubility isotherm of CO2 in PMMA at 35, 55 and 80°C: experimental data from ref 44 and predictions given by GCLF EOS and NELF model. 53

7.2.A. Solubility and volume swelling isotherm of CO2 in PEMA at 15 °C: experimental data from ref 43 and predictions given by the GCLF EOS and NELF model. 55

7.2.B. Solubility isotherm of CO2 in PEMA at 30, 40 and 55°C: experimental data from ref 44 and predictions given by GCLF EOS and NELF model. 56

7.3. Solubility isotherm of CO2 in PC at 35 °C: experimental data from ref 52 and predictions given by GCLF EOS and NELF model. 57

7.4. Solubility isotherm of CO2 in PPO at 35 °C: experimental data from ref 45 and predictions given by GCLF EoS and NELF model. 58

7.5. Solubility isotherm of EtOH in PC at 30 °C: experimental data from ref 47 and predictions given by the GCLF EoS and NELF model. 59

7.6. Solubility isotherm of m-xylene in PS at 25 °C: experimental data from ref 48 and predictions given by the GCLF EOS and NELF model. 60

8.1. Logarithmic vapor pressure and liquid density of ethane: experimental data from ref 34 and predictions given by the developed GCLF EoS. 66

8.2. Logarithmic vapor pressure and liquid density of cyclohexane: experimental data from ref 34 and predictions given by the developed GCLF EoS. 67

8.3. Logarithmic vapor pressure and liquid density of pentane: experimental data from ref 34 and predictions given by the developed GCLF EoS. 68

8.4. Logarithmic vapor pressure and liquid density of CO2: experimental data from ref 34 and predictions given by the developed GCLF EoS. 69

8.5.1. VLE of CO2/Ethane at 223.15 K: experimental data from ref 54 and predictions given by the developed GCLF EoS. 71

8.5.2. VLE of CO2/Ethane at 263.15 K: experimental data from ref 54 and predictions given by the developed GCLF EoS. 71

8.6.1. VLE of CO2/Propane at 233.15 K: experimental data from ref 54 and predictions given by the developed GCLF EoS. 73

8.6.2. VLE of CO2/Propane at 273.15 K: experimental data from ref 54 and predictions given by the developed GCLF EoS. 73

8.7.1. VLE of Ethane/Methyl Acetate at 298.15 K: experimental data from ref 54 and predictions given by the developed GCLF EoS. 74

8.7.2. Logarithmic vapor pressure and liquid density of methyl acetate: experimental data from ref 34 and predictions given by the developed GCLF EoS. 75

8.8.1. VLE of Methyl Acetate/Dodecane at 323.15 K: experimental data from ref 53 and predictions given by the GCLF EoS. 76

8.8.2. Logarithmic vapor pressure and liquid density of methyl n-butryate as a pure component: experimental data from ref 34 and predictions given by the developed GCLF EoS. 77

8.8.3. Logarithmic vapor pressure and liquid density of methyl propionate as a pure component: experimental data from ref 34 and predictions given by the developed GCLF EoS. 78

8.9.1. VLE of CO2/Methyl Acetate at 298.15 K: experimental data from ref 54 and predictions given by the developed GCLF-EoS. 79

8.9.2. VLE of CO2/Methyl Acetate at 313.15 K: experimental data from ref 54 and predictions given by the developed GCLF EoS. 80

8.10. Solubility isotherm of CO2 in PMMA at 35, 55 and 80°C: experimental data from ref 44 and predictions given by the developed GCLF EOS and NELF model. 81

9.1. Control volume for the triangular grid. 91

9.2. Heat flux and mesh element size of simple cubic (SC) cubes: solids circles are three predicted heat flux values by Fluent and dashed line is the intercept..... 93

9.3.1. Representation of simple cubic (SC) octahedron lattice. 95

9.3.2. Representation of simple cubic (SC) octahedron repeated unit. 95

9.3.3. Representation of simple cubic (SC) octahedron of the calculation domain for the smallest loading ratio (0.00195). 96

9.3.4. Representation of simple cubic (SC) octahedron mesh of the smallest loading ratio (0.00195). 96

9.3.5. Representation of simple cubic (SC) octahedron contour of the smallest loading ratio (0.00195) and lowest permeability ratio (0.001). 97

9.3.6. Representation of simple cubic (SC) octahedron contour of the smallest loading ratio (0.00195) and highest permeability ratio (1000). 97

9.3.7. Representation of simple cubic (SC) octahedron of the calculation domain for the highest loading ratio (0.165). 98

9.3.8. Representation of simple cubic (SC) octahedron mesh of the largest loading ratio (0.165). 99

9.3.9. Representation of simple cubic (SC) octahedron contour of the largest loading ratio (0.165) and lowest permeability ratio (0.001) 99

9.3.10. Representation of simple cubic (SC) octahedron contour of the largest loading ratio (0.00195) and highest permeability ratio (1000). 100

9.3.11. Representation of simple cubic (SC) octahedron mesh of the largest loading ratio (0.165) for the case of 0 & ∞ permeability ratios. 101

9.3.12. Representation of simple cubic (SC) octahedron contour of (0) permeability ratio. 101

9.3.13. Representation of simple cubic (SC) octahedron contour of (∞) permeability ratio. 102

9.4.1. Representation of face centered cubic (FCC) rhombic dodecahedron lattice. 102

9.4.2. Representation of face centered cubic (FCC) rhombic dodecahedron repeated unit. 103

9.4.3. Representation of face centered cubic (FCC) of the calculation domain rhombic dodecahedron. 103

9.5.1. Representation of body centered cubic (BCC) truncated octahedron lattice. 104

9.5.2. Representation of body centered cubic (BCC) truncated octahedron repeated unit. 104

9.5.3. Representation of body centered cubic (BCC) of the calculation domain truncated octahedron. 105

9.6.1. Representation of simple cubic (SC) cube repeated unit. 105

9.6.2. Representation of simple cubic (SC) cube of the calculation domain. 106

9.7.1. Representation of body centered cubic (BCC) sphere repeated unit. 106

9.7.2. Representation of body centered cubic (BCC) sphere of the calculation domain. 107

9.8.1. Representation of face centered cubic (FCC) sphere repeated unit. 107

9.8.2. Representation of face centered cubic (FCC) sphere of the calculation domain. 108

9.9.1. Representation of simple cubic (SC) sphere repeated unit. 108

9.9.2. Representation of simple cubic (SC) sphere of the calculation domain. 109

9.10. Ψ coefficient calculated for regular cubic lattice of sphere, as function of loading and permeability ratio. 111

9.11. Ψ coefficient calculated for regular simple cubic lattice of cubes, as function of loading and permeability ratio. 112

9.12. Ψ coefficient calculated for regular simple cubic lattice of cubes, as function of loading and permeability ratio. 113

9.13. Ψ coefficient calculated for regular face centered cubic lattice of rhombic dodecahedron, as function of loading and permeability ratio. 114

9.14. Ψ coefficient calculated for regular body centered lattice of truncated octahedron, as function of loading and permeability ratio. 115

LIST OF SYMBOLS

a^{Eq}	=	Helmholtz free energy density at equilibrium conditions (kJ m^{-3})
a^{NE}	=	Helmholtz free energy density at nonequilibrium condition (kJ m^{-3})
a_T	=	reference volume intercept in the GCLF theory at temperature T (m^3 $kmol^{-1}$)
E	=	lattice energy of the system
e_{kk}	=	group interaction energy parameter between like groups *k* (kJ/kmol)
$e_{kk,T}$	=	group interaction energy parameter, between like group of type k at temperature T (kJ/kmol)
$e_{0,k}$, $e_{1,k}$, $e_{2,k}$	=	constants in group interaction energy parameter (kJ/kmol)
f	=	fugacity (kPa)
G	=	Gibbs function (kJ)
g_c	=	athermal Guggenheim combinatorial factor (unitless)
g_{nr}	=	non-random Guggenheim combinatorial factor (unitless)
$\underline{G}$	=	molar Gibbs energy (kJ/kmol)
k_{sw}	=	swelling coefficient (unitless)
k_G	=	compressibility coefficient in the glassy region (kPa^{-1})
k_R	=	compressibility coefficient in the rubbery region (kPa^{-1})
N	=	total number of molecules in the mixture (unitless)
N_c	=	number of polymeric species
N_H	=	number of holes in the lattice (unitless)
N_i	=	number of molecules of type *i* (unitless)
N_s	=	number of solute components
$n_k^{(1)}$	=	number of group k in component 1 (unitless)
N_1	=	number of molecules of a pure component 1
P	=	pressure (kPa)
P^*	=	characteristic pressure of a mixture (kPa)
$\tilde{P}$	=	reduced pressure of a mixture (unitless)
P_1^*	=	characteristic pressure of a pure component 1 (kPa)
$\tilde{P}_1$	=	reduced pressure of a pure component 1 (unitless)
p^{Eq}	=	pressure at equilibrium condition
Q	=	canonical partition function (unitless)

Q_k	=	UNIFAC surface area parameter of group k (unitless)
q_i , q	=	molecular surface area parameters of a component *i* and a mixture, respectively (unitless)
q_1	=	molecular surface area of a component 1 (unitless)
r	=	number of lattice sites occupied by the segments of a mixture (unitless)
r_i	=	number of lattice cells occupied by one molecule of component i (unitless)
r_1	=	number of lattice cells occupied by molecules of a pure component 1 (unitless)
R	=	gas constant [= 8.314 kJ kmol^{-1} K^{-1}]
R_k	=	group reference volume parameter for group *k* (m^3 kmol^{-1})
$R_{k,T}$	=	reference volume parameter of group k at temperature, T (m^3 kmol^{-1})
$R_{0,k}$, $R_{1,k}$, $R_{2,k}$	=	constants in group reference volume parameter (m^3 kmol^{-1})
T	=	temperature (K)
T^*	=	characteristic temperature of a mixture (K)
$\tilde{T}_i$, $\tilde{T}$	=	reduced temperatures of a pure component *i* and a mixture, respectively (unitless)
$\tilde{T}_{ij}$	=	reduced temperature of a binary mixture (unitless)
T_g	=	glass transition temperature (K)
T_0	=	reference temperature [=273.15 K]
T_1^*	=	characteristic temperature of a pure component 1 (K)
$\tilde{T}_1$	=	reduced temperatures of a pure component 1 (unitless)
v	=	molar volume (m^3 kmol^{-1})
v_i^* , v^*	=	molecular reference volumes of a pure component i and a mixture, respectively (m^3 kmol^{-1})
$\tilde{v}_i$	=	reduced volume of a pure component i (unitless)
$\hat{V}_g$	=	a model parameter that depends only on temperature (m^3 kg of pol^{-1})
v_H	=	the volume of a lattice site which equals to [= 9.75 × 10^{-3} m^3 kmol^{-1}]
$\tilde{v}$, $\tilde{v}_m$	=	reduced volume of a mixture (unitless)
$\hat{V}_{pol}^{Eq}$	=	total volume of a mixture per polymer mass at equilibrium conditions (m^3 kg of pol^{-1})
$\hat{V}_{pol}^{NE}$	=	total volume of a mixture per polymer mass at nonequilibrium condition (pseudo equilibrium) (m^3 kg of pol^{-1})
$\hat{V}_{pol}^{0}$	=	dry polymer mass density at non-equilibrium condition (glassy state) (m^3 kg of pol^{-1})
$\hat{V}_{pol}^{Eq^0}$	=	specific volume of a pure polymer at equilibrium condition (m^3 kg of pol^{-1})
$v_{1,T}^*$	=	volume of cells in the lattice of a pure component 1 at temperature, T (m^3 kmol^{-1})
v_1^*	=	volume of cells in the lattice of a pure component 1 (m^3 kmol^{-1})
$\tilde{v}_1$	=	reduced volume of a pure component 1 (unitless)
x_i	=	mole fraction of component i (unitless)
z	=	coordination number [=10] (unitless)

Greek Letters

α_{mn}	=	group interaction parameters between main groups *m* and *n* (unitless)
α^{EoS}	=	thermal expansion coefficient at nonequilibrium condition using EoS (K^{-1})
α_G	=	thermal expansion coefficient at nonequilibrium condition (glassy state) (K^{-1})
α_R	=	thermal expansion coefficient at equilibrium condition (rubbery state) (K^{-1})
γ	=	the ratio of the thermal expansion coefficient from the glassy state to rubbery (unitless)
$\dot{\Gamma}_{ij}$	=	non-randomness factor for molecules of type *i* around molecules of type *j* (unitless)
δ_{ij}	=	binary interaction parameter, between segments of of *i* and *j* molecules (unitless)
δ_i	=	volume-independent parameter accounting for flexibility of component *i* molecules (unitless)
δ_1	=	volume-independent parameter accounting for flexibility of pure component 1 molecules (unitless)
$\Delta\epsilon$	=	interaction energy change (kJ $kmol^{-1}$)
ϵ^*	=	molecular interaction energy of a mixture (kJ $kmol^{-1}$)
ϵ_{ii}	=	molecular interaction energy between like molecules of type *i* (kJ $kmol^{-1}$)
ϵ_{ij}	=	molecular interaction energy between unlike molecules of type *i* and *j* (kJ $kmol^{-1}$)
ϵ_{ijh}	=	enthalpic interaction energy between unlike molecules of type *i* and *j* (kJ $kmol^{-1}$)
ϵ_{ijs}	=	entropic interaction energy between unlike molecules of type *i* and *j* (kJ $kmol^{-1}$)
ϵ_{11h}	=	enthalpic interaction energy between molecules of component 1 (kJ $kmol^{-1}$)
ϵ_{11s}	=	entropic interaction energy between molecules of component 1 (kJ $kmol^{-1}$)
$\epsilon_{11,T}$	=	molecular interaction energy between like molecules of a pure component 1 at temperature T (kJ $kmol^{-1}$)
ϵ_{11}	=	molecular interaction energy between like molecules of a pure component 1 (kJ $kmol^{-1}$)
θ	=	molecular surface area fraction of a mixture (unitless)
θ_i	=	molecular surface area fraction of component *i* including holes (unitless)
$\bar{\theta}_i$	=	molecular surface area fraction of component *i* subjected to the cells in the lattice (unitless)
$\theta_{i,P}$	=	molecular surface area fraction of the pure component *i* including holes at the same temperature and pressure as the mixture (unitless)
θ_1	=	molecular surface area fraction of component 1 including holes (unitless)
$\Theta_k^{(i)}$	=	surface area fraction of group k in the pure component *i* (unitless)
$\Theta_k^{(M)}$	=	surface area fraction of all the groups present in the mixture (unitless)

$\Theta_k^{(1)}$ = surface area fraction of group k in the pure component 1 (unitless)

μ_i^{Eq} = chemical potential of solutes in the mixture at equilibrium conditions (kJ kmol^{-1})

$\mu_i^{(M)}$ = chemical potential of component i in a binary mixture (kJ kmol^{-1})

μ_i^{NE} = chemical potential of solutes in the mixture at nonequilibrium conditions (kJ kmol^{-1})

$\mu_1^{(P)}$ = chemical potential of a pure component 1 (kJ kmol^{-1})

μ_1 = chemical potential of component 1 into mixtures (kJ kmol^{-1})

ρ_i = species mass density of all solute components (unit)

ρ_{pol}^{NE} = mass density of the polymeric species in the mixture at nonequilibrium conditions (kg of pol m^{-3})

ρ_{pol}^{PE} = density of solvent per polymer mass at nonequilibrium conditions (kg of pol m^{-3})

ρ_{pol}^{0} = dry polymer density (kg m^{-3})

σ = volume-independent parameter accounting for symmetry of mixture molecules (unitless)

σ_i = volume-independent parameter accounting for symmetry of component i molecules (unitless)

σ_1 = volume-independent parameter accounting for symmetry of pure component 1 molecules (unitless)

ϕ_i = volume fraction of component i in the mixture (unitless)

χ = compressibility ratio between glass region and rubber (unitless)

ω_i = weight fraction of low molecular weight solutes in the mixture (unitless)

ω_i^{Eq} = weight fraction of low molecular weight solutes in the mixture at equilibrium conditions (unitless)

ω_i^{NE} = weight fraction of low molecular weight solutes in the mixture at nonequilibrium conditions (unitless)

ω_1^{Eq} = weight fraction of component 1 into mixture at equilibrium condition (unitless)

ω_1^{NE} = weight fraction of component 1 into mixture at nonequilibrium condition (unitless)

ω_2 = weight fraction of a pure polymer (unitless)

Superscripts

Eq = equilibrium

(M) = mixture

NE	=	nonequilibrium
PE	=	pseudo equilibrium
(P)	=	pure
$*$	=	reducing quantities
$\sim$	=	reduced quantities
$\cdot$	=	non-randomness factor

Subscripts

c	=	combinatorial
H	=	quantity pertaining to holes
G	=	glassy state
i, j	=	component i, j
k, m, n	=	group k, m, and n
nr	=	non-random
pol	=	polymer
R	=	rubbery state
sw	=	swelling
s	=	solute component

List of abbreviations

EOS	=	equation of state
GCLF	=	group-contribution lattice-fluid
NELF	=	nonequilibrium lattice fluid
NET-GP	=	nonequilibrium thermodynamics of glassy polymers
PC	=	polycarbonate
PEMA	=	poly(ethyl methacrylate)
PMMA	=	poly(methyl methacrylate)
PPO	=	poly(2,6-dimethyl phenylene oxide)
PS	=	polystyrene

ACKNOWLEDGEMENTS

I would like to thank my family, especially my mother and sisters for their kindly encouragement, support, and love gave my efforts meaning.

I would like to thank Professor Ferruccio Doghieri for his suggestions, support, and helpful criticisms throughout my higher studies (Master & Ph.D) at University of Bologna. His contributions have always made my research more valuable and enjoyable.

Vorrei ringraziare la mia famiglia, in particolare mia madre e le sorelle per il loro gentile incoraggiamento, sostegno e amore che hanno dato un senso ai miei sforzi.

Vorrei ringraziare il Professore Ferruccio Doghieri per i suoi suggerimenti, supporto e utili critiche durante i miei studi superiori (Master & Ph.D) presso l'Università di Bologna. I suoi contributi hanno sempre reso la mia ricerca più preziosa e piacevole.

Papers are in Process:

[1] Development a group contribution method for the prediction of gas/vapor solubility coefficient in glassy polymers that is based on Lee & Danner approach and the objective work is to study the phase behaviour in solvent/polymer at glassy state by using Non-Equilibrium Lattice Fluid model (NELF) and to develop a predictive tool for gas or vapor solubility that could be applied in a number of different applications: membrane gas separation, barrier materials for polymer-based gas sensors, drug delivery devices.

[2] The description of the gas transport properties in composite systems through the use of Fluent, objective work is to explore models aimed at extending the Maxwell-Wiener relation for the gas permeability in composite systems.

[3] A new group contribution mixing rule is based on the Panayiotou and Vera approach for the prediction of gas/vapor solubility coefficient in glassy polymers and the objective work is to study the phase behaviour in solvent/polymer at glassy state by using Non-Equilibrium Lattice Fluid model (NELF) and to develop a predictive tool for gas or vapor solubility that could be applied in a number of different applications: membrane gas separation, barrier materials for polymer-based gas sensors, drug delivery devices.

Chapter 1
INTRODUCTION

The investigation of phase equilibria behaviour for the prediction of the thermodynamics properties of solvent and polymers solutions has become crucial in many industrial applications. Recently, many models had been exhibited in prediction VLE conditions: UNIFAC free volume model [1], group contribution Flory EoS [2,3], and ultimately Lee and Danner approach, that has been succeeded to predict the equilibria phase behaviour of polymeric systems for pure component and binary mixture [4,5] by developing the group-contribution method based on Panayiotou and Vera lattice-fluid equation of state (LF-EoS). Besides that, Panayiotou and Vera EoS has shown an optimal result in correlating the phase equilibria in polymer-solvent systems [6,7]. Thus, it has been selected as a starting point for developing a group-contribution lattice-fluid EoS, together with different mixing rules for interaction energy proposed by [High, Danner, Hamedi, and Lee] [8,9], and [Hamedi and coworkers] [10]. While GCLF- EoS shows a very good prediction capability for the analysis of vapor/gas in polymer solutions at molten/rubbery equilibrium state in many applications, polymers are processed and used at below glass transition temperature that is considered as non-equilibrium condition. Therefore, to address this specific condition, [Doghieri and Sarti] [11] have developed a model that solves this kind of phase behaviour below glass transition temperature by employing pseudo equilibrium polymer mass density as an additional state variable. As a result of that, most of thermodynamic properties can be calculated and analysed, such as solubility gas into homopolymer and copolymers at various pressures.

In what follows a brief discussion is offered of essential features of lattice-fluid theories, with reference to earlier versions (chapter 3) first and then to the model of Panayiotou and Vera which is of direct interest of this work (chapter 4). Characteristic of group contribution methods are then presented in chapter 5, both in general terms and for the specific approach considered by Danner and co-workers with reference to lattice fluid theory.

A short description follows of the non-equilibrium lattice-fluid approach, which includes most recent developments and consider a new formulation built to facilitate the use of predictive procedures for the evaluation of non-equilibrium parameters (chapter 6). The overall predictive procedure set up in this work for the estimation of gas and vapor solubility in glassy polymer is finally described in chapter 7, in which several results are shown as obtained from its application to the case VLE of few conventional glassy polymers with both gaseous and vapor species.

The additional effort devoted to the analysis of an alternative approach to the group contribution estimation of the energy both homogeneous and heterogeneous interaction between segments in the lattice is then discussed in chapter 8. The last chapter of this work summarizes the results obtained from the numerical analysis of effective permeability in composite media and it specifically addresses the effect of shape, arrangement and permeability ratio for the case of isotropic composite media obtained through the ordered dispersion of isotropic inclusions.

It is worthful to address a general representation of this work, departing from a mathematical expression namely, the effective permeability of gas or vapour in glassy polymers, P_{eff}, as shown:

$$P_{eff} = f\left(Geometry, \phi\ ,\ P^{(d)},\ P^{(c)}\right) \tag{1.1}$$

Where ϕ is the disperse loading in the matrix. $P^{(d)}$ is the permeability of gas or vapour in the disperse phase. $P^{(c)}$ is the permeability of gas or vapour in the continuous phase.

Fifty-four years ago, [Crank and Park] [12] showed a mathematical expression for representing the permeability coefficient departing from Fick's law [13] to describe the permeability coefficient and its association to the diffusion and solubility coefficients, as follows:

$$F = \frac{D\ (C_1 - C_2)}{l} \tag{1.2}$$

Where F is the flow rate of gas or vapour per unit area of membrane's section, C_1 is the concentration of gas or vapour that exists on the surface of the membrane or diffuses across the membrane and this mechanism is termed "sorption", C_2 is the concentration of gas or vapour that exists on the other surface of the membrane or releases at atmosphere and this mechanism is named "desorption", l is the thickness of the membrane, and D is the diffusion coefficient in which it controls the quantity of the diffused gas or vapour across the membrane.

Eq.1.2 has another relevant expression that is more applicable for predicting the permeability coefficient, P , as follows:

$$F = \frac{P\ (p_1 - p_2)}{l} \tag{1.3}$$

Where p_1 and p_2 are the pressure of gas or vapour in the membrane and the pressure of gas or vapour out of the membrane from the other side, respectively.

There is a linear relationship between the concentration of gas or vapour and the external vapour pressure, given by:

$$C = Sp \tag{1.4}$$

where S is the solubility coefficient.

By equating [Eq.1.2 & 1.3], it gives the ultimate expression for the permeability coefficient, P, as follows:

$$P = DS \tag{1.5}$$

It could be noted that the solubility coefficient can be calculated by modelling a predictive tool that combines two models a group-contribution method (GC) [4,5,10,14,15] and nonequilibrium thermodynamics of glassy polymers (NET-GP) [11]. GC method is selected due to its ability to express the thermodynamic properties behaviour when there are no sufficient characteristic properties of chemical compounds by utilizing solo the chemical structure. Besides that, NET-GP has been chosen because of its capability to interpret the thermodynamics properties behaviour of polymers at below glass transition temperature, T_g in which polymer material is transformed from liquid to rubbery, and ultimately to a stiff or glassy upon cooling [16]. Furthermore, polymer has a free volume that allows gas or vapor to diffuse between polymers' chains. The free volume shows a low effect of segmental mobility when the temperature below glass transition temperature, namely glassy polymers [Matteucci et al.] [17]. In addition, it arises to study the thermodynamics properties behaviour of gas or vapour particularly in glassy polymers due to increasing demand by industrial and commercial enterprises. Moreover, the interested group-contribution method that has been selected to be developed at this work, is relied on Panayiotou and Vera EoS [7,8] that was evolved by manipulating lattice-hole theory. Interestingly, Panayiotou and Vera EoS showed accurate results in the literature. Thus, it has been selected as an optimal departure to extend from GC method to NET-GP.

Ultimately, the solubility coefficient model that is referred to as "nonequilibrium group contribution lattice fluid" model (NE-GCLF) can be designed to be applied based on a minimum number of properties

as inputs such as glass transition temperature, T_g, compressibility ratio,χ, chemical structure of polymer, M_n and the ratio of the thermal expansion coefficient from the glassy to rubbery state,γ.

It could be noted that the NE-GCLF model has been implemented in a mathematical tool (MATLAB) for the purpose of highly achieving precision in both calculation and plotting. However, there are some difficulties that may encounter at current work which are the lack of experimental data and properties (i.e., compressibility and glass transition temperature) in the literature. A similar modelling approach is followed for calculating the diffusion coefficient.

Along with modelling permeability coefficients, analysis of diverse geometries considering the effect of chemical structure of polymer matrix, characterizing disperse phase, disperse arrangement and its loading.

For a better understanding to the effective permeability of gas or vapour in polymer composites, it is essential to introduce the relative permeability expression, P_r, as shown:

$$P_r = \frac{P_{eff}}{P_c} \tag{1.6}$$

Maxwell model [18] presented a predictive model that can study the permeation of species in composite materials. His model is composed of two objects: (i) sphere within a surface and (ii) the other one without a surface, alternatively an extended sphere. The spheres are arranged regularly and separately from each other with a view to allow the course of the current to pass. The model is well effective when the spheres are far from each other and vice versa it shows a deviation from the ideality because the model works at low loadings of spherical particles approximately $(\phi_d \leq 0.2)$. Moreover, it does not take into consideration the particle shape or distribution.

Maxwell's model expression is given by:

$$P_{eff} = \frac{P_d+2P_c - 2\phi\,(P_c-P_d)}{P_d+2P_c + \phi\,(P_c-P_d)}\,P_c \tag{1.7. A}$$

By substituting the permselectivity [19], $\alpha_{d/c}$ in [Eq. 1.7. A], it results the following expression:

$$P_{eff} = \frac{2\,(1-\phi)+\alpha\,(1+2\phi)}{(2+\phi)+\alpha\,(1-\phi)} \quad ; \quad \alpha_{d/c=\frac{P_d}{P_c}} \tag{1.7. B}$$

It can be noted that the permselectivity demonstrates the ideal capability to separate fluids.

It can be stated that Maxwell's model can be applied in several applications which have different driving forces such as pressure, concentration … etc., for predicting the performances of composite membranes.

As it has been shown that Maxwell's model demonstrates a deviation when the loading is higher than 0.2. At present work, verifying the validity of empirical Nielsen model extending the Maxwell-Wiener-Nielsen through the use of a CFD software (FLUENT) tool. A new coefficient, Ψ can be introduced to optimize more complex geometries with different loadings and permeability ratios which disperse phase can be almost compacted to the continuous (matrix phase) by reaching approximately 0.99 out of 1.

Chapter 2
MOTIVATION

The future vision of renewable and sustainable energy has played a crucial role around the world, through development of modern separation technologies to preserve energy while minimizing waste and reducing emission of volatile organic compounds, VOCs. In this respect, membrane technologies proved to represent good alternative over traditional separation processes in the industries, such as absorption, adsorption, and distillation, owing to their advantages [20]: (i) low energy consumption and capital costs [21], (ii) consistent production with high performance [22], (iii) ease of operating management [23,24].

Mass transport properties of low molecular weight species in polymers are of major importance to the performance of separation processes which make use of dense polymer membranes. The latter is typically the case of gas separation, pervaporation and organic solvent nanofiltration processes. In these fields, and especially in the case of gas separation, great attention has been devoted in recent years to the use of high free volume glassy materials for the preparation of separation membranes, and to the development of suitable composites, in which domains of an organic or inorganic phase are dispersed into a polymer matrix (mixed matrix membranes, MMM). Interest in glassy membranes is motivated by their superior selectivity, with respect to rubbery membranes, while the routes developed for the preparation of MMM allow, in principle, to optimize mass transport properties of the composite system with respect to specific target separations, by combining permeability of the matrix and selectivity of dispersed phase.

To the optimal design of material for the preparation of membranes, the availability of reliable tools for the prediction of key mass transport properties as gas/vapor solubility and diffusivity is crucial. Several well-established models, based on solid thermodynamic foundations, are indeed available for the representation of mass transport properties of low molecular weight species in bulk rubbery polymers, from lattice fluid to free volume theory, which can be easily applied when key experimental data are available for volumetric and viscosity properties of pure polymer and solute components. Significant efforts have also been done to extend the use of the latter tools to the case of polymeric species for which necessary experimental data are missing. In this respect, several approaches, based on group contribution methods, have been proposed, combined with specific thermodynamic models for equilibrium phases. Similar reliable tools still miss, in this respect, for the case of polymer-solute mixture below the glass transition temperature, where non-equilibrium condition need to be addressed to properly represent the thermodynamic behaviour. On a different side, studies must be mentioned which

have presented in the technical literature and aimed at interpreting the effect of loading, disperses domains and arrangement on effective permeability of composite materials. Despite the efforts, the tools developed remain substantially empirical in nature, except for the case of simple geometries of dilute dispersion of spheroids, for which exact solutions are known (Maxwell-Garnett type models).

The aim of this work is to contribute to the development of predictive tools for the mass properties of composite materials prepared after glassy polymers. In this view, two distinct approaches have been taken. The first is aimed at extending to the case of glassy materials, the capability of modelling approaches for gas/vapor solubility, based on group contribution methods, already proposed in the technical literature for the case of polymer-solute mixtures above the glass transition temperature. The latter result will ultimately allow for the prediction of solubility coefficient of low molecular weight species in polymeric materials for which key equilibrium volumetric properties are not available. In fact, this is the case of several materials of interest in separation applications, for which the glass transition temperature exceeds the degradation temperature, thus preventing the direct experimental exam of equilibrium properties. The second approach considered in this work is aimed at the detailed analysis of the effect of shape, loading, arrangement and permeability ratio of dispersed domains on effective permeability in composite material. This problem is addressed through the numerical evaluation of the latter property in a number of different geometries, paying special attention to the uncertainty of numerical results, trying to recognize patterns for the effect of permeability ratio which could be useful in representing the deviations from Maxwell results in general conditions. In this respect, what is developed in this work is a first attempt to identify possible forms of generalized Maxwell type models and, to this aim, the case of isotropic ordered geometries is first addressed.

It is also worthwhile to mention here that the tools for thermodynamic and transport properties addressed in this work will be useful also in a number of applications different from membrane separation. Indeed, predicting gas/vapor transport properties in glassy materials is essential also in the design of polymer-based gas/vapor sensors, of that of drug delivery devices, in the optimization of devolatilization as well as foaming processes, just to mention few cases. As it refers to the predictive tools for effective permeability in composite materials, it is useful to mention that the same mathematical problem arises in the calculation of effective thermal conductivity or electrical permittivity of dielectric material and that results developed in this work could be easily transferred to these related problems, pertinent to rather different fields.

Chapter 3
EARLY LATTICE FLUID THEOIES

3.1.1. Flory Lattice Fluid Theory:

More than eighty years ago, Flory [25] investigated a statistical mechanical treatment by studying the thermodynamic properties of polymer-solvent system considering a lattice structure (quasi-solid). In his work, he discussed how the polymer and solvent were arranged on the lattice sites through the analysis of mixing entropy.

It is worthful to indicate the expression for mixing entropy, ΔS_{mixing} and the partial molar entropy of dilution for component 1 in a binary ideal mixture, $\Delta \bar{S}_1$, as given by:

$$\Delta S_{mixing} = -R\ (n_1 \ln X_1 + n_2 \ln X_2\ ) \qquad (3.1.1.1)$$

$$\Delta \bar{S}_1 = -R \ln X_1 \qquad (3.1.1.2)$$

where n_1 and n_2 are the numbers of moles for component 1 and component 2, respectively, X_1 and X_2 the mole fraction of component 1 and component 2 in the mixture, respectively, and R is a gas universal constant which is equal to 8.314 $J/mol.K$.

Flory had addressed the problem of mixing entropy for the case of a low molecular weight component and a polymer following few simplified assumptions. The assumptions include (i) quasi-solid lattice in the liquid, (ii) interchange ability of segments of the polymer chain with solvent; the cell of hypothetical lattice maybe be occupied either by a solvent molecule or a segment of a polymer chain, (iii) independence of lattice constants on composition, (iv) all polymers' molecules are assumed to have the same size; the average concentration of polymer segments in cells adjacent to cells unoccupied by the polymeric are equal the average concentration.

Flory's expression was derived after the application of the lattice statistical thermodynamic approach to the evaluation of configurational entropy in which the above mixture can be described, as follows:

$$\Delta S_{mixing} = -k\left[n \ln\left(\frac{n}{n+xN}\right) + N \ln\left(\frac{xN}{n+xN}\right)\right] \quad (3.1.1.3)$$

where n is the number of molecules of a pure solvent, N is the number of polymer molecules, x is the number of segments of a polymer chain, and k is Boltzmann's constant.

It can be noted that if the value of x in (Eq. 3.1.1.3) is equal to 1, then (Eq. 3.1.1.3) will turn to the fundamental expression that is (Eq. 3.1.1.1).

Alternatively,

$$\Delta S_{mixing} = -k[n \ln v_1 + N \ln v_2] \quad (3.1.1.3.A)$$

Where $v_1$and v_2 are the volume fraction of solvent and polymer, respectively.

Differentiating (Eq. 3.1.1.3) with respect to n, it turns out the partial molar entropy of solvent, as shown:

$$\Delta \bar{S}_1 = -R \ln(1 - v_2) - R(1 - 1/x)v_2 \quad (3.1.1.4)$$

Correspondingly,

$$\Delta \bar{S}_2 = -R \ln(1 - v_1) - R(1 - 1/x)v_1 \quad (3.1.1.5)$$

The heat of mixing can be represented, as follows:

$$\Delta H = BV_1 V_2 n N/(nV_1 + NV_2) \quad (3.1.1.6)$$

where B is a constant for a pair of polymer molecules (liquid state). V_1 and V_2 are the molar volumes of solvent and polymeric solute, respectively.

Flory considered that the molar volume of the polymer is equal to the number of segments in a polymer molecule multiplied by the molar volume of solvent, as follows:

$$V_2 = xV_1 \tag{3.1.1.7}$$

Differentiating (Eq.3 .1.1.7) with respect to n, it gives the partial molar heat of solvent, as follows:

$$\Delta\bar{H}_1 = BV_1v_2^2 \tag{3.1.1.8}$$

Similarly,

$$\Delta\bar{H}_2 = BV_2v_1^2 = Bx\,V_1v_1^2 \tag{3.1.1.9}$$

The partial molar free energy can be calculated through the combination of (Eq. 3.1.1.4) and (Eq. 3.1.1.5), as given by:

$$\Delta\bar{F}_1 = RT\ln(1-v_2) + RT\ln(1-1/x)\,v_2 + BV_1v_2^2 \tag{3.1.1.10}$$

$$= -RTv_2[1/x + (1-K)\,v_2/2 + v_2^2/3] \tag{3.1.1.10.A}$$

Similarly,

$$\Delta\bar{F}_2 = RT\,[\ln(1-v_1) - (x-1)v_1 + Kx\,v_1^2/2] \tag{3.1.1.10.B}$$

where $K = 2BV_1/RT$.

It could be mentioned that when K is higher than 1, then x becomes large, the region of partial miscibility is reached. In addition, miscibility gap is obtained when the heat of mixing is much greater than zero, according to (Eq. 3.1.1.8) and (Eq. 3.1.1.9). Thus, to study the phase equilibria of a binary system, the relevant compositions v_2 and v_2' to that system must obey the following expressions:

$$\Delta\bar{F}_1(v_2) = \Delta\bar{F}_1(v_2') \, , \Delta\bar{F}_2(v_2) = \Delta\bar{F}_2(v_2') \tag{3.1.1.11}$$

$$K(\text{critical}) = \left(1 + \sqrt{x}\right)^2 / x \tag{3.1.1.12}$$

Where $\Delta\bar{F}_1(v_2)$ is the partial molar free energy of the solvent; as $\Delta\bar{F}_1$decreases as v_2 increases from zero to unity.

It can be noted that if x is great, then, the critical value of K is slightly greater than unity and it approaches unity as x approaches infinity; continuing if the K is larger, then, two phases will co-exist in equilibrium. Moreover, when K exceeds the critical value, there exists a pair of values (v_2 and v_2') which satisfies the equilibrium conditions (Eq. 3.1.1.11) and when K is very near K(critical), it is permissible to set $\Delta\bar{F}_1(v_2') = 0$ and to compute v_2' from K using (Eq. 3.1.1.9).

The roots can be calculated by taking the differentiation of (Eq. 3.1.9), with respect to v_2 and equating to zero, as follows:

$$Kxv_2^2 - (Kx - x + 1)v_2 + 1 = 0 \tag{3.1.1.13}$$

The two solutions for the two roots $(\pm v_2)$ can be calculated, if the maximum and minimum of $\Delta\bar{F}_1$ are equal and (Eq. 3.1.12) satisfies its condition, then,

$$v_2 = \frac{Kx - (x-1) \pm \left[(Kx - x + 1)^2 - 4Kx\right]^{\frac{1}{2}}}{2Kx} \tag{3.1.1.14}$$

By substituting (Eq. 3.1.1.12) in (3.1.1.14),

$$v_2(\text{critical}) = 1/\left(1 + \sqrt{x}\right) \tag{3.1.1.15}$$

The critical composition, at which the two phases become identical, according to (Eq. 3.1.1.15), occurs when x is large.

In summary, it can be said that the thermodynamic properties of polymer solutions are frequently described in terms of the Flory-Huggins equation, which gives the free enthalpy change occurring when a non-crystalline polymer is mixed with a solvent.

For any given polymer-solvent pair, it contains a characteristic parameter, χ , called "Flory interaction parameter", which reflects the intermolecular forces between the molecules in the solution.

The corresponding formulation of Flory-Huggins free enthalpy of mixing is:

$$\frac{\Delta G_m}{RT} = n_1 \ln \Phi_1 + n_2 \ln \Phi_2 + \chi \Phi_1 \Phi_2 (n_1 + m n_2) \qquad (3.1.1.16)$$

In (Eq.3.1.1.16), ΔG_m is defined as the free enthalpy of mixing; the "liquid-like", disoriented polymer with the solvent; n_1 and n_2 refer to the number of moles of solvent and polymer, respectively. Φ_1 and Φ_2 are the volume fractions of solvent and polymer, respectively, as follows:

$$\Phi_1 \equiv \frac{n_1}{n_1 + m n_2} \text{ and } \Phi_2 \equiv \frac{m n_2}{n_1 + m n_2} \qquad (3.1.1.17)$$

where m is the ratio of molar volumes of polymer and solvent, and χ, is the Flory interaction parameter; a dimensionless quantity which is a function of the interaction energy characteristic of a given solvent-solute pair.

If (Eq. 3.1.1.16) is used to describe the thermodynamic properties of polymer solutions, then, the problem of predicting polymer solubility is equivalent to that of predicting reasonably accurate values of the Flory interaction parameter. In (Eq. 3.1.1.18), χ is a free enthalpy parameter, which is considered to include both entropy and enthalpy contributions, as follows:

$$\chi = \chi_S + \chi_H \qquad (3.1.1.18)$$

Huggins' derivation for the free energy of mixing predicts that the entropy parameter, $\chi_S = 1/z$, where z is the lattice coordination number; however, many workers have found χ_S empirically to have a value of approximately 0.3 to 0.4.

The parameter is:

$$\chi_H = \frac{v_1}{RT} \quad (\delta_1 - \delta_2)^2 \qquad (3.1.1.19)$$

Where v_1 is the solvent molar volume, and where δ_1 and δ_2 are the solubility parameters of solvent and polymer, respectively.

The condition of (Eq.3.1.1.19) to be used is that it allows only positive values for χ_H. Thus, if χ tends to have a value less than 0.5, it means that χ_H has a very small value, and therefore the solubility parameters of the polymer and solvent must have very closely values. Furthermore, the approximate equality of the solubility parameters of polymer and solvent is a useful for priori test of the suitability of a given solvent for a given polymer.

It could be noted that (Eq.3.1.1.19) is applied only to nonpolar systems and is not valid for systems containing polar molecules or for those where specific interactions are present.

3.1.2. Flory Equation of State [EoS]:

Fifty-eight years ago, Flory et al. interpreted and correlated the properties of macro molecular liquids and their solutions by linking the molecular characteristics with the thermodynamic properties of such liquids that can be employed in investigating several thermodynamic properties such as glass transition temperature [26]. Thus, Flory and co-workers had formulated a partition function for chain liquids. Their motivation was to represent the intermolecular energy and its volume in the cell model. They started from assuming a linear chain consisting of repeating units, n for a certain molecule that is terminated with a certain atom (i.e., $\mathrm{H}-(\mathrm{CH}_2)_n-\mathrm{H}$). They had been indicated that the terminal groups may exert intermolecular forces varying from those of the mid-chain repeating units and imagined the chain is subdivided into x segments. The segment does not correspond to repeating unit (i.e., $x \neq n$). The segment, x is proportional to the "hard core" molecular volume v^*.

The configuration partition function of the liquid is written as follows:

$$Z = Z^{\dagger}\left[\gamma\left(v^{1/3} - {v^*}^{1/3}\right)^3\right]^{xNc} \exp(-E_0/kT) \tag{3.1.2.1}$$

$$E_0 = -xNs\eta/2v \tag{3.1.2.2}$$

$$\eta \cong (s_m/s)^2\eta_m\left[1 + \left(s_e{\eta_e}^{1/2}/s_m{\eta_m}^{1/2}\right)/x\right]^2 \tag{3.1.2.3}$$

Where E_0 is the intermolecular energy. $Z^{\dagger}$ is the number of ways of arranging the segments of N molecules over a spatial array of xN sites in the lattice model and the combinatorial factor; $Z^{\dagger}$ is assumed to be independent of volume and temperature. γ is a geometric constant. η is the mean interaction between a segment pair in the liquid. η_m, η_{em} , η_e characterize interactions between sites on two neighbouring mid-chain segments, between a mid-chain and a terminal segment site, and between two terminal sites, respectively.

By substituting (Eq. 3.1.2.2) in (Eq. 3.1.2.1), together with introducing reduced variables, an expression can be obtained, as follows:

The statistical form of the simple configurational integral:

$$Z = Z^{\dagger}(\gamma v^*)^{xNc}\left(\tilde{v}^{1/3} - 1\right)^{3xNc} e^{(xNc/\tilde{v}\tilde{T})} \tag{3.1.2.4.A}$$

The classical form of the simple configurational integral:

$$Z = (nV^*)^n\left(\tilde{v}^{1/3}\right)^{3Cn} e^{-eq\epsilon/RT\tilde{v}} \quad (3.1.2.4.B)$$

$$Z^{fv} = (nV^*)^n\left(\tilde{v}^{1/3}\right)^{3Cn} \quad (3.1.2.5)$$

$$Z^{Att} = e^{-eq\epsilon/RT\tilde{v}} \quad (3.1.2.6)$$

$$\tilde{v} = v/v^* \quad (3.1.2.7)$$

where $\tilde{v} = V/V^*$, V^* is the molar hard-core volume, and ϵ is the average configurational potential energy per segment surface area, q.

$$\tilde{T} = T/T^* = 2v^*ckT/s\eta \quad (3.1.2.8)$$

Ultimately, the equation of state can be obtained from (Eq. 3.1.2.4.A), and it can be expressed in reduced form, as shown:

$$\tilde{p}\tilde{v}/\tilde{T} = \tilde{v}^{1/3}/\left(\tilde{v}^{1/3} - 1\right) - 1/\left(\tilde{v}\tilde{T}\right) \quad (3.1.2.9)$$

$$\tilde{p} = p/p^* = 2pv^{*2}/s\eta \quad (3.1.2.10)$$

Alternatively,

$$\tilde{p}/\tilde{\rho}^2 = \tilde{T}/\tilde{\rho}\left(1 - \tilde{\rho}^{1/3}\right) - 1 \quad (3.1.2.11)$$

$$\tilde{p} = pv^*/ckT^* \quad (3.1.2.12)$$

It could be mentioned that the equation of state differs as the parameter c changes, i.e., when c is equal to 1, it shows (Eq. 3.1.2.11). In addition, the three parameters, namely, v^*,c, and the product $s\eta$, serve to characterize the chain molecule according to (Eq. 3.1.2.4.A) and (Eq. 3.1.2.11).

Based on that, the equation of state reduces to parametric form.

The first of the parameters is alleged to be the same for all homologs of the series; this follows from the manner of defining a segment and the assumed linearity of xv^* with n. The other parameters are considered to depend asymptotically on n.

Thermodynamic properties can be deduced from Flory EoS such as the coefficient of thermal expansion α, the coefficient of compressibity κ, and the thermal pressure coefficient γ (not to be confused with the previous γ), may be exhibited in terms of the reduced variables as:

$$\alpha = v^{-1}(\partial v/\partial T)_p = \left(\tilde{T}/T\tilde{v}\right)\left(\partial\tilde{v}/\tilde{T}\right)_{\tilde{p}} \quad (3.1.2.13)$$

$$\kappa = -v^{-1}(\partial v/\partial p)_T = -(\tilde{p}/p\tilde{v})(\partial\tilde{v}/\tilde{p})_{\tilde{T}} \quad (3.1.2.14)$$

$$\gamma = (\partial p/\partial T)_v = \alpha/\kappa = \left(\tilde{T}p/T\tilde{p}\right)\left(\partial\tilde{p}/\partial\tilde{T}\right)_{\tilde{v}} \quad (3.1.2.15)$$

3.2. Sanchez and Lacombe Lattice Fluid Theory:

3.2.1. Pure Lattice Fluid:

Sanchez and Lacombe lattice fluid theory [27] is a statistical mechanical model that is based solely on three molecular parameters that are required to describe a real fluid: ϵ_i^*,v_i^*, and r_i^0. The three molecular parameters can be calculated once the three equation of state parameters, T_i^*, P_i^*, and ρ_i^* are evaluated.

$$\epsilon_i^* = N_A k T_i^* \tag{3.2.1.1}$$

$$r_i^0 = (1 \times 10^3 \times M_w P_i^*)/(N_A k T_i^* \rho_i^*) \tag{3.2.1.2}$$

$$v_i^* = M_w/(\rho_i^* r_i^0) \tag{3.2.1.3}$$

where ϵ_i^* is the interaction energy between molecules of type i in the pure component, T_i^*, P_i^*, and ρ_i^* are the characteristic of temperature, pressure, and density of a pure component i, respectively, r_i^0 is the number of occupied sites by the pure component molecules of type i in the lattice, the superscript (^{0}) is referred to the pure fluid, and v_i^* is the molecular close-packed volume.

The minimum reduced Gibbs free energy can be expressed after several substitutions, as follows:

$$G/(Nr\epsilon^*) \equiv \tilde{G} = -\tilde{\rho} + \tilde{P}\tilde{v} + \tilde{T}\left[(\tilde{v}-1)\ln(1-\tilde{\rho}) + \frac{1}{r}\ln(\tilde{\rho}/\omega)\right] \tag{3.2.1.4}$$

$$\tilde{T} \equiv T/T^* \quad T^* \equiv \epsilon^*/k \tag{3.2.1.5}$$

$$\tilde{P} \equiv P/P^* \quad P^* \equiv \epsilon^*/v^* \tag{3.2.1.6}$$

$$\tilde{v} \equiv \rho^*/\rho \equiv 1/\tilde{\rho} \tag{3.2.1.7}$$

$$\omega = \delta r/\sigma e^{r-1} \tag{3.2.1.8}$$

where ω is the number of configurations available to a r-mer in the close-packed "pure state", δ is a parameter used to characterize the flexibility of pure component molecules, σ is a parameter utilized to characterize the symmetry of pure component molecules, and $\tilde{T}$, $\tilde{P}$, $\tilde{v}$, and $\tilde{\rho}$ are the reduced temperature, pressure, volume, and density.

The equation of state for the system is estimated by equating the partial differentiation of reduced free energy with respect to the reduced volume at fixed reduced temperature and pressure to zero, as follows:

$$\partial\tilde{G}/\partial\tilde{v}\big|_{\tilde{T},\tilde{P}} = 0 \tag{3.2.1.9.A}$$

which yields to the following expression:

$$\tilde{\rho}^2 + \tilde{P} + \tilde{T}\left[\ln(1-\tilde{\rho}) + \left(1-\frac{1}{r}\right)\tilde{\rho}\right] = 0 \qquad (3.2.1.9.B)$$

It should be mentioned that $\tilde{\rho}$ is a dependent variable because it is calculated at given $(\tilde{T}, \tilde{P})$, with regard to the minimization of the free energy, while $\tilde{P}$ and $\tilde{T}$ are independent variables.

(Eq. 3.2.1.9.B) shows the complete thermodynamic description of the model fluid; all other thermodynamic properties can be deduced from the standard thermodynamic expressions, e.g., the thermal expansion coefficient, α, and isothermal compressibility, β, as shown:

$$\alpha \equiv \frac{1}{V}\left.\frac{\partial V}{\partial T}\right|_P = -\left.\frac{\partial \ln\tilde{\rho}}{\partial T}\right|_P \qquad (3.2.1.10.A)$$

$$T\alpha = \frac{1+\tilde{P}\tilde{v}^2}{\tilde{T}\tilde{v}\,[1/(\tilde{v}-1)+1/r]-2} \qquad (3.2.1.10.B)$$

$$\beta \equiv -\frac{1}{V}\left.\frac{\partial V}{\partial P}\right|_T = -\left.\frac{\partial \ln\tilde{\rho}}{\partial P}\right|_T \qquad (3.2.1.11.A)$$

$$P\beta = \frac{\tilde{P}\tilde{v}^2}{\tilde{T}\tilde{v}\,[1/(\tilde{v}-1)+1/r]-2} \qquad (3.2.1.11.B)$$

3.2.2. Mixed Lattice Fluid:

[Sanchez and Lacombe] [28] have extended the lattice-fluid theory to mixture by using "combining rules"; these combining rules are essential in all statistical and mechanical theories in which they can be employed as preliminary characteristics that lead finally to investigate the VLE behaviour.

Prior to proceeding, it is essential to understand the mechanism of this mixing rule considering how the characteristics of a mixture differ from a pure one.

The mer volume in the lattice for a pure component varies from one to another, whereas in the case of mixture, it differs slightly in which it depends on the concentration that results from the average characteristic value of pure components, as shown:

$$v^* = \phi_1^0\, v_1^* + \phi_2^0\, v_2^* \tag{3.2.2.1}$$

$$\phi_1^0 = \frac{\phi_1}{\phi_1 + \nu\phi_2} = 1 - \phi_2^0 \tag{3.2.2.2}$$

$$\nu \equiv v_1^*/v_2^* \tag{3.2.2.3}$$

$$\phi_1 = \frac{m_1/\rho_1^*}{m_1/\rho_1^* + m_2/\rho_2^*} = 1 - \phi_2 \tag{3.2.2.4}$$

$$m_2 = 1 - m_1 \tag{3.2.2.5}$$

Where ${\phi_1}^0$ is the close packed volume of component 1 in the mixture. m_1 and m_2 are the mass fractions of component 1 and 2, respectively.

The number of sites that occupied by the molecules of type i in the mixture, as follows:

$$r_i = (r_i^0\, v_i^*)/v^* \tag{3.2.2.6}$$

The total number of sites that occupied by the molecules, as follows:

$$r \equiv x_1 r_1 + x_2 r_2 \tag{3.2.2.7}$$

$$x_1 = \left(m_1/M_{w_1}\right)/\left(m_1/M_{w_1} + m_2/M_{w_2}\right) = 1 - x_2 \tag{3.2.2.8}$$

where x_1 and x_2 are the mole fractions of component 1 and 2, respectively.

The total characteristic pressure is given by:

$$P^* = \phi_1 P_1^* + \phi_2 P_2^* + \phi_1 \phi_2 \Delta P^* \quad (3.2.2.9)$$

$$\Delta P^* \equiv P_1^* + P_2^* - 2P_{12}^* \quad (3.2.2.10)$$

$$P_{12}^* = \sqrt{P_1^* P_2^*}\,(1 - k_{12}) \quad (3.2.2.11)$$

where k_{12} is an adjustable parameter.

The interaction energy of the mixture between two sites in the lattice, as follows:

$$\epsilon^* = P^* v^* = (\phi_1 P_1^* + \phi_2 P_2^* - \phi_1 \phi_2 \Delta P^*)(\phi_1^0 v_1^* + \phi_2^0 v_2^*) \quad (3.2.2.12)$$

The total characteristic temperature is given by:

$$T^* = T\left[\left(\phi_1/\tilde{T}_1 + \nu\,\phi_2/\tilde{T}_2\right)/(\phi_1 + \nu\phi_2) - \phi_1\phi_2 X\right] \quad (3.2.2.13)$$

where,

$$X \equiv (\Delta P^* v^*)/(N_A k T) \quad (3.2.2.14)$$

The reduced temperature $\tilde{T}$ and pressure $\tilde{P}$ of the mixture are defined similarly as a pure lattice fluid in (3.2.1.5-6).

The configurational Gibbs free energy G of a binary mixture is given by:

$$G \equiv rN\epsilon^* \tilde{G} \quad (3.2.2.15)$$

$$\tilde{G} = -\tilde{\rho} + \tilde{P}\tilde{v} + \tilde{T}\tilde{v}\left[(1-\tilde{\rho})\ln(1-\tilde{\rho}) + \frac{\tilde{\rho}}{r}\ln\tilde{\rho}\right] + \tilde{T}\left[\frac{\phi_1}{r_1}\ln\phi_1 + \frac{\phi_2}{r_2}\ln\phi_2\right] \quad (3.2.2.16)$$

where $\tilde{G}$ is the reduced Gibbs free energy.

The chemical potential of component 1 in the mixture can be obtained by taking the partial derivative of (Eq. 3.2.2.15) with respect to the number of molecules of a component 1 in the mixture at a certain temperature, pressure, and the number of molecules of a component 2 in the mixture, as follows:

$$\mu_1 \equiv \frac{\partial G}{\partial N_1}\Big|_{T,P,N_2} \tag{3.2.2.17}$$

$$\mu_1 = N_A kT[\ln \phi_1 + (1 - r_1/r_2)\phi_2 + r_1^0 \tilde{\rho} X_1 \phi_2^2] + r_1^0 kT \left\{-\tilde{\rho}/\tilde{T}_1 + \tilde{P}_1 \tilde{v}/\tilde{T}_1 + \tilde{v}\left[(1 - \tilde{\rho})\ln(1 - \tilde{\rho}) + \frac{\tilde{\rho}}{r_1^0}\ln \tilde{\rho}\right]\right\} \tag{3.2.2.18}$$

The expression of the chemical potential of component 2, μ_2 in the mixture can be calculated by interchanging the indices 1 by 2.

The above chemical potential of either component 1 or 2 leads to the following conditions:

- If the concentration of component 1 in the mixture equals to 1, then the chemical potential of component 1 turns to the chemical potential of component 1 in the pure state, as shown by:

$$\mu_1(\phi_1 = 1) \equiv \mu_1^0 \tag{3.2.2.19}$$

- The Flory-Huggins chemical potentials can be recovered when the temperature is low or the pressure is high, then, the reduced densities can approach their maximum value of unity (as $\tilde{\rho}\ and\ \tilde{\rho}_1 \to 1$):

$$(\mu_1 - \mu_1^0)/(N_A kT) \to \ln \phi_1 + (1 - r_1/r_2)\phi_2 + r_1^0 X_1 \phi_2^2 \tag{3.2.2.20}$$

- ΔP^* or X_1 parameter can characterize a binary mixture whereas all the remaining parameters are known from the pure components.

It could be noted that it is convenient to characterize the interaction in terms of a dimensionless parameter ζ which measures the deviation of P_{12}^* from the geometric mean, as follows:

$$\zeta = P_{12}^*/(P_1^* P_2^*)^{1/2} \tag{3.2.2.21}$$

And (Eq. 3.2.2.10) becomes:

$$\Delta P^* = P_1^* + P_2^* - 2\zeta (P_1^* P_2^*)^{1/2} \quad (3.2.2.22)$$

The change of mixing volume is defined by:

$$\Delta V_m / V_0 = \tilde{v}/(\phi_1 \tilde{v}_1 + \phi_2 \tilde{v}_2) - 1 \quad (3.2.2.23)$$

Where V_0 is the ideal volume of the mixture.

The heat of mixing:

$$\Delta H_m / RT = r\{ \tilde{\rho}\phi_1\phi_2 X + v^*[\phi_1 P_1^*(\tilde{\rho}_1 - \tilde{\rho}) + \phi_2 P_2^*(\tilde{\rho}_2 - \tilde{\rho})]/RT\} \quad (3.2.2.24)$$

The entropy of mixing ΔS_m is:

$$\Delta S_m/R = -r\left\{\frac{\phi_1}{r_1}\ln\phi_1 + \frac{\phi_2}{r_2}\ln\phi_2 + \tilde{v}\left[(1-\tilde{\rho})\ln(1-\tilde{\rho}) + \frac{\tilde{\rho}}{r}\ln\tilde{\rho}\right]\right\} + \frac{r}{\phi_1 + v\phi_2}\left\{\phi_1\tilde{v}_1\left[(1-\tilde{\rho}_1)\ln(1-\tilde{\rho}_1) + \frac{\tilde{\rho}_1}{r_1^0}\ln\tilde{\rho}_1\right] + v\phi_2\tilde{v}_2\left[(1-\tilde{\rho}_2)\ln(1-\tilde{\rho}_2) + \frac{\tilde{\rho}_2}{r_2^0}\ln\tilde{\rho}_2\right]\right\} \quad (3.2.2.25)$$

It can be mentioned that the first terms of the above equation are the Flory-Huggins combinatorial entropy terms.

3.2.3. Alternative Mixing Rules for Sanchez and Lacombe LF model:

3.2.3.1. Modified mixing rule which uses two fitting parameters k_{ij} and l_{ij}:

The mixing rule reported by McHugh et al. [29] for the segment volume v^* of the mixture, as follows:

$$v^* = \sum \sum \varphi_i \, \varphi_j \, v_{ij}^* \quad (3.2.3.1.1)$$

$$v_{ij}^* = \frac{1}{2}\left(v_i^* + v_j^*\right)\left(1 - l_{ij}\right) \quad (3.2.3.1.2)$$

$$\phi_i = \frac{x_i r_i}{r} \quad (3.2.3.1.3)$$

where ϕ_i is the segment fraction of component i and l_{ij} is the interaction size parameter.

It can be noticed that there is an adjustable parameter (l_{ij}) that has been added to (Eq. 3.2.3.1.1), compared to the total molecular close packed volume that was introduced by Sanchez and Lacombe in the original method, [see Eq. (3.2.2.1)].

The segment energy, ϵ^* is defined by:

$$\epsilon^* = \frac{\sum \sum \phi_i \phi_j \epsilon_{ij}^* v_{ij}^*}{v^*} \quad (3.2.3.1.4)$$

$$\epsilon_{ij}^* = \sqrt{\epsilon_i^* \epsilon_j^*}\,(1 - k_{ij}) \quad (3.2.3.1.5)$$

Where k_{ij} is the interaction energy parameter between component i and j.

The mixing rule proposed by McHugh et al. which divides the interaction parameters into the energy parameter k_{ij} and the size parameter l_{ij} was shown to be more effective than the original mixing rule.

$$\frac{\mu_i}{RT} = \left(\ln \phi_i + 1 - \frac{r_i}{r}\right) + \ln \tilde{\rho} + r_i\left[-\frac{\tilde{\rho}}{\tilde{T}} - \left(\frac{1}{\tilde{\rho}} - 1\right)\ln(1-\tilde{\rho}) + \frac{\tilde{P}\tilde{v}}{\tilde{T}}\right] + \frac{z}{r}\left[\frac{nr}{v^*}\left(\frac{\partial v^*}{\partial n_i}\right)_{n_j,T}\right] - \frac{\tilde{\rho}}{\tilde{T}}\left[\frac{nr}{\epsilon^*}\left(\frac{\partial \epsilon^*}{\partial n_i}\right)_{n_j,T}\right] \quad (3.2.3.1.6)$$

$$z = \frac{Pv}{RT} = r\left[-\frac{1}{\tilde{\rho}}\ln(1-\tilde{\rho}) - \left(1 - \frac{1}{r}\right) - \frac{\tilde{\rho}}{\tilde{T}}\right] \quad (3.2.3.1.7)$$

$$\frac{nr}{v^*}\left(\frac{\partial v^*}{\partial n_i}\right)_{n_j,T} = \frac{1}{v^*}\left[2r_i\left(-v^* + \sum \phi_j v_{ij}^*\right)\right] \quad (3.2.3.1.8)$$

$$\frac{nr}{\epsilon^*}\left(\frac{\partial \epsilon^*}{\partial n_i}\right)_{n_j,T} = \frac{1}{\epsilon^* v^*}\left[2r_i(-\epsilon^* v^*) + \sum \phi_j\, \epsilon_{ij}^* v_{ij}^*\right] - \left[\frac{nr}{v^*}\left(\frac{\partial v^*}{\partial n_i}\right)_{n_j,T}\right] \quad (3.2.3.1.9)$$

3.2.3.2. Mixing rule proposed by West et al.[30]:

$$v^* = \sum_{i=1}^{n} \sum_{j=1}^{n} \phi_i\, \phi_j v_{ij}^* \quad (3.2.3.2.1)$$

$$v_{ij}^* = \left(\frac{v_{ii}^{*1/3} + v_{jj}^{*1/3}}{2}\right)^3 \quad (3.2.3.2.2)$$

$$\epsilon^* \sum_{i=1}^{n} \sum_{j=1}^{n} \phi_i\, \phi_j \epsilon_{ij}^* \quad (3.2.3.2.3)$$

$$\epsilon_{ij}^{*} = \left(\epsilon_{ii}^{*}\epsilon_{jj}^{*}\right)^{1/2}\zeta_{ij} \qquad (3.2.3.2.4)$$

Where ζ_{ij} is a binary interaction parameter and ϕ_i is the site fraction of component i.

$$\frac{\mu_i^{LF}}{kT} = \ln\phi_i + \left(1+\frac{r_i}{r}\right) + r_i\tilde{\rho}\left(\sum_{j=1}^{n}\phi_j\,\chi_{jj} - \sum_{j=1}^{n}\ \sum_{k=j+1}^{n}\phi_j\,\phi_k\chi_{jk}\right) + r_i\left[-\frac{\tilde{\rho}}{\tilde{T}_i} + \frac{\tilde{P}_i\tilde{v}}{\tilde{T}} + (\tilde{v}-1)\ln(1-\tilde{\rho}) + \frac{1}{r_i}\ln\tilde{\rho}\right] \qquad (3.2.3.2.5)$$

where χ_{ij} is the classic Flory-Huggins interaction term:

$$\chi_{ij} = \frac{\left(\epsilon_{ii}^{*}+\epsilon_{jj}^{*}-2\epsilon_{ij}^{*}\right)}{kT} \qquad (3.2.3.2.6)$$

$$\frac{1}{r} = \sum_{i=1}^{n}\frac{\phi_i}{r_i} \qquad (3.2.3.2.7)$$

3.2.3.3. Mixing rule proposed by [Sanchez and Panayiotou] [31]:

$$\epsilon_{ij}^{*} = \frac{1}{2}\left(\epsilon_{ii}^{*}+\epsilon_{jj}^{*}\right) - \frac{1}{2}RT \qquad (3.2.3.3.1)$$

Chapter 4
THERMODYNAMIC EQUATION OF STATE

4. Panayiotou and Vera Equation of State [EoS]:

4.1. Statistical Mechanics of the Lattice-Fluid Equation of State for a Pure Component:

Decades ago, Panayiotou and Vera developed an equation of state [6,7]. Starting from the following:

$$P = RT \left(\frac{\partial \ln Q}{\partial v}\right)_{T,N_1} \tag{4.1.1}$$

$$v = (N_H v_H + N_1 r_1 v_H) \tag{4.1.2}$$

$$v_1^* = N_1 r_1 v_H \tag{4.1.3}$$

v is the total volume of the lattice, N_H is the number of holes in the lattice, v_h which corresponds to (9.75 × 10 -3 m3 kmol^{-1}) that has been considered to be correspondent to a methylene group in poly(ethylene) [7], N_1 is the number of molecules of a pure component 1, r_1 is the number of lattice cells occupied by molecules of a pure component 1, and v_1^* is the volume of cells in the lattice of a pure component 1 and it can be considered as the first adjustable parameter.

The canonical partition function, Q is defined by:

$$Q = \left(\frac{\delta_1}{\sigma_1}\right)^{N_1} g_c g_{NR} \; e^{\left(\frac{-E}{RT}\right)} \tag{4.1.4}$$

Where $\delta_1$and σ_1 are volume-independent parameters accounting for flexibility and symmetry of component 1 molecules, g_c is the random combinatorial term, g_{NR} is the non-random combinatorial correction factor, and E is the lattice energy of the system.

EoS can be derived by taking the partial derivative of Q with respect to v, fixing T and N_1 as shown in (Eq.4.1.1) along with the substitution of conventional reduced quantities:

$$\tilde{P}_1 = \frac{P}{P_1^*} = \frac{2\,P\,v_h}{z\,\epsilon_{11}} \qquad \tilde{T}_1 = \frac{T}{T_1^*} = \frac{2\,RT}{z\,\epsilon_{11}} \qquad \tilde{v}_1 = \frac{v}{v_1^*} \tag{4.1.5}$$

$$\epsilon_{11} = \epsilon_{11h} + T\epsilon_{11s} \tag{4.1.5.A}$$

z is the coordination number; the number of the closest neighbours' sites to the central site in the lattice. Panayiotou and Vera had assumed the coordination number equals to 10 since the base of the lattice can accommodate the chemical structure that leads to an accurate result, ϵ_{11} is the molecular interaction energy between like molecules of a pure component 1, ϵ_{11h} is the enthalpic interaction energy between molecules of component 1, and ϵ_{11s} is the entropic interaction energy between molecules of component 1 and they can be considered as the second adjustable parameter and the third one, respectively.

$\tilde{P}_1$, $\tilde{T}_1$ and $\tilde{v}_1$ are reduced quantities of pressure, temperature, and volume, respectively.

Eventually, EOS (Random approximation) can be obtained, as follows:

$$\frac{\tilde{P}_1}{\tilde{T}_1} = ln\ \frac{\tilde{v}_1}{\tilde{v}_1 - 1} + \frac{z}{2}\ ln\left(\frac{\tilde{v}_1 + q_1/r_1 - 1}{\tilde{v}_1}\right) - \frac{\theta_1^2}{\tilde{T}_1} \tag{4.1.6}$$

$$\theta_1 = \frac{q_1}{r_1(\tilde{v}_1 - 1) + q_1} \tag{4.1.7}$$

θ_1 denotes the molecular surface area fraction of component 1 including holes, and q_1 is the molecular surface area of a component 1.

$$zq_1 = (z-2)r_1 + 2 \tag{4.1.8}$$

zq_1 is the number of contact sites by component 1 molecules, $(z-2)$ are the interaction sites; two of these sites are taken up by bonded neighbours, and (+2) is added in (Eq. 4.1.8) because there is only one site at the end of the lattice.

The chemical potential of a pure component 1 has a significant role in the phase equilibrium. It can be obtained from the canonical partition function, as follows:

$$-\frac{\mu_1^{(P)}}{RT} = \left(\frac{\partial\ ln\ Q}{\partial N_1}\right)_{T,v} \tag{4.1.9}$$

After several differentiations, ultimate of chemical potential of a pure component 1 form as follows:

$$-\frac{\mu_1^{(P)}}{RT} = ln\frac{\delta_1}{\sigma_1} + \ln q_1\ + \ln\frac{(1-\theta_1)^{r_1}}{\theta_1}\ + \frac{\theta_1}{\tilde{T}_1}\ (q_1 + r_1\tilde{v}_1\theta_1) \tag{4.1.10}$$

$\mu_1^{(P)}$denotes the chemical potential of a pure component 1.

4.2. Statistical Mechanics of the Lattice-Fluid Equation of State for Mixtures:

A good start to determine the EoS for a mixture [7] is given by:

$$P = RT \left(\frac{\partial \ln Q}{\partial v}\right)_{T,N_i} \tag{4.2.1}$$

The expression for the canonical partition function of the mixture, Q, is written in a similar way to the expression of the canonical partition function for the pure component with considering the product of multi-components as defined by:

$$Q = \prod_i \left(\frac{\delta_i}{\sigma_i}\right)^{N_i} g_c g_{NR}\, e^{\left(\frac{-E}{RT}\right)} \tag{4.2.2}$$

The expression for calculating the reduced variables remains the same as a pure component expression,

$$\tilde{P} = \frac{P}{P^*} = \frac{2\,P\,v_h}{z\;\epsilon^*} \tag{4.2.3}$$

$$\tilde{T} = \frac{T}{T^*} = \frac{2\,R\,T}{z\,\epsilon^*} \tag{4.2.4}$$

$$\tilde{v} = \frac{v}{v^*} \tag{4.2.5}$$

Where $\tilde{P}, \tilde{T}, \tilde{v}$ are reduced of pressure, temperature, and volume of a mixture, respectively. P^* and T^* are characteristic of pressure and temperature. ϵ^* is the molecular interaction energy among molecules of a mixture. v^* is the molecular reference volume of a mixture.

The molecular interaction energy of a mixture, ϵ^*, as follows:

$$\epsilon^* = \bar{\theta}_i\,\epsilon_{ii} + \bar{\theta}_j\epsilon_{jj} - \bar{\theta}_i\;\bar{\theta}_j\,\dot{\Gamma}_{ij}\,\Delta\epsilon \tag{4.2.6}$$

$$\Delta\epsilon = \epsilon_{ii} + \epsilon_{jj} - 2\epsilon_{ij} \tag{4.2.7}$$

$$\epsilon_{ij} = \epsilon_{ijh} + T\epsilon_{ijs} \tag{4.2.8}$$

$$\bar{\theta}_i = \frac{x_i\;q_i}{q} \tag{4.2.9}$$

ϵ_{ii} is the molecular interaction energy between like molecules of type i, $\dot{\Gamma}_{ij}$ is non-randomness factor for molecules of type i around molecules of type j, $\Delta\epsilon$ is the difference of the molecular interaction energy between unlike molecules of type i and j, ϵ_{ij} is the molecular interaction energy of molecules between

unlike molecules of type i and j, ϵ_{ijh} is the enthalpic interaction energy between unlike molecules, ϵ_{ijs} is the entropic interaction energy between unlike molecules of type i and j. $\bar{\theta}_i$ is the molecular surface area fraction of component i subjected to the cells in the lattice, and x_i is the mole fraction of component i.

The number of lattice cells occupied by molecules, r, as follows:

$$r = \sum x_i \, r_i \tag{4.2.10}$$

$$r_i = \frac{v_i^*}{v_h} \tag{4.2.11}$$

Where r_i is number of lattice cells occupied by one molecule of component i, v_i^* is the molecular reference volume of component i.

The total molecular surface area parameter of a mixture, q, as follows:

$$q = \sum x_i \, q_i \tag{4.2.12}$$

$$zq_i = (z-2)r_i + 2 \tag{4.2.13}$$

q_i represents the effective chain length of molecule i. zq_i is the number of contact sites by the molecule i.

The molecular surface area fraction of a mixture, θ, as follows:

$$\theta = \sum x_i \, \theta_i \tag{4.2.14}$$

$$\theta_i = \frac{q_i N_i}{rN(\tilde{v}-1)+qN} \tag{4.2.15}$$

θ_i denotes the molecular surface area fraction of component i including holes.

The EoS of random approximation for a mixture in terms of reduced variables is:

$$\frac{\tilde{P}}{\tilde{T}} = ln \, \frac{\tilde{v}}{\tilde{v}-1} + \frac{z}{2} \, ln \left(\frac{\tilde{v} + q/r - 1}{\tilde{v}} \right) - \frac{\theta^2}{\tilde{T}} \tag{4.2.16}$$

The chemical potential of component i in a binary mixture, $\mu_i^{(M)}$:

$$-\frac{\mu_i^{(M)}}{RT} = ln\phi_i + ln\frac{\tilde{v}_i}{\tilde{v}} + q_i \, ln\left(\frac{\tilde{v}}{\tilde{v}-1} \quad \frac{\tilde{v}_i - 1}{\tilde{v}_i}\right) + 2q_i \left(\frac{\theta_{i,P-\theta_i}}{\tilde{T}_i} - \frac{\theta_j}{\tilde{T}_{ij}}\right) \tag{4.2.17}$$

$$\phi_i = \frac{x_i\, v_i^*}{\sum_j x_j\, v_j^*} = \frac{x_i\, r_i}{\sum_j x_j\, r_j} \tag{4.2.18}$$

$$\tilde{T}_{ij} = \frac{2\,R\,T}{z\,\epsilon_{ij}} \tag{4.2.19}$$

where $\theta_{i,P}$ is the molecular surface area fraction of the pure component i including holes at the same temperature and pressure as the mixture, $\tilde{T}_{ij}$ is the reduced temperature of a binary mixture, $\tilde{v}_i$ is the reduced volume of component i in the mixture, and φ_i is the volume fraction of component i in the mixture.

Chapter 5

GROUP CONTRIBUTION METHOD

5.1. Introduction to Group Contribution Methods [GCM]:

Industrial chemical process design requires a separation for mixtures, especially studying the behaviour of fluid phase equilibrium, and because of limited experimental data or empirical correlations, group contribution methods are introduced for the prediction of several thermodynamic properties. The basic idea moves from considering that while thousands of chemical compounds are of interest in chemical technology, the number of functional groups which compose them is much smaller. In addition, assuming that a physical property of a fluid is the sum of contributions formed of the molecule's functional groups, the contribution constructed by one group is supposed to be independent of that constructed by another group in which the molecule contains several different groups such as a molecule made by alkane and alcohol. Interestingly, it assists to acquire a technique for correlating the properties of a very large number of fluids in the matter of a much smaller number of parameters which characterize the contributions of individual groups.

5.2. Group Contribution Methods:

5.2.1. UNIFAC model:

UNIFAC model (UNIQUAC Functional-Group Activity Coefficients) is a result of combination of the solution-of-groups concept with a model for activity coefficients based on an extension of the quasi-chemical theory of liquid mixtures, namely Universal Quasi-Chemical (UNIQUAC) which holds two adjustable parameters that were derived from the extension of Guggenheim's quasi-chemical theory of liquid mixtures. UNIFAC method is used for calculating activity coefficients in the matter of parameters that are identified in the sizes and surface areas of individual functional groups, and energetic interactions between groups. Size and area constants for groups were evaluated from pure component and molecular structure data. Group- interactions constants were evaluated from phase equilibrium data for mixtures containing water, alcohol, ketones, amines, esters, ethers, aldehydes, chlorides, nitriles, paraffines, olefines, aromatic hydrocarbons, and other organic liquids.

UNIQUAC equation of mixture for the activity coefficient of (molecular) component i is defined by:

$$\ln \gamma_i = \ln \gamma_i^c + \ln \gamma_i^R \qquad (5.2.1.1)$$

combinatorial term residual term

Where γ_i^c is the combinatorial term which results from the difference in molecular size and it can be evaluated by using the Flory-Huggins equation. γ_i^R is the residual term which results from the molecular interactions and Wilson equation can be applied to its calculation.

5.2.2. GC-Flory EoS:

Holten-Andersen and co-workers [2] have represented a new group-contribution model for predicting phase equilibria in polymer solutions. The model is based on an equation of state that is extended from Flory. The equation contains a free volume term, which leads to the correct ideal gas limit. The model can correlate and predict with good accuracy both pure-component PVT properties and vapor-liquid equilibria of mixtures containing polymers. The model by Flory et al. has been modified on three points, the purpose of which is to render the model applicable for associating mixtures and to enable the introduction of the group-contribution approach.

Firstly, the free volume term of Flory in (Eq. 3.1.2.5) has been changed, as follows:

$$Z^{FV} = \left[nV^* \left(\tilde{v}^{1/3} - 1 \right)^3 \left(\frac{\tilde{v}^{1/3} - 1}{\tilde{v}^{1/3}} \right)^{3C} \right]^n \qquad (5.2.2.1)$$

The above expression is unlike the Flory expression as it leads to the correct ideal gas limit, i.e., $Z^{FV} \rightarrow V$ as $V \rightarrow \infty$.

The attractive term has been changed on two points: The first alteration considers the attractive potential of two molecules to be the sum of two different contributions: (i) an energy of random orientations of two molecules and (ii) an energy of favorable orientations or favorable packing configurations of the two molecules. This difference has been found advantageous in expressing several phenomena met in polymer solution thermodynamics.

This separation of the attractive energy leads to the following form of the attractive part of the partition function:

$$Z^{ATT} = e^{\left[-\frac{znq\epsilon_0}{2RT\tilde{v}}\right]} \left[\left(1-\omega+\omega\, exp(-\epsilon_\omega b/RT\tilde{v})\right)\right]^{2nq/2b} \qquad (5.2.2.2)$$

Random orientation + favorable orientations

In the above equation, ϵ_0 is the potential energy per sement-surface area of random packing configurations. ϵ_ω is the extra energy contribution from packing into more favorable configurations. ω is a measure of the relative number of favorable configurations. b is a measure of the number of segment units engaged in the favored orientations.

The second alteration of the attractive term concerns its extension to mixtures, where a non-random UNIQUAC-like expression has been adopted instead of the random mixing expression of the Flory model:

$$Z_{mix}^{ATT} = exp\left\{-\sum_i \frac{1}{2} z q_i n_i \left(a_{ii} - RT \ln \sum_j \theta_j\, exp\left(-\Delta a_{ji}/RT\right)\right)/RT\right\} \qquad (5.2.2.3)$$

$$\Delta a_{ji} = \left(a_{ji} - a_{ii}\right)s \qquad (5.2.2.4)$$

$$a_{ji} = \epsilon_{0,ji}/\tilde{v} - (RT/b)\ln\left\{1+\omega\left(exp\left(-b\epsilon_{\omega ji}/RT\tilde{v}\right)-1\right)\right\} \qquad (5.2.2.5)$$

Where a_{ji} is the Helmholtz energy of interaction. s is the number of segment units.

It can be mentioned that there is only one binary parameter that is a_{ji}, which is equal to a_{ij}, and it is used for system without hydron bonding. Thus, for hydrogen-bonding systems, it has been noticed that one parameter is not sufficient to describe the systems. Therefore, binary vapor-liquid equilibria data has been correlated by introducing an extra binary entropic interaction parameter, ΔS_{ji}^{hb}, in the attractive or residual term:

$$\Delta a_{ji} = \left(a_{ji} - a_{ii} - T\Delta S_{ji}^{hb}\right)s \qquad (5.2.2.6)$$

This additional entropy parameter for hydrogen-bonding components is assumed independent of density, and therefore, it does not affect the equation of state.

From the expressions given above, all necessary thermodynamic quantities may be derived. The main equations are given below.

The Gibbs mixing function is formed of three terms: i) combinatorial, ii) free volume, iii) attractive, as shown in the following:

$$\Delta G^{Mixing}/RT \approx \Delta A/RT = \sum_i n_i \ln \varphi_i + \sum_i n_i \left[3(1+c_i)\ln\frac{\tilde{v}_i^{1/3}-1}{\tilde{v}^{1/3}-1} - C_i \ln\frac{\tilde{v}_i}{\tilde{v}}\right] + \sum_i \frac{1}{2} z(q_i n_i/RT)\left[a_{ii}(\tilde{v}) - a_{ii}(\tilde{v}_i) - RT\ln\sum_j \theta_j \exp\left(-\Delta a_{ji}/RT\right)\right] \quad (5.2.2.7)$$

Combinatorial + free volume + attractive

Where $\tilde{v}_i$ is the pure component reduced volume and $\tilde{v}$ the reduced volume of the mixture.

The chemical potential is given in the following:

$$\Delta\mu_i/RT = \ln\varphi_i + 1 - \frac{\varphi_i}{x_i} + 3(1+C_i)\ln\frac{\tilde{v}_i^{1/3}-1}{\tilde{v}^{1/3}-1} - C_i\ln\frac{\tilde{v}_i}{\tilde{v}} + \frac{1}{2}zq_i\left[\frac{1}{RT}\left(a_{ii}(\tilde{v}) - a_{ii}(\tilde{v}_i)\right) + 1 - \ln\sum_j \theta_j \exp\left(-\Delta a_{ji}/RT\right) - \sum_j\left(\theta_j \exp\left(-\Delta a_{ij}/RT\right)/\sum_k \theta_k \exp\left(-\Delta a_{kj}/RT\right)\right)\right] \quad (5.2.2.8)$$

The pressure is given by:

$$P = \frac{nRT}{V}\left(\frac{\tilde{v}^{1/3}+C}{\tilde{v}^{1/3}-1}\right) + \frac{E}{nV^*\tilde{v}} \quad (5.2.2.9)$$

For a mixture, [Flory and co-workers] [26] proposed a simple linear mixing rule for the hard-core volume and C parameter, as follows:

$$C = \sum_i n_i C_i/n \quad (5.2.2.10)$$

$$V^* = \sum_i n_i V_i^*/n \quad (5.2.2.11)$$

and energy E is given by,

$$E = \sum_i \frac{1}{2} z q_i n_i \left\{\epsilon_{ii} + \frac{\sum_j \theta_j \exp\left(-\Delta a_{ji}/RT\right)\Delta\epsilon_{ji}}{\sum_k \theta_k \exp\left(-\Delta a_{ki}/RT\right)}\right\} \quad (5.2.2.12)$$

$$\epsilon_{ji} = \epsilon_{0,ji}/\tilde{v} + \frac{\omega \exp(-b\epsilon_{\omega,ji}/RT\tilde{v})}{1+\omega(\exp(-b\epsilon_{\omega,ji}/RT\tilde{v})-1)}\frac{\epsilon_{\omega,ji}}{\tilde{v}} \quad (5.2.2.13)$$

$$\Delta\epsilon_{ji} = \epsilon_{ji} - \epsilon_{ii} \quad (5.2.2.14)$$

There are only five molecular parameters for expressing this model which are V_i^*, q_i ,C_i , $\epsilon_{0,ji}$, $\epsilon_{\omega,ji}$ and only two parameters for hydrogen bonding systems which are ΔS_{ij}^{hb}, ΔS_{ji}^{hb}.

The following group-contribution expressions are adopted for the calculation of these parameters:

$$V_i^* = \sum_m 21.238\, R_m \quad (5.2.2.15)$$

$$q_i = \sum_m Q_m \quad (5.2.2.16)$$

$$C_i = -0.640 + \sum_m C_m^{MC} R_m^{MC} + \sum_m C_m^{BG} R_m^{BG} \quad (5.2.2.17)$$

$$\epsilon_{0,ji} = \sum_m \theta_m^{(i)} \sum_n \theta_n^{(j)}\, \epsilon_{nm} \quad (5.2.2.18)$$

$$\epsilon_{\omega,ji} = -\left[\epsilon_{\omega,jj}\epsilon_{\omega,ii}\right]^{1/2} \quad (5.2.2.19)$$

$$\Delta S_{ji}^{hb} = \sum_m \theta_m^{(i)} \sum_n \left(\theta_n^{(j)} - \theta_n^{(i)}\right) \Delta S_{nm}^{hb} \quad (5.2.2.20)$$

where R_m and Q_m are nonadjustable parameters that retrieved from UNIFAC. C_m^{MC} is a degree of freedom group parameter for groups located in the main chain. The quantity C_m^{BG} is the degree of freedom parameter for branch point groups (e.g., the CH group in propane, 2-methyl). C_m^{BG} can be calculated through a correlation related to C_m^{MC}. R_m^{MC} and R_m^{BG} are group volume parameters that obtained from UNIFAC. $\epsilon_{\omega,jj}$ is a pure-component molecular parameter. ϵ_{nm} and ΔS_{nm}^{hb} are a group-interaction parameters. C_m^{MC}, ϵ_{mn} are adjustable group parameters for hydrogen bonding components. ΔS_{mn}^{hb} is adjustable parameter and determined experimentally. m and n refer to groups m and n indexes. i and j refer to i and j molecules.

5.2.3. Developed GC-Flory EoS:

Thirty-two years ago, [Chen and co-workers] [3] presented an equation of state by extending a group-contribution of the Flory equation. Their motivation was to develop an equation that is similar to Flory but simpler than the Holten-Andersen model. They introduced a new correlation for the degree of freedom parameter, C. The energy interaction parameters are based on group-group interactions, and the C parameters are calculated by using the group-contribution approach. They indicated that the new equation of state can predict vapor-liquid equilibria for a large variety of mixtures of polymers and solvents over a wide range of temperatures with a good accuracy.

Holten-Andersen model has been changed on the following:

In the Holten-Andersen EoS, the attractive potential between two molecules was expressed as the sum of energy of random orientations, ϵ_0, and of favourable orientations, ϵ_ω. This distinction is meant to be advantageous in describing a number of phenomena met in polymer solutions, as well as for pure compounds. This type of treatment appears to be physically reasonable, but it causes the model to be complex to use.

Chen and co-workers have developed an attractive energy partition function that is similar to the Flory expression as shown in (Eq. 3.1.2.6), as follows:

$$Z^{Att} = e^{\left[-\frac{znq\epsilon_0}{2RT\tilde{v}}\right]} \tag{5.2.3.1}$$

The energy has been changed compared to Holten-Andersen and others work [2], as follows:

$$E = \sum_i \frac{1}{2} z q_i n_i \left\{ \epsilon_{ii} + \frac{\sum_j \theta_j \exp\left(-\left(\Delta\epsilon_{ji} - T\Delta S_{ji}^{hb}\right)/RT\right)\Delta\epsilon_{ji}}{\sum_j \theta_j \exp\left(-\left(\Delta\epsilon_{ki} - T\Delta S_{ki}^{hb}\right)/RT\right)} \right\} \tag{5.2.3.2}$$

A new correlation for the C parameter of component i has been introduced instead of the simple, linear temperature dependency of the C parameter in the Holten-Andersen model as shown in (Eq.5.2.2.17), as follows:

$$C_i = \sum_n \nu_{n,i} \left[C_{T_0,n} + C_{T,n} \left(\frac{1}{T} - \frac{1}{T_0} \right) \right] + \sum_n \frac{R_n}{\sum_m R_m} C_n{}^0 \tag{5.2.3.3}$$

where $\nu_{n,i}$ is the number of group n in molecule i, the reference temperature T_0 is taken as 298.15K, R_n is the normalized van der Waals volume for group n given as in the UNIFAC model [Fredenslund et al.,

1977] [32], and $C_{T_0,n}$, $C_{T,n}$ and $C_n{}^0$ are the temperature-independent term, the temperature coefficient, and a constant term for group n taking into account special effects.

The temperature dependence of the C parameter is rigorously introduced into the Helmholtz free energy. Thus, a new energy expression is obtained, replacing (Eq.5.2.3.2):

$$E = \sum_i \frac{1}{2} z q_i n_i \left\{ \epsilon_{ii} + \frac{\sum_j \theta_j \exp\left(-\left(\Delta\epsilon_{ji} - T\Delta S_{ji}^{hb}\right)/RT\right)\Delta\epsilon_{ji}}{\sum_k \theta_k \exp\left(-\left(\Delta\epsilon_{ki} - T\Delta S_{ki}^{hb}\right)/RT\right)} \right\} - 3R \ln\left(\frac{\tilde{v}^{1/3}-1}{\tilde{v}^{1/3}}\right) \sum_i n_i \left[\frac{dC_i}{d(1/T)}\right] \quad (5.2.3.4)$$

In summary, it can be said that Chen and co-workers have obtained a predictive model for correlating the data of pure polymers and solvents with good accuracy and even better than those of the Holten-Andersen. Their model can be applied over a wider range of temperature compared to Holten-Andersen model.

5.2.4. GC-Sanchez and Lacombe EoS:

[Constantinou and Gani, 1994] [33] developed a group contribution method that can evaluate the lattice-fluid (LF) scaling constants of the polymers and it has been shown to be very successful in estimating various thermophysical properties of simple fluids. This method can be applied in two steps. First step, the fundamental step has contributions from first-order functional groups such as those currently applied for the estimation of mixtures properties [Fredenslund et al., 1977] [32]. Second step has a set of second-order groups which have the first-order groups as building blocks. The identity of the second-order groups is dependent on the concept of conjugation operators. Based on this method, the molecular structure of a compound is as a number of conjugate forms and the property of a compound is a linear combination of these conjugate form contributions. Each conjugate form is an idealized structure with integer-order localized bonds and integer charges on the atoms. The purely covalent conjugate form is the dominant conjugate form, and the ionic forms are the recessive conjugates, which can be obtained from the dominant form by a rearrangement of electron pairs. A conjugation operator describes a particular pattern of electron rearrangement and, when applied to a dominant conjugate, yields an entire class of recessive conjugates. The property of a compound is evaluated by calculating and combining the properties of its conjugate forms through conjugation operators. The group identification focuses on the operators which correspond to the significant conjugate forms, that is, the operators with significantly high contributions than the other. The structure of a second-order group ought to the distinct sub-chain of at least one significant conjugation operator; i.e., the CH3COCH2 second-order group incorporates the $O = C - C$, the $O = C - C - H$, and the $C - C - C - H$ operators. The structure of a second-order group has to adjacent first-order groups as building blocks, and it should

be as small and simple as possible. Certainly, the performance of second-order groups (as with first-order groups) is independent of the molecules in which the groups occur.

Constantinou and Gani' method for the estimation of a property X of a compound is as follows. Let C_i be the contribution of the first-order group of type i, which occurs Ni times, and D_j be the contribution of the second-order group of type j, which occurs M_j times in the compound. By selecting a simple function $f(X)$ of the property X, as follows:

$$f(X) = \sum_i N_i C_i + W \sum_j M_j D_j \qquad (5.2.4.1)$$

The constant W is equal to 1 when there are second-order groups contributing to the property and equal to 0 when only first-order groups are contributing. The selection of the function $f(X)$ is based on some principles as well. It has to achieve additivity in the contributions C_i and D_j and to exhibit the best possible fit of the experimental data. Furthermore, it should be able to provide sufficient extrapolating behaviour and, therefore, a wide range of applicability. The determination of the (adjustable) parameters C_i and D_j of the model is categorized into a two-step regression analysis. In the first step, W is set equal to 0 and the regression is carried out in order to determine the contributions C_i of the first-order groups. In the second step, W is set equal to 1 and the contributions D_j of the second-order groups are estimated through regression. Thus, the contribution of the first-order groups is independent of that of the second-order groups and the contribution of the second-order groups serves as a correction to the first-order approximation.

5.3. Calculation of the Molecular Parameters for Panayiotou and Vera EoS through Group Contributions for Pure Component:

Group Contribution Method [GCM] can be employed to study a particular thermodynamic property based on the chemical structure. Moreover, it depends mainly on molecular parameters. The molecular parameters contribute to solving EoS.

High [14] developed the molecular parameters, ϵ_{11h} , ϵ_{11s}, and v_1^* of Panayiotou and Vera. However, instead of adjusting three parameters, High has adjusted four parameters: $\epsilon_{11,300\,K}$, $\epsilon_{11,400\,K}$, $v^*_{1,300\,K}$, and $v^*_{1,400\,K}$ by using a linear expression in the range of 300 K to 400 K.

Furthermore, High has expanded v_1^* by adding the temperature used a group contribution expression for calculating all groups of component 1 at 300K and 400K. Whereas Panayiotou and Vera assumed v_1^* as independent parameter. v_1^* is obtained by taking the interpolation between calculated values, $v^*_{1,300}$ and $v^*_{1,400\,K}$. The value of v_1^* is modified by adding a linear expression which is used for estimating the value of v_1^* at the temperature of interest.

The molecular interaction energy between molecules of component 1,ϵ_{11} is calculated at the temperature of interest as follows:

$$\epsilon_{11} = \epsilon_{11,300\,\mathrm{K}} + \frac{(\epsilon_{11,400\,K} - \epsilon_{11,300\,K})}{100}(T - 300) \qquad \text{[Linear]} \qquad (5.3.1)$$

$\epsilon_{11,300}$, $\epsilon_{11,400}$ are the interaction energy between molecules at 300K and 400K, respectively.

The group contribution expression for calculating the interaction energy between molecules at 300K and 400K, as follows:

$$\epsilon_{11,T} = \sum_k \sum_m \Theta_k^{(1)} \Theta_m^{(1)} \left(e_{kk,T}\, e_{mm,T}\right)^{1/2} \qquad (5.3.2)$$

$\sum_k \sum_m$ are the summations of all groups of a certain compound and presence.

$e_{kk,T}$ is an interaction energy constant of group k at 300K and 400K.

The surface area fraction of group k in the pure component 1 at group k is defined by:

$$\Theta_k^{(1)} = \frac{n_k^{(1)} Q_k}{\sum_p n_p^{(1)} Q_p} \tag{5.3.3}$$

$n_k^{(1)}$ denotes the number of group k in component 1, $\Theta_k^{(1)}$ is the surface area fraction of group k in component 1, Q_k is the dimensionless surface area parameter of group k as utilized in the UNIFAC method [32].

The molecular reference volume of component 1, v_1^* is estimated at the temperature of interest from the following:

$$v_1^* = v_{1,300\,\mathrm{K}}^* + \frac{(v_{1,400\,K}^* - v_{1,300\,K}^*)}{100}\ (T - 300) \quad \text{[Linear]} \tag{5.3.4}$$

$$v_{1,\mathrm{T}}^* = a_T + \sum_k n_k^{(1)}\ R_{k,\mathrm{T}} \tag{5.3.5}$$

$v_{1,300\,K}^*, v_{1,400\,K}^*$ are the molecular reference volume of component 1 at 300K and 400K, respectively.

a_T is universal constant which is added to maintain the calculation. It can be noted that High had chosen 0.021231 for a_{300} and 0.022373 for a_{400}.

$R_{k,T}$ is the molecular reference volume constant of group k at 300K and 400K.

[Lee and Danner] [5] have developed (Eq.5.3.4) by eliminating the universal constant, a_T from (Eq.5.3.5) because it does not make a significant change in the result. Additionally, (Eq.5.3.4) is no longer linear.

The molecular reference volume of a pure component i, v_i^* as follows:

$$v_i^* = \sum_k n_k^{(i)} R_k \tag{5.3.6}$$

The molecular group reference volume of k, R_k has been replaced of being parameter in (Eq.5.3.5) to a variable in (Eq.5.3.7) as follows:

$$R_k = \frac{1}{10^3}\left[R_{0,k} + R_{1,k}\left(\frac{T}{T_0}\right) + R_{2,k}\left(\frac{T}{T_0}\right)^2\right] \quad \text{[Quadratic]} \tag{5.3.7}$$

where T_0 is arbitrarily set to 273.15 K.

$R_{0,k,}R_{1,k\,,}R_{2,k}$ are the molecular reference volume constants of group k.

The molecular interaction energy between molecules of component i, given by:

$$\epsilon_{ii} = \sum_k \sum_m \Theta_k^{(i)}\Theta_m^{(i)}(e_{kk}\, e_{mm})^{1/2} \qquad (5.3.8)$$

Lee and Danner [5] have modified, $e_{kk,T}$ from constant to variable, [see Eq.5.3.2 & Eq. 5.3.9], as follows:

$$e_{kk} = e_{0,k} + e_{1,k}\left(\frac{T}{T_0}\right) + e_{2,k}\left(\frac{T}{T_0}\right)^2 \qquad \text{[Quadratic]} \qquad (5.3.9)$$

$e_{0,k,}e_{1,k\,,}e_{2,k}$ are the molecular interaction energy constants of group k.

Table 5.1 and 5.2 subgroups were retrieved from the paper of Lee and Danner [5] and the handbook of Danner and High [15] for the purpose of using them at present work, respectively.

$R_{0,k,}R_{1,k\,,}R_{2,k}$ in [Eq.5.3.7], and $R_{k,300K}$, $R_{k,400K}$ in [Eq.5.3.4] are estimated by the best fitting to the liquid density of the Daubert and Danner experimental data [34].

$e_{0,k,}e_{1,k\,,}e_{2,k}$ in [Eq.5.3.9] and $e_{k,300K}$, $e_{k,400K}$ in [Eq.5.3.1] are estimated by the best fitting to the vapor pressure of the Daubert and Danner experimental data [34].

TABLE 5.1

Group Interaction Energy and Reference Volume Parameters [Linear]

Group	$e_{kk,300}$	$e_{kk,400}$	$R_{k,300}$	$R_{k,400}$	Q_k
CH3	640.87	640.79	0.01596	0.01628	0.848
CH2	943.33	987.68	0.01522	0.01518	0.540
C	5378.38	7731.24	0.00854	0.00762	0.150
ACH	975.38	971.62	0.01054	0.01035	0.400
AC	5452.73	6771.48	0.00623	0.00680	0.120
AC-CH3	994.41	1022.68	0.02465	0.02456	0.968
AC-CH	2780.93	3281.53	0.02733	0.02643	0.348
-COO-	1341.67	1308.80	0.02236	0.02327	0.880
-OH	1867.92	1466.87	0.00685	0.00752	1.200
-O-	868.47	679.56	0.00670	0.00606	0.240

TABLE 5.2

Group Interaction Energy and Reference Volume Parameters [Quadratic]

Main group	subgroup	e_0	e_1	e_2	R_0	R_1	R_2	Q_k
CH2	**CH3**	642.019	10.186	-4.817	25.979	-0.388	0.814	0.848
	CH2	919.390	-67.757	78.384	14.089	2.039	-0.963	0.540
C	**C**	1480.016	1125.680	1967.093	-11.793	7.681	-5.795	0.150
ACH	**ACH**	1132.433	-209.906	78.217	12.189	1.834	-0.389	0.400
ACCH2	**ACCH3**	959.652	-11.693	33.812	26.370	3.136	-1.092	0.968
	ACCH	2134.993	-232.701	560.421	2.933	7.462	-4.174	0.348
COO	**COO**	2182.434	-782.011	226.335	14.091	10.712	-3.344	0.880
OH	**OH**	9229.525	-7980.168	2105.795	4.862	14.325	-3.989	0.584
CO2	**CO2**	570.152	149.875	-49.995	8.808	33.2832	-9.353	1.112

5.4. Calculation of the Molecular Parameters through Group Contributions for Mixtures:

[High and Danner] [8] has used a geometric mixing rule for calculating the interaction energy between unlike molecules, ϵ_{ij} , as follows:

$$\epsilon_{ij} = \left(\epsilon_{ii}\ \epsilon_{jj}\right)^{1/2} \tag{5.4.1}$$

$$\delta_{ij}=0 \qquad \text{[MR0]} \tag{5.4.2}$$

where ϵ_{ii} is the molecular interaction energy between like molecules of type i.

Lee and Danner [5] have developed a binary mixing rule, as follows:

$$\epsilon_{ij} = \left(\epsilon_{ii}\ \epsilon_{jj}\right)^{1/2}\ (1-\ \delta_{ij}) \tag{5.4.3}$$

$$\delta_{ij} = \sum_m\ \sum_n\ \Theta_m^{(M)}\Theta_n^{(M)}\alpha_{mn} \qquad \text{[MR1]} \tag{5.4.4}$$

Where α_{mn} is a binary interaction parameter between m group and n.

$$\Theta_k^{(M)} = \frac{\sum_i n_k^{(i)} Q_k}{\sum_p \sum_i n_p^{(i)} Q_p} \tag{5.4.5}$$

where $\Theta_k^{(M)}$ is the surface area fraction of all the groups present in the mixture.

[Hamedi and co-workers] [10] have proposed an alternative mixing rule that can handle more than one mixture instead of a binary mixture [see Eq.5.4.4], an example is a triple-mixture, as follows:

$$\delta_{ij} = \sum_m\ \sum_n\ \Theta_m^{(i)}\Theta_n^{(j)}\alpha_{mn} \qquad \text{[MR2]} \tag{5.4.6}$$

$$\Theta_k^{(i)} = \frac{n_k^{(i)} Q_k}{\sum_p n_p^{(i)} Q_p} \tag{5.4.7}$$

where $\Theta_k^{(i)}$ is the surface area fraction of group k in component i.

The molecular reference volume of a mixture, v^* as follows:

$$v^* = \sum x_i\ v_i^* \tag{5.4.8}$$

Where x_i is the mole fraction of component i.

Table 5.3 illustrates the parameters of group interaction. The binary interaction parameter was predicted independently of temperature by the best fitting of bubble point and dew point for the temperature and pressure, and then compared to experimental data of DECHEMA [35-40].

Table 5.3

Group Binary Interaction Parameters (α_{mn}) [Quadratic]

m\n	CH2	C	ACH	ACCH2	COO	OH	CO2 [MR1]	CO2 [MR2]
CH2	0.0000	0.2033	0.0363	-0.0064	0.0211	0.3994	0.1262	0.2994
C		0.0000	0.0202	-0.3946	0.0000	1.2601	0.0000	0.0000
ACH			0.0000	0.0116	-0.1408	0.1031	0.1130	0.2483
ACCH2				0.0000	0.0415	0.3770	0.0027	0.0278
COO					0.0000	-1.4501	-0.1850	-0.4739
OH						0.0000	0.0000	0.0000
CO2 [MR1]							0.0000	0.0000
CO2 [MR2]								0.0000

Lee and Danner have mentioned that there was not adequate binary VLE data available to calculate values for all the subgroups. Thus, as in the UNIFAC method, values were obtained only for the main groups as defined in Table 5.2. The group binary interaction parameters, α_{mn} , are given in Table 5.3 The group binary interaction parameters between like groups, α_{mm}, are set to zero and α_{mn} is equal to α_{nm}.

Chapter 6

NONEQUILIBIRUM LATTICE FLUID [NELF]

6. NELF Model for Gas Solubility in Glassy Polymers:

6.1. Early Version:

The nonequilibrium thermodynamics of glassy polymers (NET-GP) was proposed by [Doghieri and Sarti] [11]. NET-GP approach extends EoS description of thermodynamic properties of amorphous phase from equilibrium conditions above glass transition temperature (T_g) to non-equilibrium conditions below (T_g). NET-GP can be applied to any EoS by using the properties and tools of the equation of state. NELF approach can be used for the equilibrium of Helmholtz Free Energy Density, a^{Eq}, as follows:

$$a^{Eq} = a^{Eq}\left(T, P, \{\rho_i\}_{i=1,N_c}\right) \qquad 1 \le i \le N_c \qquad (6.1.1)$$

Where T is the temperature of the system, ρ_i is the species mass density of all solute components $(1 \le i \le N_s)$ and polymeric species $(i = N_c)$.

The main idea of the NET- GP is by assuming the mass density of the polymeric species in the mixture $\left(\rho_{pol}^{NE}\right)$ as an order parameter for the description of the nonequilibrium state at a certain temperature, T and pressure, p and the mass fraction of low molecular weight solutes in the mixture, ω_i. Helmholtz free energy can then be considered at nonequilibrium condition, as follows:

$$a^{NE} = a^{NE}\left(T, p, \omega_i^{NE}, \rho_p\right) \qquad 1 \le i \le N_s \qquad (6.1.2)$$

[Doghieri and Sarti] [11] have assumed the mass density of the polymer as an internal state variable (its rate of variation in time depends on the state of the system). By applying the second law of thermodynamic.

The following condition is derived for Helmholtz free energy density in non-equilibrium conditions, as follows:

$$a^{NE} = a^{Eq}\left(T, p, \omega_i^{Eq}, \rho_p\right) \qquad 1 \le i \le N_s \qquad (6.1.3)$$

This approach can be applied parallelly to thermodynamic expression of the chemical potential of solutes in the mixture at non equilibrium state, μ_i^{NE}, as follows:

$$\mu_i^{NE} = \mu_i^{NE}(T, p, \omega_i, \rho_{pol}) = \mu_i^{Eq}(T, P, \rho_i) \quad (6.1.4)$$

The later assumption for the evaluation of solubility in glassy polymers that has been accounted a swelling coefficient, k_{sw} as an adjustable parameter, as follows:

$$\rho_{pol}^{PE}(T, f_i(T, p, \omega_i)) = \rho_{pol}^{0}(T)\left[1 - \left(k_{sw}\, f_i(T, p)\right)\right] \quad (6.1.5)$$

where ρ_{pol}^{PE} is the density of solvent per polymer mass at nonequilibrium condition, and $\rho_{pol}^{0}(T)$ is the dry polymer density that has been taken from the experimental data.

6.2. Recent Version:

[Minelli and Doghieri] [41] developed a rheological tool by addressing the polymer behaviour in a sorption experiment below the glass transition temperature. A simplification of the spectrum of relaxation times in which the distribution is considered to be bimodal with a constant ratio between ("hard" and "soft" element).

Parallelly, it can calculate the total volume of mixture per polymer mass at nonequilibrium condition (pseudo equilibrium), as follows:

$$\hat{V}_{pol}^{NE}(T, p, \omega_1^{NE}) = \chi\, \hat{V}_{pol}^{Eq}(T, p, \omega_1^{Eq}) + (1 - \chi)\, \hat{V}_g(T) \quad (6.2.1)$$

$$\chi = \frac{k_G}{k_R} \quad (6.2.2)$$

where $\hat{V}_{pol}^{Eq}(T, p, \omega_1^{Eq})$ is the total volume per polymer mass at equilibrium condition at specific temperature, pressure, and mass fraction of solute, χ is the compressibility ratio between glass region

and rubber and k is the compressibility coefficient; the partial derivative of specific volume with respect to pressure, p at constant temperature, T multiplies by the negative reciprocal of the average volume, and $\hat{V}_g(T)$ is a model parameter depends only on temperature.

The specific volume of a pure polymer at equilibrium, $\hat{V}_{poly}^{Eq^0}$ can be calculated after an equilibrium EoS. $\hat{V}_{poly}^{0}$ is meant as the dry polymer mass density at non-equilibrium glassy state, can be estimated from literature data, using the following expression:

$$\hat{V}_{poly}^{0}(T, p \cong 0) = \hat{V}_{poly}^{Eq^0}(T_g, p \cong 0) \times [1 + \alpha_g \times (T - T_g)] \quad (6.2.3)$$

$$\alpha_G = \frac{1}{\hat{V}}\left(\frac{\partial \hat{V}}{\partial p}\right)_T \quad (6.2.4)$$

α_G is the thermal expansion coefficient; the partial derivative of specific volume with respect to temperature, T at constant pressure, p, multiplied by the reciprocal of the average volume.

Chapter 7

NELF AND GCLF COMBINATION [NEGCLF-EOS]

7.1. Introduction to NEGCLF-EOS:

At present work, a predictive tool has been evolved that combines two models: a group contribution lattice-fluid equation of state (GCLF-EoS) and nonequilibrium lattice fluid (NELF); the group contribution method depends mainly on the chemical structure. As a result of this combination, a new model is produced that is referred to as "nonequilibrium group contribution lattice fluid" model (NE-GCLF). NE-GCLF model is designed to be applied based on a minimum number of properties as inputs, to study thermodynamic properties such as the solubility of gas/vapour into glassy polymers.

The polymer properties that are required for the application of NE-GCLF procedure are glass transition temperature,T_g ,compressibility ratio,χ ,chemical structure of polymer and the ratio of the thermal expansion coefficient from the glassy to rubbery state, γ.

Obviously, the group interaction energy parameters [$e_{0,k}$, $e_{1,k}$, $e_{2,k}$], reference volume parameters [$R_{0,k}$, $R_{1,k}$, $R_{2,k}$] and the surface area parameter, Q_k need also to be known for all functional groups participating to polymer and solvent structure.

The compressibility ratio of polymer, the glass transition temperature and the ratio of the thermal expansion coefficient properties are used in NELF for calculating the total volume per polymer mass at nonequilibrium condition (glassy state), $\hat{V}_{poly}^{NE}$.

The chemical structure is composed of groups and contributes to counting the number of the molecular reference volume of a certain component.

The thermal expansion coefficient is used at present work because the temperature of the system is lower than the glass transition temperature, as follows:

$$\alpha_g(p \cong 0) = \alpha^{EoS}\,\gamma \tag{7.1.1}$$

$$\gamma = \left(\frac{\alpha_G}{\alpha_R}\right) \tag{7.1.2}$$

γ is the estimated ratio of the thermal expansion coefficient from the glassy to rubbery state. The availability of the ratio at (Eq.7.1.1) because the calculated thermal expansion coefficient at nonequilibrium condition using EoS, α^{EoS} must get a bit closer to the thermal expansion coefficient at rubbery state, α_R , that is measured experimentally.

In order to study the solubility of penetrant species into solid polymers, the chemical potential of component 1 into mixtures, μ_1 at temperature, T, mass fraction of component 1 into mixture at nonequilibrium condition, ω_1^{NE}, and the total volume per polymer mass at nonequilibrium condition, $\hat{V}_{pol}^{NE}$ must be equal to the chemical potential of a pure component 1, $\mu_1^{(G)}$, as follows:

$$\mu_i\left(T, \omega_1^{NE}, \hat{V}_{pol}^{NE}\right) = \mu_1^{(G)}(T, p) \tag{7.1.3}$$

The total volume per polymer mass, $\hat{V}_{pol}^{NE}$ is calculated by substituting (Eq.6.2.3) in (Eq.6.2.1), as follows:

$$\hat{V}_{pol}^{NE}(T, p, \omega_1^{NE}) = \chi\, \hat{V}_{pol}^{Eq}\left(T, p, \omega_1^{Eq}\right) + (1 - \chi)\, \frac{\hat{V}_{poly}^{0}(T, p \cong 0) - \chi\, \hat{V}_{poly}^{Eq^0}(T, p \cong 0)}{(1 - \chi)} \tag{7.1.4}$$

Where $\hat{V}_{Poly}^{0}(T, p \cong 0)$ is the specific volume of polymer at system temperature and low pressure at nonequilibrium condition (glassy state) and $\hat{V}_{poly}^{Eq^0}(T, p \cong 0)$ is the specific volume of polymer at system temperature and low pressure at equilibrium condition (rubbery state) which is calculated by solving EoS of a pure component from (Eq.4.1.6) which satisfies the equilibrium condition of known pressure, as follows:

$$p = p^{Eq}\left(T, \omega_2 = 1, \hat{V}_{poly}^{Eq^0}(T, p \cong 0)\right) \tag{7.1.5}$$

ω_2 denotes the mass fraction of a pure polymer.

The equation of the specific volume of polymer at nonequilibrium condition (glassy state), $\hat{V}_{poly}^{0}(T, p \cong 0)$, (Eq.6.2.3) is substituted in (Eq.7.1.4), as shown:

$$\hat{V}_{pol}^{NE}(T, p, \omega_1^{NE}) = \chi\, \hat{V}_{pol}^{Eq}\left(T, p, \omega_1^{Eq}\right) + \hat{V}_{poly}^{Eq^0}\left(T_g, p \cong 0\right)\left[1 + \alpha_g\left(T - T_g\right)\right] - \chi\, \hat{V}_{poly}^{Eq^0}(T, p \cong 0) \tag{7.1.6}$$

The expression of thermal expansion coefficient, α_g , (Eq.7.1.1-2) is substituted in (Eq.7.1.6), as shown:

$$\hat{V}_{pol}^{NE}(T,p,\omega_1^{NE}) = \chi\,\hat{V}_{pol}^{Eq}\left(T,p,\omega_1^{Eq}\right) + \hat{V}_{Poly}^{Eq^0}\left(T_g\,,p\cong 0\right)\left[1+\alpha^{EoS}\left(\frac{\alpha_G}{\alpha_R}\right)\left(T-\ T_g\right)\right] -$$

$$\chi\,\hat{V}_{poly}^{Eq^0}(T,p\cong 0) \qquad (7.1.7)$$

The total volume per polymer mass, $\hat{V}_{poly}^{Eq}$ at temperature, T, pressure, p, mass fraction of component 1 into mixture at equilibrium condition, ω_1^{Eq} , is calculated by solving EoS of a mixture from (Eq.4.2.16), as follows:

$$p = p^{Eq}\left(T,\omega_1^{Eq},\hat{V}_{poly}^{Eq}\left(T,p,\omega_1^{Eq}\right)\right) \qquad (7.1.8)$$

The chemical potential of component 1 into mixtures, μ_1 at temperature, T, equilibrium mass fraction of component 1 into mixture, ω_1^{Eq} and the total volume per polymer mass, $\hat{V}_{pol}^{Eq}$ must be equal to the chemical potential of a pure component 1 , $\mu_1^{(G)}$, as follows:

$$\mu_i\left(T,\omega_1^{Eq},\hat{V}_{pol}^{Eq}\left(T,p,\omega_1^{Eq}\right)\right) = \mu_1^{(G)}(T,p) \qquad (7.1.9)$$

7.2. Solubility Prediction in Polymer-Solute Systems:

To proceed in the calculation, it is essential to express the first case of mixing rule that requires to estimate a linear expression for ϵ_{11} which is a function of two variables $\epsilon_{11,300\,K}$ and $\epsilon_{11,400\,K}$. The two variables are calculated from (Eq.5.3.2). The surface area fraction of group k of component 1, $\Theta_k^{(1)}$ which is a function of ϵ_{11} , it can be estimated by (Eq.5.3.3). The surface area parameter of group k, Q_k and the two constants $e_{\mathrm{kk,300K}}$ and $e_{\mathrm{kk,400K}}$ are retrieved from Table 5.1.

First case, v_1^* is represented in a linear expression as function of two variables $v_{1,300K}^*$ and $v_{1,400K}^*$, [see Eq.5.3.4]. The two variables $v_{1,300K}^*$ and $v_{1,400K}^*$ are calculated from a group contribution expression that is given in (Eq. 5.3.5) and the two constants $R_{k,300K}$ and $R_{k,400K}$ are retrieved from Table 5.1.

Second case, the molecular interaction energy between two components i and j, ϵ_{ij} which requires to estimate a binary interaction variable δ_{ij} that is illustrated in mixing rule 1 [MR1], [see Eqs. 5.4.3-4]. e_{kk} is a function of the molecular interaction energy variable between like groups that can be calculated quadratically by (Eq.5.3.9). The constants of energy ($e_{0,k}$, $e_{1,k}$, $e_{2,k}$) are retrieved from Table 5.2. One more variable, $\Theta_k^{(M)}$ is estimated by (Eq.5.4.5) and the surface area group parameter, Q_k [that is requested to calculate $\Theta_k^{(M)}$] is retrieved from Table 5.2.

The calculation of δ_{ij} for the third case MR2 is similar to MR1 excluding the variable $\Theta_k^{(i)}$ that can be estimated by (Eq.5.4.7). The expression of v_{i}^* that follows Lee and Danner approach is a function of molecular reference volume variable of group k as shown in (Eq.5.3.6) that can be calculated quadratically from (Eq.5.3.7). The contents of reference volume for a group k, ($R_{0,k}$, $R_{1,k}$, $R_{2,k}$) can be retrieved from Table 5.2.

Table 7.1 shows the five different types of the polymers (PEMA, PMMA, PC, PS, PPO) that are used at this work. It also illustrates the properties of polymers such as the ratio of thermal expansion coefficient from glassy to rubbery state which retrieved from [Zoller] [42], compressibility factors, and the glass transition temperature of each polymer were retrieved from different references.

Table 7.1

The Properties of Polymers

Polymers	$\left(\frac{\alpha_G}{\alpha_R}\right)$	**Ref.**	**χ**	**Ref.**	**T_g [°C]**	**Ref.**
PEMA	0.57	[42]	0.83	[41]	61	[43]
PMMA	0.45		0.69	[49]	120	[44]
PC	0.43		0.69	[41]	150	[41]
PS	0.42		0.68	[41]	92	[41]
PPO	0.27		0.46	[52]	210	[45]

7.3. Results and discussion for solubility prediction in glassy polymers:

7.3.1. Solubility Prediction in Poly (methyl methacrylate) + CO2 system:

Koros et al.[44] investigated the sorption of carbon dioxide (CO_2) in poly(methyl methacrylate) (PMMA) at various temperatures experimentally, the polymer utilized in his study was earned from Aldrich Chemical Co., Milwaukee, WI. Koros measured the molecular weight of the PMMA using solution viscosity in butanone and found it to be equivalent to 599,000 g/mole. Koros measured the sorption isotherms after such pre-treatments were reproducible as long as the maximum sorption never exceeded 20 atm. Compressibility parameter, χ was not available in the Koros et al. paper [44]. Thus, it has been retrieved from Minelli and Doghieri paper [49]. (Eqs.7.1.1-2) were applied for estimating the PMMA ratio of thermal expansion coefficient from glassy to rubbery state, which is equivalent to 0.45 [Zoller][42].

At this system, it has been applied (Eq.5.4.1) for the first case [mixing rule 0, MR0]. For the second case, [mixing rule 1, MR1] was applied for calculating δ_{12} using EoS, registered value of the MR1 equals to 0.0205 and 0.0772 for the mixing rule 2 [MR2] as a third case.

It could be noted that the surface area parameter, Q_k is equivalent to 1.200 for ester group (-COO-) as it was published by [Danner and High] [15], however, this value was in contrary to Fredenslund [1] Q_k which is equivalent to 0.880. Therefore, the value that was published by Fredenslund has been selected. There was not available group interaction energy and reference volume parameters for CO2 as shown in Table 5.1. Thus, it has been taken the constants of group interaction energy and reference volume ($e_{0,k}$, $e_{1,k}$, $e_{2,k}$, $R_{0,k}$, $R_{1,k}$, $R_{2,k}$) that are shown in Table 5.2 for calculating CO2 considering all cases [MR0, MR1, MR2].

Koros et al.' experimental data expressed the solubility of carbon dioxide (CO2) in poly (methyl methacrylate) (PMMA) at various pressures for different temperatures. Fig. 7.1.A shows the predicted results from the NEGCLF model at both cases [MR1, MR2]. They succeeded in general term but failed in the temperature range compared to experimental data. In addition, both cases exhibited the same result at low pressure because they have the same properties. Fig. 7.1.B shows a quite similar trendlines for the case [MR0]. However, mixing rule 1 is remained the best.

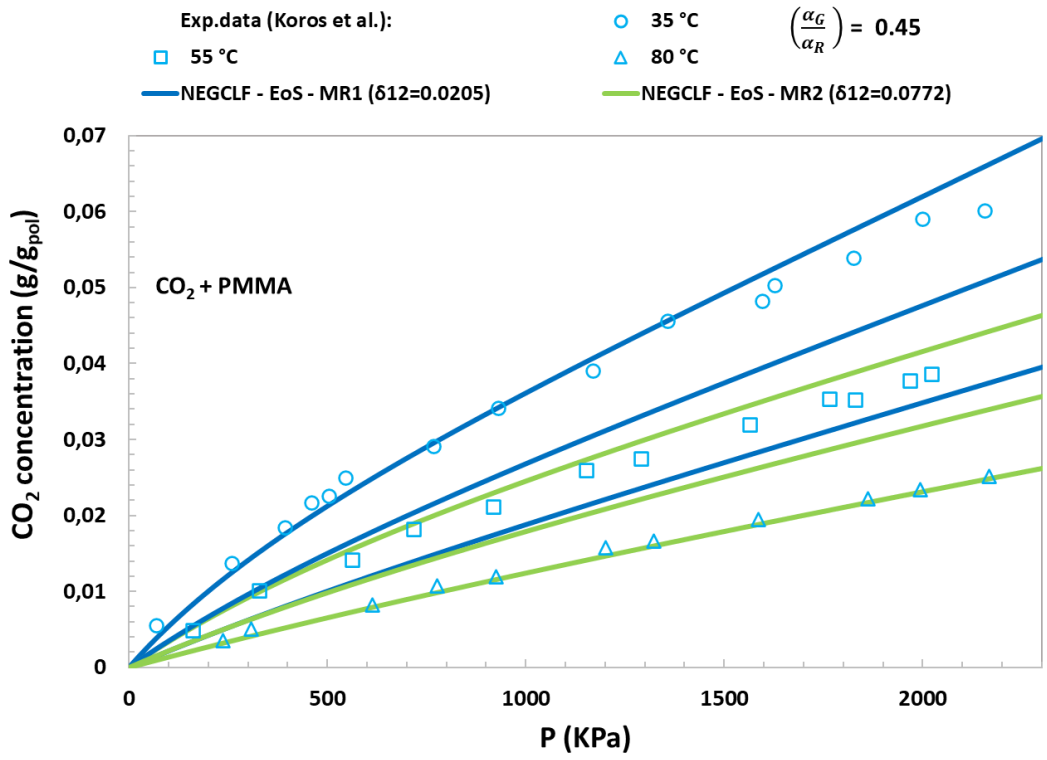

Fig 7.1.A. Solubility isotherm of CO2 in PMMA at 35, 55 and 80°C: experimental data from ref 44 and predictions given by GCLF EoS and NELF model.

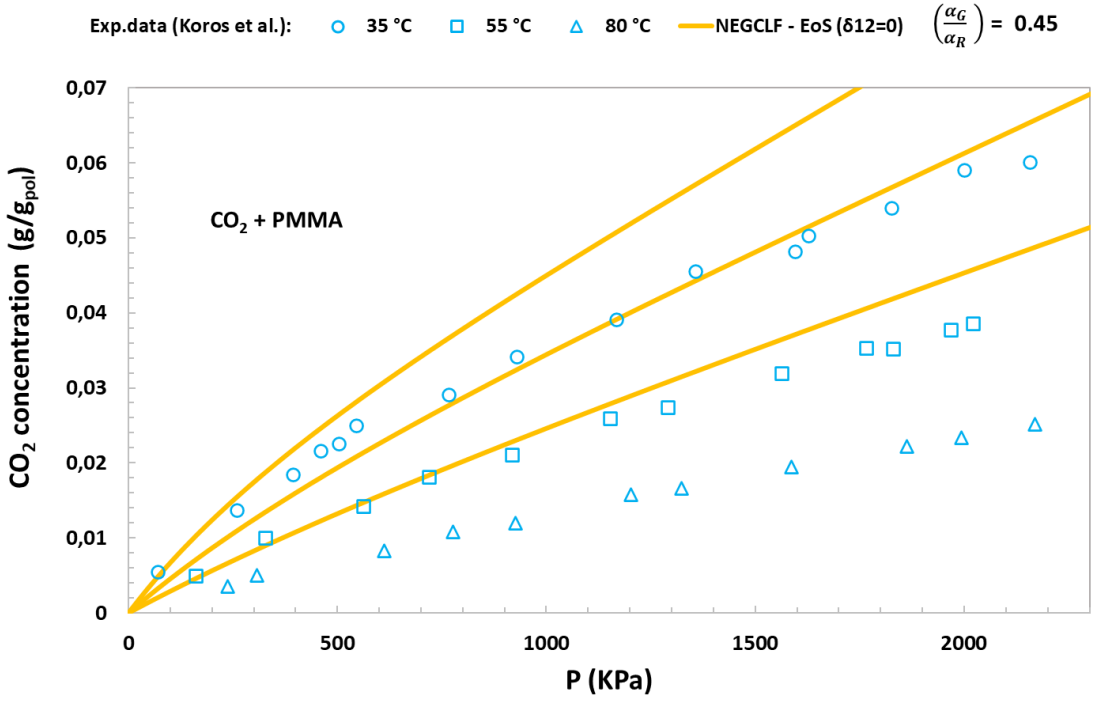

Fig. 7.1.B. Solubility isotherm of CO2 in PMMA at 35, 55 and 80°C: experimental data from ref 44 and predictions given by GCLF EoS and NELF model.

7.3.2. Solubility Prediction in Poly (ethyl methacrylate) + CO2 system:

Kamiya et al [43] have prepared poly (ethyl methacrylate) (PEMA) by radical polymerization, the glass transition temperature T_g was 61°C that was determined by taking the average of several methods: thermal dilation, the Arrhenius plot of gas permeability, and evaluated by differential scanning calorimetry (DSC). Kamiya and co-workers have determined sorption under pressure up to 50 atm in the temperature range 15 to 85°C and measured with an electric microbalance (Cahn model 2000) settled in a high-pressure chamber [50,51]. The molecular weight of PEMA was not available in the paper of Kamiya et al. Thus, the value was taken from Koros et al. paper [44] which is equivalent to 309,000 g/mole. The compressibility parameter, χ was not available in the Kamiya et al paper. Therefore, it has been retrieved from Minelli and Doghieri paper [41]. (Eqs.7.1.1-2) were applied for estimating the PEMA ratio of the thermal expansion coefficient from glassy to rubbery state, which is equivalent to 0.57 [Zoller] [42].

At this system, it has been used (Eq.5.4.1) for the first case [MR0] and for the second case, it has been applied [MR1] for calculating δ_{12} using EoS which is equivalent to 0.0188 and 0.1088 for [MR2] as a third case. Similar to the previous case, the surface area parameter, Q_k for ester group (-COO-) is equal to 0.880 and it has been used a quadratic expression for calculating the properties of CO2 for all three cases: [MR0, MR1, MR2].

Fig. 7.2.A-B show the prediction of CO2 solubility in PEMA for the three cases: MR0, MR1, and MR2. Fig. 7.2.A represents the ability of the model to predict the volume of CO2 in the mixture per polymer mass. Fig. 7.2.B expressed linear trendlines compared to PMMA due to the glass transition temperature closeness to the predicted temperatures.

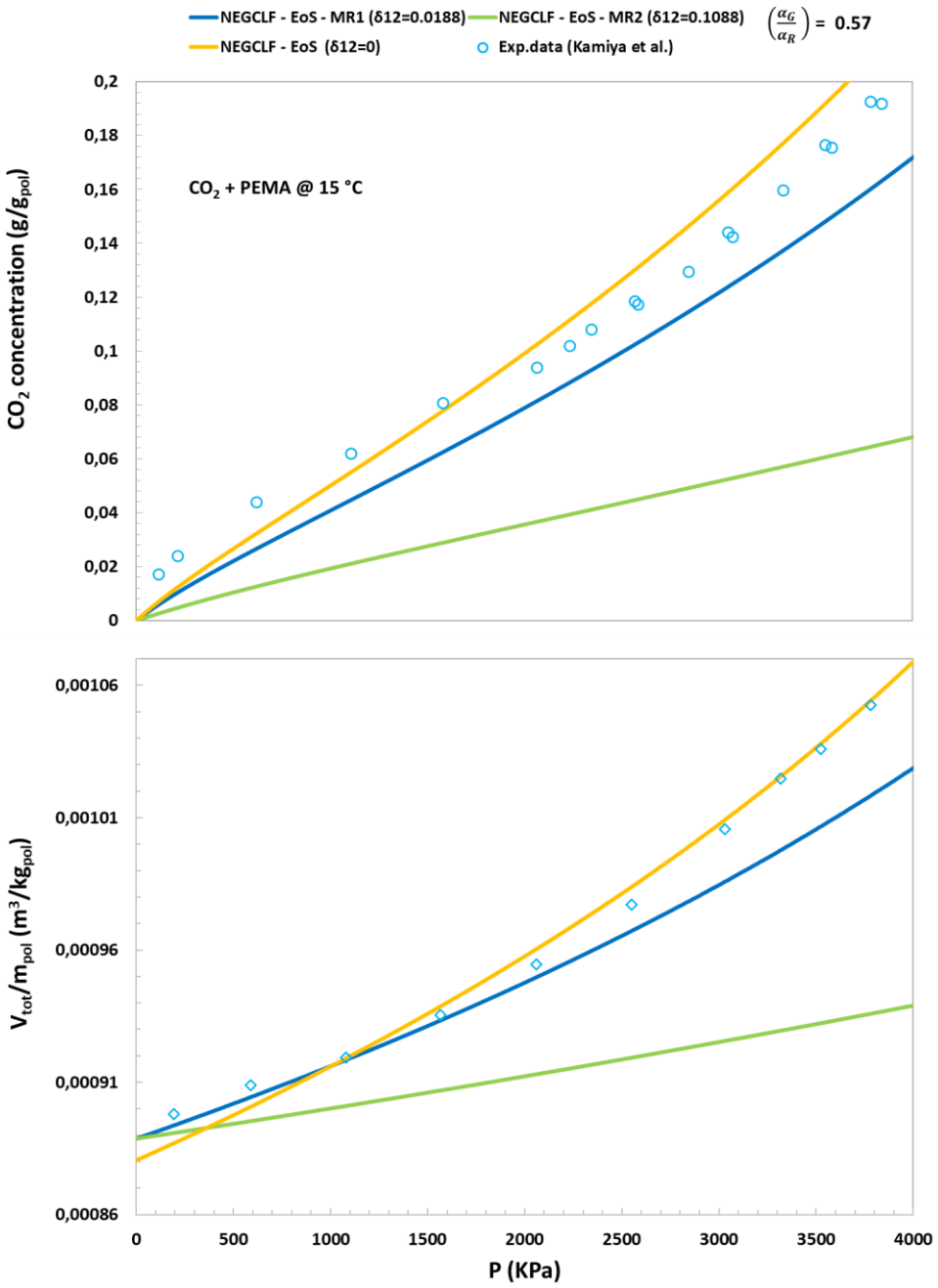

Fig. 7.2.A. Solubility and volume swelling isotherm of CO2 in PEMA at 15 °C: experimental data from ref 43 and predictions given by the GCLF EoS and NELF model.

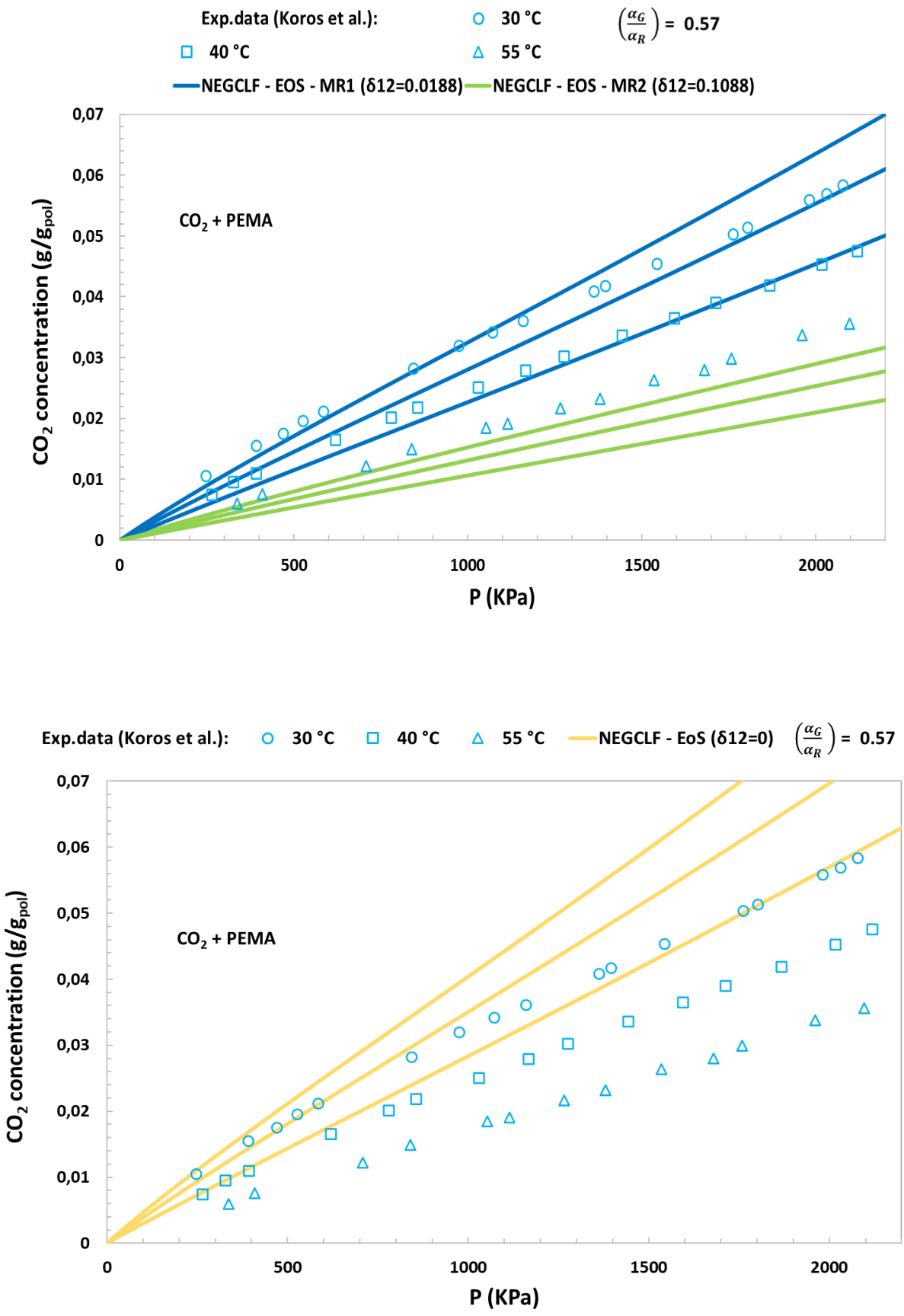

Fig 7.2.B. Solubility isotherm of CO2 in PEMA at 30, 40 and 55°C: experimental data from ref 44 and predictions given by GCLF EoS and NELF model.

7.3.3. Solubility Prediction in Polycarbonate + CO2 system:

[Fleming and Koros] [52] applied 1000 psia of pressure for the measurement of carbon dioxide (CO_2) sorption in polycarbonate at 35°C and it has been indicated that the isothermal dilatometry measurements exposure of polycarbonate. The measurement of pure gas sorption was made with a pressure decay cell design. Fleming and Koros did not mention the molecular weight. Therefore, it has been assumed [Mn=110000]. (Eqs.7.1.1-2) were applied for estimating the PC ratio of the thermal expansion coefficient from glassy to rubbery state which is equivalent to 0.43 [Zoller] [42]. Similar to the previous cases, it has been used the quadratic expression for calculating the properties of CO2 for the case of MR0 due to the lack of parameters in Table 5.1. Furthermore, there was not available ether group (-O-) parameters in Table 5.2 for the calculating the value of e_{kk} and R_k quadratically for both cases [MR1, MR2]. Thus, it has been utilized the parameters $e_{kk,300K}$, $e_{kk,400K}$, $R_{k,300K}$, and $R_{k,400K}$ that available in Table 5.1 for expressing them in a linear expression. Fig. 7.3 shows a satisfactory result of the carbon dioxide solubility in polycarbonate at diverse pressures.

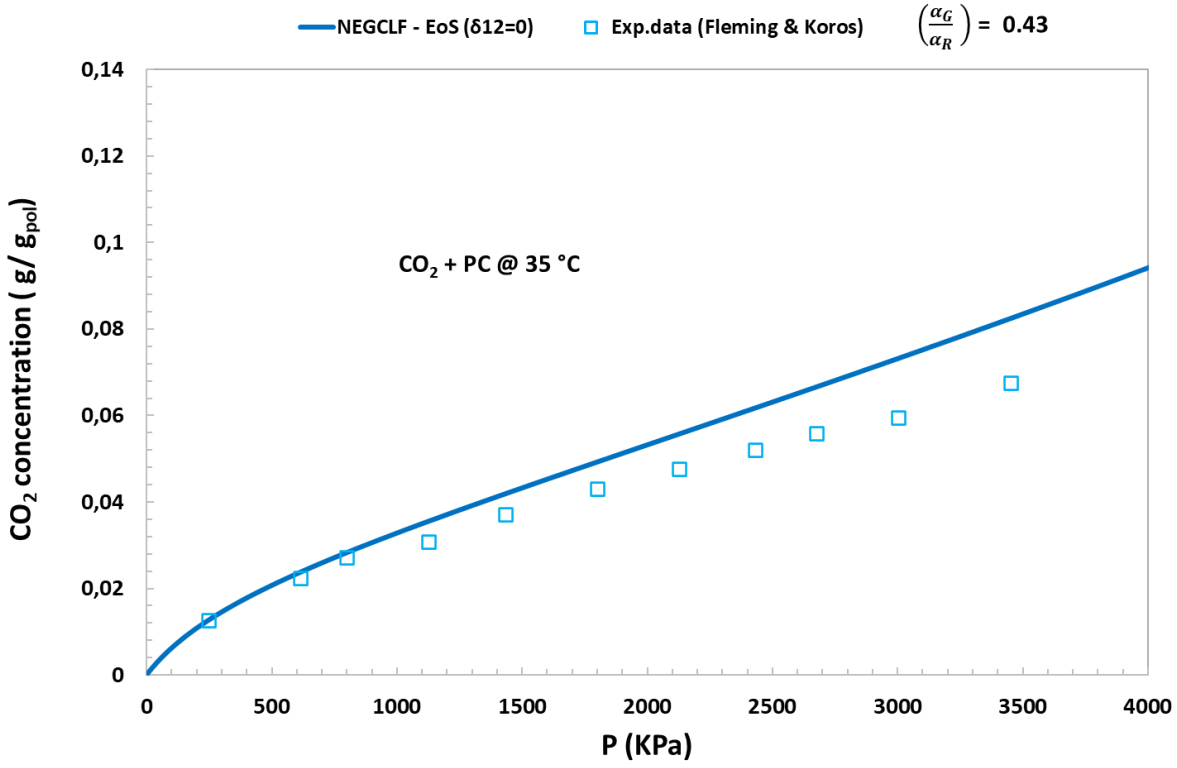

Fig. 7.3. Solubility isotherm of CO2 in PC at 35 °C: experimental data from ref 52 and predictions given by GCLF EoS and NELF model.

7.3.4. Solubility Prediction in Poly (2,6-dimethyl phenylene oxide) + CO2 system:

Chern et al. [45] measured the phase behaviour of carbon dioxide (CO_2) and poly (2,6-dimethyl phenylene oxide) (PPO) by utilizing a dual-transducer barometric device at 35°C, and the glass transition temperature, T_g equals to 210°C that was evaluated by a differential scanning calorimeter operated at 20°C heating rate. Chern did not indicate the molecular weight. Therefore, it has been presumed [Mn=110000]. Compressibility parameter, χ was not available in the paper of Chern et al [45]. Thence, it was retrieved from Minelli and Sarti paper [52]. (Eqs.7.1.1-2) were applied for estimating the PPO ratio of thermal expansion coefficient from glassy state to rubbery, which is equivalent to 0.27 [Zoller] [42]. Like the previous cases, it has been used quadratic expression for calculating the properties of CO2 for the case of MR0 due to the lack of parameters in Table 5.1 and there were not ether group (-O-) parameters for the two cases MR1, and MR2. Therefore, a linear expression has been used. Fig 6.4 illustrates the amount of carbon dioxide (CO2) sorption in poly (2,6-dimethyl phenylene oxide) (PPO) at varying pressures. It shows a good fitting to experimental data.

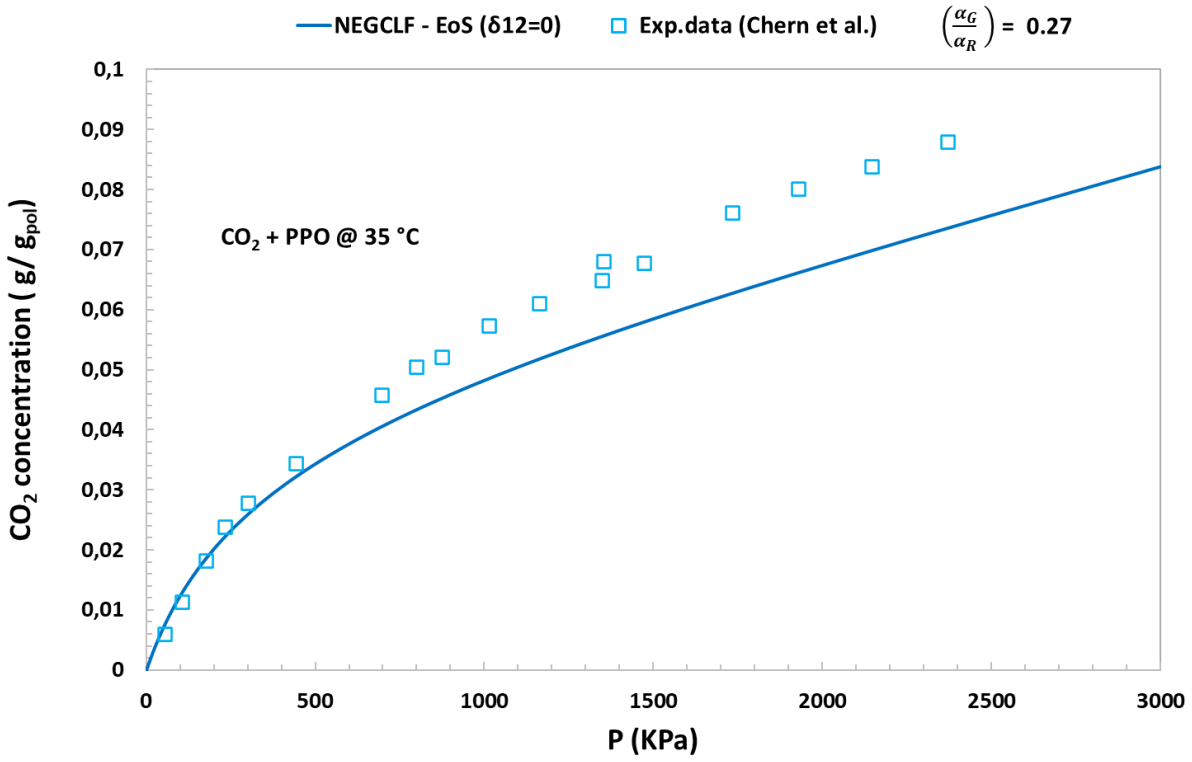

Fig. 7.4. Solubility isotherm of CO2 in PPO at 35 °C: experimental data from ref 45 and predictions given by GCLF EoS and NELF model.

7.3.5. Solubility Prediction in Polycarbonate + EtOH system:

Hwang et al. [47] measured the phase equilibrium of ethanol and polycarbonate by using a Sartorius M25D-V vacuum electro microbalance cell [MB] at 30°C, [Mn = 24000]. Glass transition temperature, T_g and compressibility, χ parameters had not been stated by Hwang et al [47]. For that reason, the two parameters have been retrieved from Minelli and Doghieri paper [41]. Similar to the previous cases, the surface area parameter, Q_k for ester group (-COO-) is equal to 0.880 and there were not available ether group (-O-) parameters for the two cases [MR1, MR2]. Thus, a linear expression has been used in MR0. Fig. 7.5 shows the activity effect of the weight concentration of ethanol in polycarbonate at diverse pressures. It does not exhibit a satisfactory result because this type of mixing rule is not good at mixing polar compound with non-polar one.

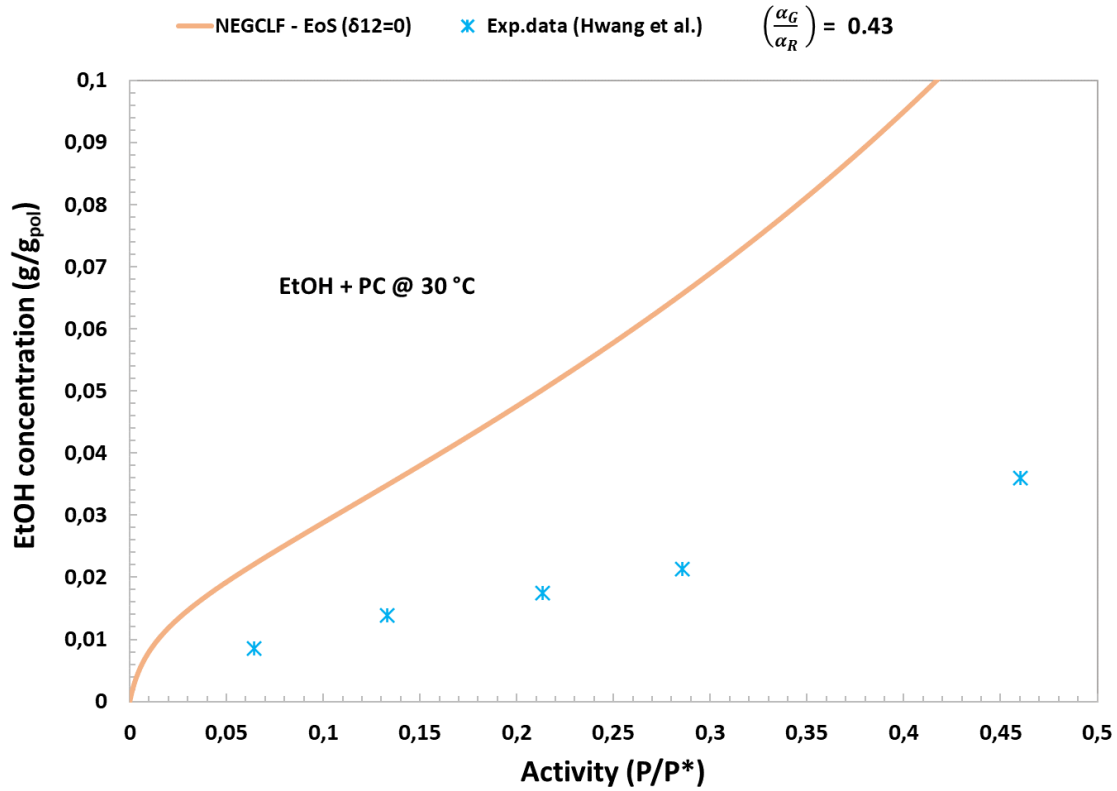

Fig. 7.5. Solubility isotherm of EtOH in PC at 30 °C: experimental data from ref 47 and predictions given by the GCLF EoS and NELF model.

7.3.6. Solubility Prediction in Polystyrene + m-xylene system:

Tsutusi et al.[48] investigated the solubility of m-xylene in atactic polystyrene (APS) at 25°C and the averaged molecular weight was [Mn = 280000]. The glass transition temperature, T_g and compressibility, χ parameters were not available in the Tsutusi et al. paper [48]. Therefore, the two values have been retrieved from [Minelli and Doghieri] paper [41]. (Eqs.7.1.1-2) were applied for estimating the PS ratio of thermal expansion coefficient from glassy to rubbery state which is equivalent to 0.42 [Zoller] [42]. It has been applied the first case of mixing rule [MR0], MR1 in which the binary interaction variable equals to 0.0110 and MR2 in which the binary interaction variable equals to 0.00744 and MR2 in which the binary interaction variable equals to 0.00744. It has also been used a direct prediction for all cases due to the availability of parameters in both Tables 5.1 and 5.2.

Fig. 7.6 illustrates the amount of m-xylene concentration in polystyrene (PS) at varied activity of pressures to m-xylene vapour pressure. Three predicted plots of the models show a quite similar trendlines. Mixing rule 1 is kept the closest one to the experimental data.

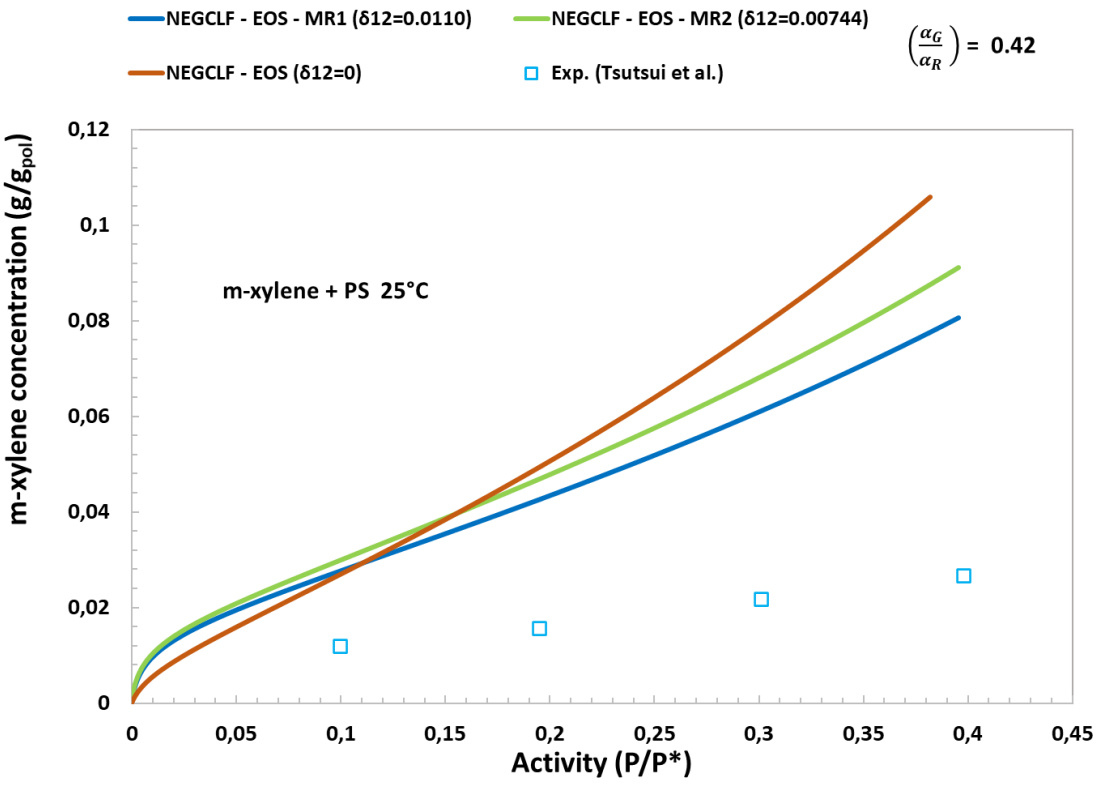

Fig. 7.6. Solubility isotherm of m-xylene in PS at 25 °C: experimental data from ref 48 and predictions given by the GCLF EoS and NELF model.

7.4. Conclusions of Solubility Part I:

GCLF EOS has been used within the NELF approach for pure prediction of gas solubility in glassy polymer and the results were compared for the use of different mixing rule for the expression of binary interaction parameter. Quantitative predictions obtained for CO2 solubility isotherm in a large pressure interval are interesting while, apparently, “mixture-based” MR1 mixing rule performed better than “component-based” MR2 mixing rule.

From the work that it has been done at the prediction of gas or vapour in glassy polymers using EoS with three different mixing rule; molecular weight does not affect mixing rule 1 [MR1] because of the interaction of molecules between segments whereas it affects mixing rule 2 [MR2]. A convenient extension of data for group contribution is necessary in order to apply the predictive procedure to a broader class of polymeric materials.

Chapter 8

DEVELOPMENT OF A GROUP CONTRIBUTION MIXING RULE

8.1. Introduction to the Developed GCLF - EoS:

At this chapter, it has been evolved a group contribution mixing rule that deals with a pure component and a mixture following the Panayiotou and Vera EoS that were introduced in [Eq.4.1.6, and Eq.4.2.16] for a pure component and a mixture, respectively. Firstly, the mixing rule is employed to express the molecular reference interaction energy between similar groups or different ones. Secondly, the mixing rule of molecular reference volume is kept the same for a pure component and a mixture because it is not a function of temperature. The mixing rule is applicable in predicting the thermodynamic properties such as the solubility of gas or vapor into rubbery polymers or glassy ones.

8.1.1. Mixing Rule for A Pure Component and Mixtures:

The mixing rule refers to the estimation of interaction energy between segment of component "i" and that of component "j" as a function of the group surface area of group-to-group interaction energy parameter:

$$\epsilon_{ij} = \sum_m \sum_n \Theta_m^{(i)} \Theta_n^{(j)} e_{mn} \qquad \text{[MR3 \& MR4]} \qquad (8.1.1.1)$$

$$e_{mn} = e_{mn_h} + e_{mn_s} T \qquad (8.1.1.2)$$

Where ϵ_{ij} is the interaction energy between segments of component "i" and "j", $\Theta_m^{(i)}$ is the surface area fraction of group m in the pure component i, e_{mn} is the molecular reference interaction energy between group m and n, e_{mn_h} is the molecular enthalpic interaction energy parameter between group m and n, e_{mn_s} is the molecular entropic interaction energy parameter between group m and n. T is the temperature of the system.

It could be noted that the above mixing rule also works for the case "$i = j$" (homogeneous interaction) as well as for that in which "$i \neq j$" (heterogeneous interaction).

The molecular reference volume of component i, as follows:

$$v_i^* = \sum_m R_m^0 \qquad (8.1.1.3)$$

Where R_m^0 is the molecular reference volume constant of group m.

The molecular reference volume of a mixture, v^* is calculated similarly to (Eq.5.4.8), with taken into consideration the difference of v_i^*.

8.2. Prediction of the Molecular Reference Volume, Enthalpic Interaction Energy and Entropic Interaction Energy Parameters and Results:

The developed GCLF – EoS is applicable in predicting the thermodynamic properties considering the molecular reference volume, enthalpic interaction energy, entropic interaction energy as adjustable parameters.

At this chapter, it has been predicted the results of a pure component based on the best fitting to the Daubert and Danner experimental data [34], and it is worth to mention that the interested thermodynamic properties that have been selected are the vapor pressure, P* for predicting the molecular enthalpic and entropic interaction energies and the liquid density, ρ_{liq} for predicting the molecular reference volume constant. For the case of mixture, it has been analysed the phase behaviour of vapor-liquid equilibria for predicting the parameters of the molecular reference volume and interaction energy of groups. The vapor pressure, P* was used as a thermodynamic property, and it was predicted by finding the best fitting to the DECHEMA experimental data [53,54].

It could be stated that mixing rule 3 [MR3] and mixing rule 4 [MR4] that represented in (Eq. 8.1.1.1) are set for a pure component and a mixture one, respectively.

Table 8.1 shows the predicted parameters of the molecular enthalpic interaction energy between group m and n for the following groups: CH3, CH2, CH3COO and CO2. The molecular enthalpic interaction energy between CH3COO and CH3COO demonstrates the highest rate of energy whereas the molecular enthalpic interaction energy parameter between CH3 and CH3COO exhibits the lowest rate of energy.

Table 8.1

Group Binary of the Molecular Enthalpic Interaction Energy Parameters (e_{mn_h})

m\n	CH3	CH2	CH3COO	CO2
CH3	673.87	760	457	701.38
CH2		821.2	738	1036.55
CH3COO			1687	1198.03
CO2				1002.4

Table 8.2 represents predicted parameters of the molecular entropic interaction energy between group m and n for the following groups: CH3, CH2, CH3COO and CO2. The molecular entropic interaction energy between CH3COO and CH3COO illustrates the lowest rate of entropy whereas the molecular entropic interaction energy parameter between CH3 and CH3COO expresses the highest rate of entropy.

Table 8.2

Group Binary of the Molecular Entropic Interaction Energy Parameters (e_{mn_S})

m\n	CH3	CH2	CH3COO	CO2
CH3	-0.16	0.01	0.68	-0.33
CH2		0.25	0.47	-0.65
CH3COO			-2.13	-1.07
CO2				-0.99

Table 8.3 shows predicted parameters of the molecular reference volume and the surface area for the following groups: CH3, CH2, CH3COO and CO2. The surface area of the following groups: CH3, CH2, C, and CH3COO were retrieved from Fredenslund et al. book [32], while CO2 was retrieved from Hamedi et. al. paper [10]. It should be noted that the surface area constant of carbon (C) is equal to zero because it has no surfaces around its atom.

Table 8.3

Group Reference Volume, R_m and Surface Area Parameters, Q_k

Group	R_m^0	Q_k	Ref.
CH3	0.02572	0.848	
CH2	0.016464	0.540	[32]
C	0.000	0.000	
CH3COO	0.065	1.728	
CO2	0.04	1.112	[10]

8.2.1. Prediction of the Molecular Reference Volume, Enthalpic Interaction Energy and Entropic Interaction Parameters of CH3 CH3 Using the Properties of Vapor Pressure and Liquid Density of Ethane:

Fig. 8.1 illustrates the predicted results of the logarithmic of vapor pressure, P* and liquid density,ρ_{liq} of ethane at the temperature range of 90.35 to 273K. The predicted results by GCLF-EoS for the logarithm of vapor pressure fits well to the Daubert and Danner experimental data [34]. Whereas, the predicted results of liquid density, ρ_{liq} do not show a satisfactory result. However, the predicted results of liquid density do not affect this work compared to the predicted results of the logarithm of vapor pressure, P*. MR3 is applied for predicting the parameters of molecular reference volume constant of a group CH3, R^0_{CH3}, enthalpic interaction energy between like groups CH3 and CH3, $e_{CH3-CH3_h}$, and entropic interaction energy between like groups CH3 and CH3, $e_{CH3-CH3_s}$. The parameters of the molecular enthalpic and entropic interaction energies of CH3 CH3 can be found in Tables 8.1-2, whereas the reference volume and the surface area of group CH3 parameters are given in Table 8.3, the surface area constant of CH3, Q_{CH3} was retrieved from Fredenslund et al. book [32] which is equal to 0.848.

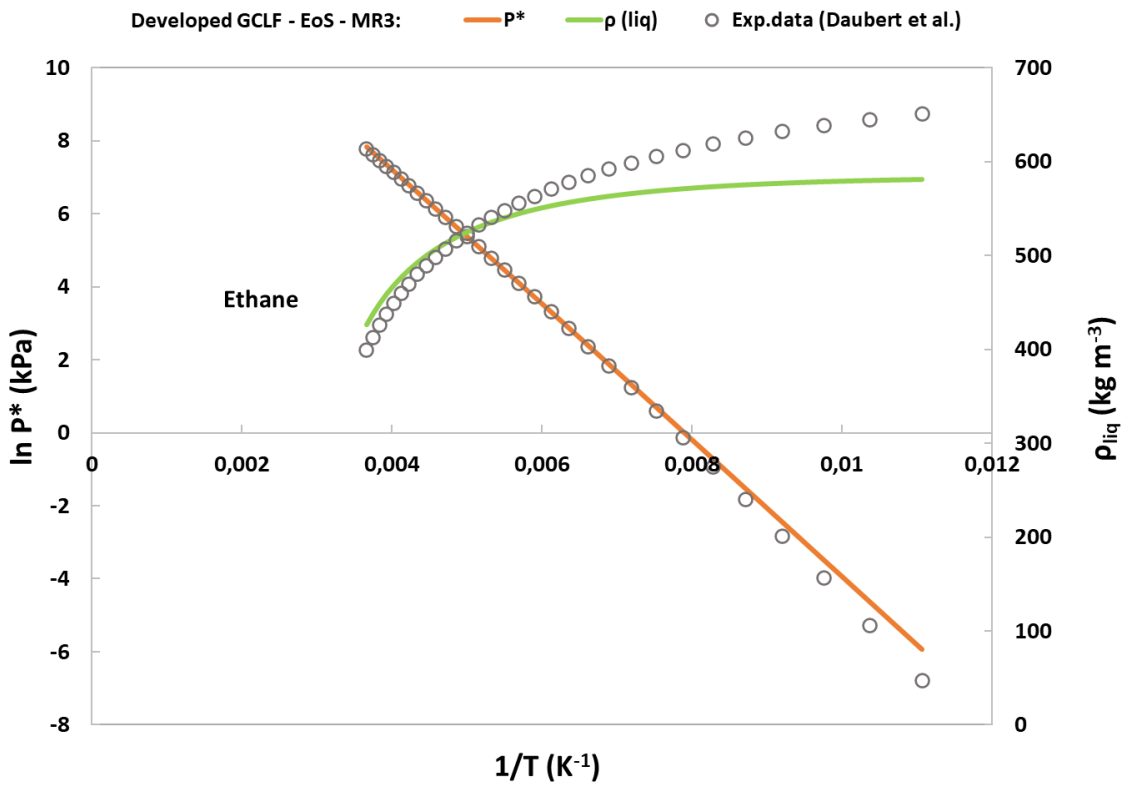

Fig. 8.1. Logarithmic of vapor pressure and liquid density of ethane: experimental data from ref 34 and predictions given by the developed GCLF EoS.

8.2.2. Prediction of the Molecular Reference Volume, Enthalpic Interaction Energy and Entropic Energy Interaction Parameters of CH2 CH2 Using the Properties of Vapor Pressure and Liquid Density of Cyclohexane:

Fig. 8.2 shows the prediction of the logarithmic of vapor pressure, P* and liquid density, ρ_{liq} of cyclohexane at the temperature range of 279.69 to 498.19 K. Interestingly, the predicted results of the logarithmic of vapor pressure and liquid density fit perfectly to the Daubert and Danner experimental data [34]. As previous case [ethane], it has been applied MR3 for predicting the parameters of molecular reference volume of a group CH2, R^0_{CH2}, enthalpic interaction energy between like groups CH2 and CH2, $e_{CH2\,CH2_h}$ and entropic interaction energy between like groups CH2 and CH2, $e_{CH2\,CH2_s}$, [parameters, see Table 8.1-3]. It has been found that the surface area constant of cycles [cy-CH2] in the article that was published by [Lee and Danner] [5], is equal to the normal alkanes [CH2]. Thus, it has been taken the surface area constant of CH2, Q_{CH2} from the Fredenslund et al. book [32] which is equal to 0.540.

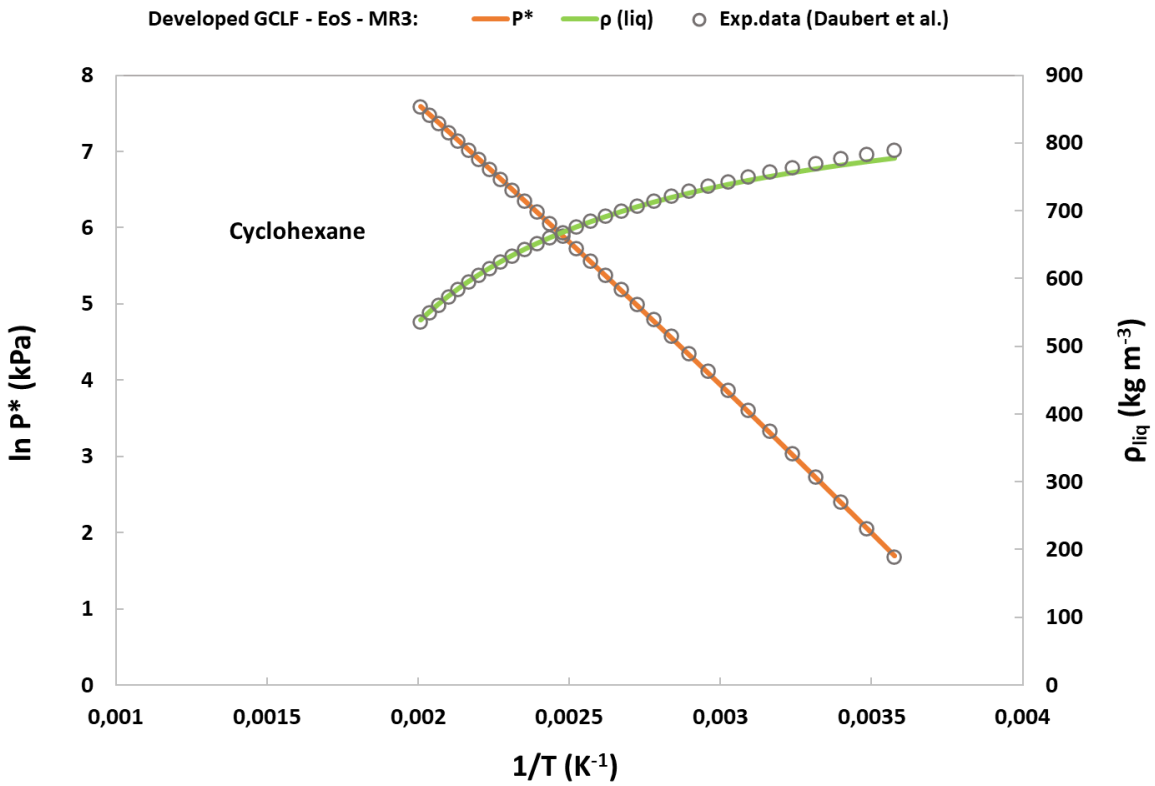

Fig. 8.2. Logarithmic of vapor pressure and liquid density of cyclohexane: experimental data from ref 34 and predictions given by the developed GCLF-EoS.

8.2.3. Prediction of the Molecular Enthalpic Interaction Energy and Entropic Interaction Energy Parameters of CH2 CH3 Using the Properties of Vapor Pressure and Liquid Density of Pentane:

Fig. 8.3 represents the prediction of the logarithmic of vapor pressure, P* and liquid density,ρ_{liq} at the temperature range of 143.42 to 422.73 K. The predicted results by GCLF-EoS for the logarithmic of vapor pressure fit appropriately to the Daubert and Danner experimental data [34]. On the other hand, the predicted results by GCLF-EoS for the liquid density,ρ_{liq} do not show a reasonable result. However, as it has been clarified in the previous case [ethane] that the predicted results of liquid density do not influence this work contrary to the predicted results of the logarithmic of vapor pressure. Furthermore, MR3 is used for predicting the parameters of molecular enthalpic interaction energy between unlike groups CH2 and CH3, $e_{CH2\ CH3_h}$and entropic interaction energy between unlike groups CH2 CH3, $e_{CH2\ CH3_s}$, [parameters, see Table 8.1-2].

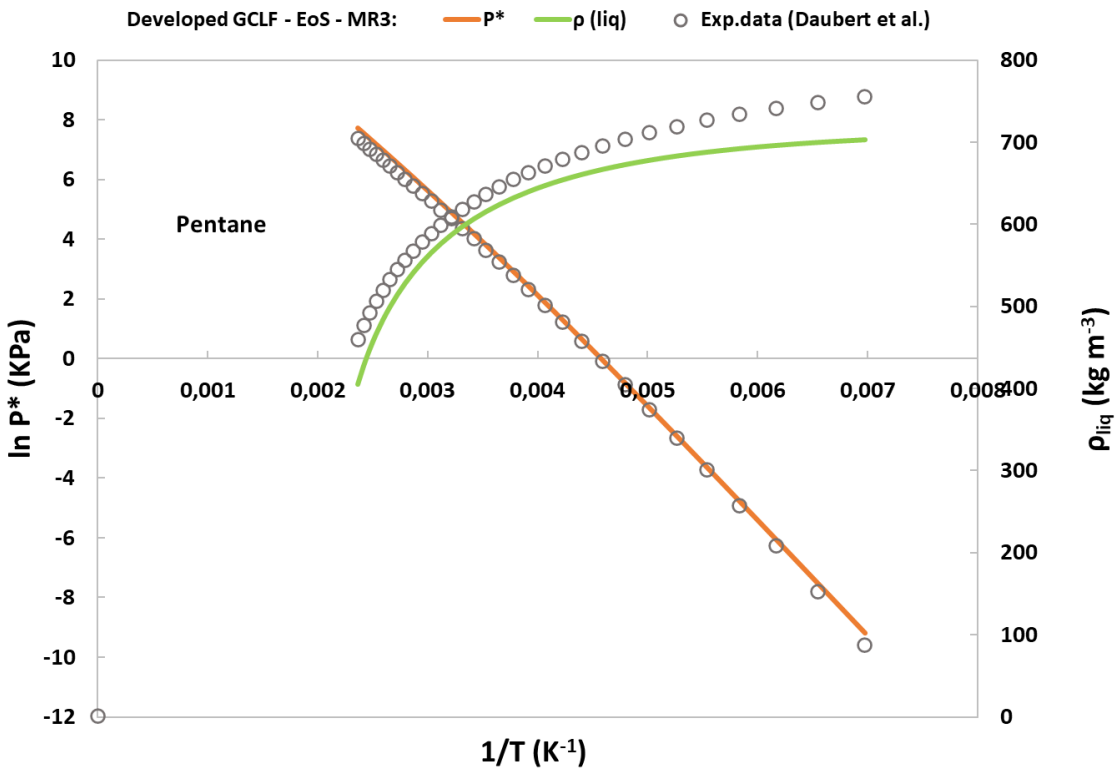

Fig. 8.3. Logarithmic of vapor pressure and liquid density of pentane: experimental data from ref 34 and predictions given by the developed GCLF EoS.

8.2.4. Prediction of the Molecular Reference Volume, Enthalpic Interaction Energy and Entropic Interaction Energy Parameters of CO2 CO2 Using the Properties of Vapor Pressure and Liquid Density of Carbon Dioxide:

Fig. 8.4 illustrates the prediction of the logarithmic of vapor pressure, P* and liquid density, ρ_{liq} at the temperature range of 216.58 to 273K. The predicted results by GCLF-EoS for the logarithmic of vapor pressure match accurately to the experimental data that were proposed by [Daubert and Danner] [34]. Whereas, the predicted results of liquid density, ρ_{liq} do not lead to a convenient result. However, liquid density does not affect this work compared to the predicted vapor pressure, P*. Similarly to previous cases for a pure component, it has been applied MR3 for predicting the parameters of molecular reference volume of a group CO2, R_{CO2}, enthalpic interaction energy between like groups CO2 and CO2, $e_{CO2\,CO2_h}$, and entropic interaction energy between like groups CO2 and CO2, $e_{CO2\,CO2_s}$, [parameters, see Table 8.1-3]. The surface area constant of CO2, Q_{CO2} was not available in the book of Fredenslund et al. [32]. Thus, it has been taken the value of Q_{CO2} from the paper of Hamedi et al. [10] which is equal to 1.112.

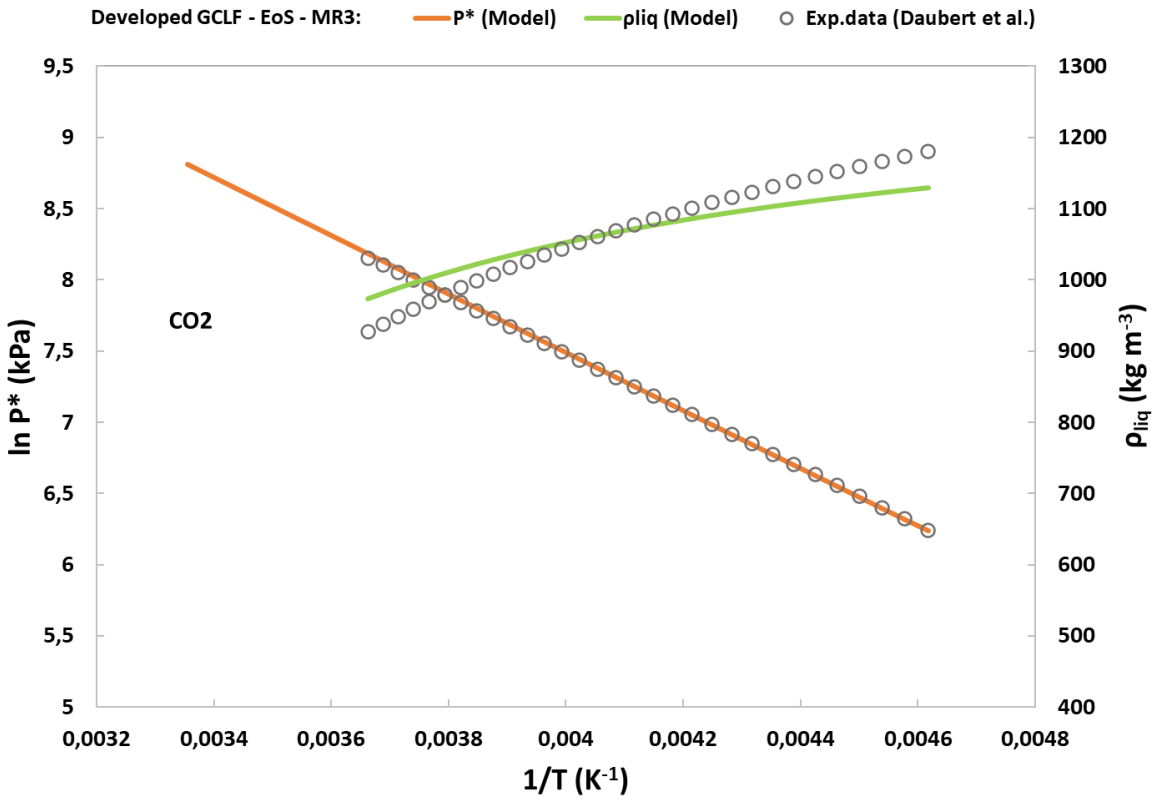

Fig. 8.4. Logarithmic of vapor pressure and liquid density of carbon dioxide (CO2): experimental data from ref 34 and predictions given by the developed GCLF EoS.

8.2.5. Prediction of the Molecular Enthalpic Interaction Energy and Entropic Interaction Energy Parameters of CO2 CH3 Using the Properties of Vapor or Liquid Equilibria of CO2/Ethane:

Figs 8.5.1-2 show the prediction of the vapor pressure, P* at two different temperatures 223.15 and 263.15 K that was analyzed by investigating the phase behaviour of vapor and liquid equilibria of carbon dioxide and ethane. As it has been noticed in the two figures that the difference between the predicted vapor pressure by GCLF-EoS and the ideal one with respect to the mass fraction of CO2 is fitted suitably to the DECHEMA experimental data [54].

It is worthful to mention that MR4 is applied for predicting the parameters of molecular enthalpic interaction energy between unlike groups CO2 and CH3, $e_{CO2\,CH3_h}$, [parameters, see Table 8.1-2]. Furthermore, it has been calculated the entropic interaction energy between unlike groups CO2 and CH3, $e_{CO2\,CH3_S}$ by interpolating the molecular enthalpic interaction energy linearly considering the maximum temperature and the minimum one, ultimately, the interaction energy between unlike groups is calculated at the temperature of interest, [see Eq. 8.1.1.1-2]. For an accurate estimation an objective function has been used by taking the quadratic difference of the experimental vapor pressure and the calculated one as shown in (Eq.8.4.2). Hence, the confident value that had been taken into consideration was the minimized one.

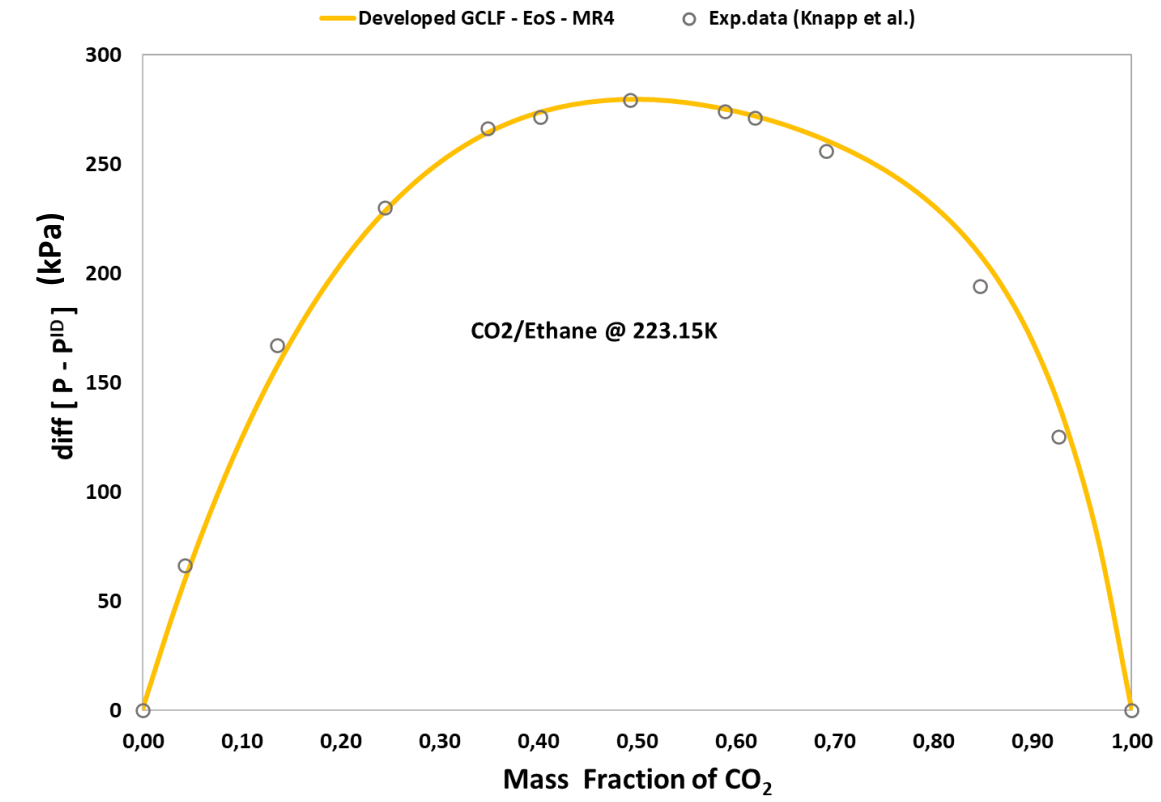

Fig. 8.5.1. VLE of CO2/Ethane at 223.15 K: experimental data from ref 54 and predictions given by the developed GCLF EoS.

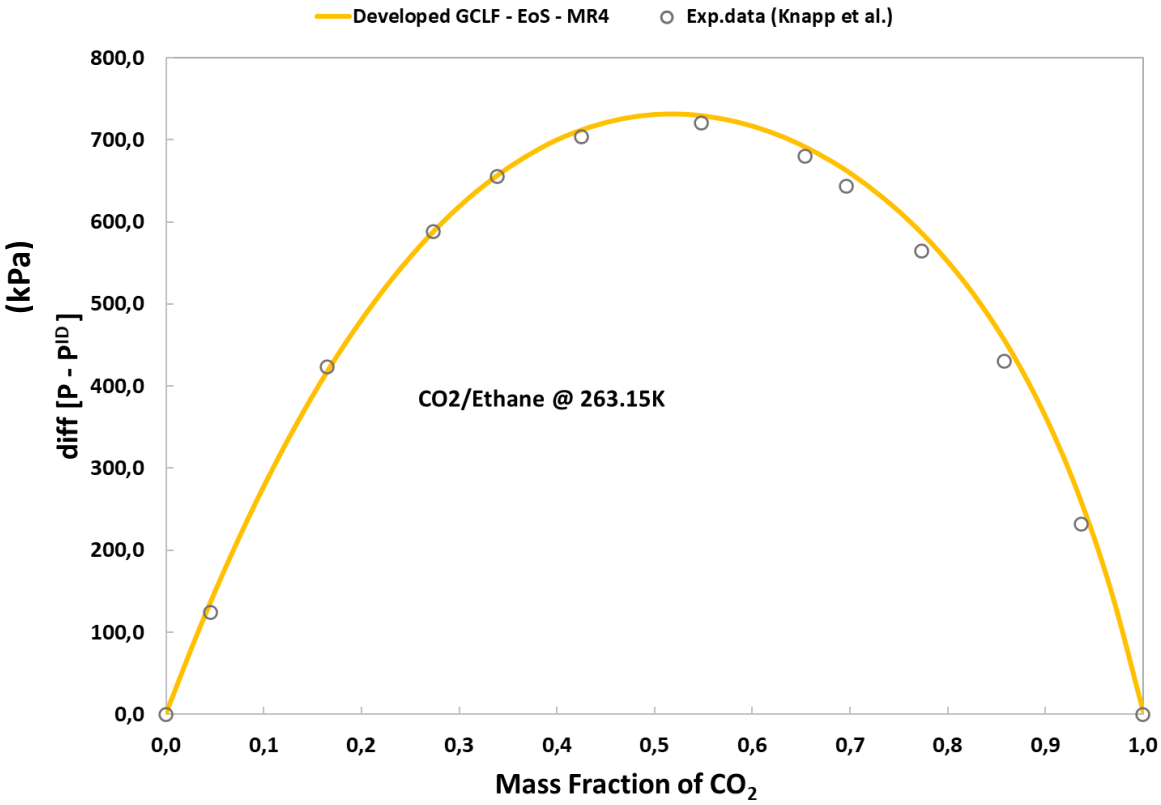

Fig. 8.5.2. Predicted VLE of CO2/Ethane at 263.15 K: experimental data from ref 54 and predictions given by the developed GCLF EoS.

8.2.6. Prediction of the Molecular Enthalpic Interaction Energy and Binary Entropic Interaction Energy Parameters of CO2 CH2 Using the Properties of Vapor/Liquid Equilibria of CO2/Propane:

Figs 8.6.1-2 illustrate the prediction of the vapor pressure, P* at two different temperatures 233.15 and 273.15 K that was analyzed by studying the phase behaviour of vapor and liquid equilibria of carbon dioxide and propane. The difference between the predicted vapor pressure by GCLF-EoS and the ideal one with respect to the mass fraction of CO2 is fitted well to the DECHEMA experimental data [54] as shown in Fig 8.6.1 whereas Fig 8.6.2 shows a partial match to the experimental data. Similar to the previous case, MR4 is applied for predicting the parameters of molecular enthalpic interaction energy between unlike groups CO2 and CH2, $e_{CO2\,CH2_h}$, [parameters, see Table 8.1-2]. Similar to the previous case, the molecular entropic interaction energy between unlike groups CO2 and CH2, $e_{CO2\,CH2_s}$ has been estimated by interpolating the molecular enthalpic interaction energy parameter linearly taking into consideration the maximum temperature and minimum one, eventually the interaction energy between unlike groups can be calculated at the temperature of interest, [see Eq. 8.1.1.1-2], along with that, an objective function has been used by taking the quadratic difference of the experimental vapor pressure and the calculated one as given in (Eq.8.4.2). Consequently, the verified value that had been taken into account was the minimized one.

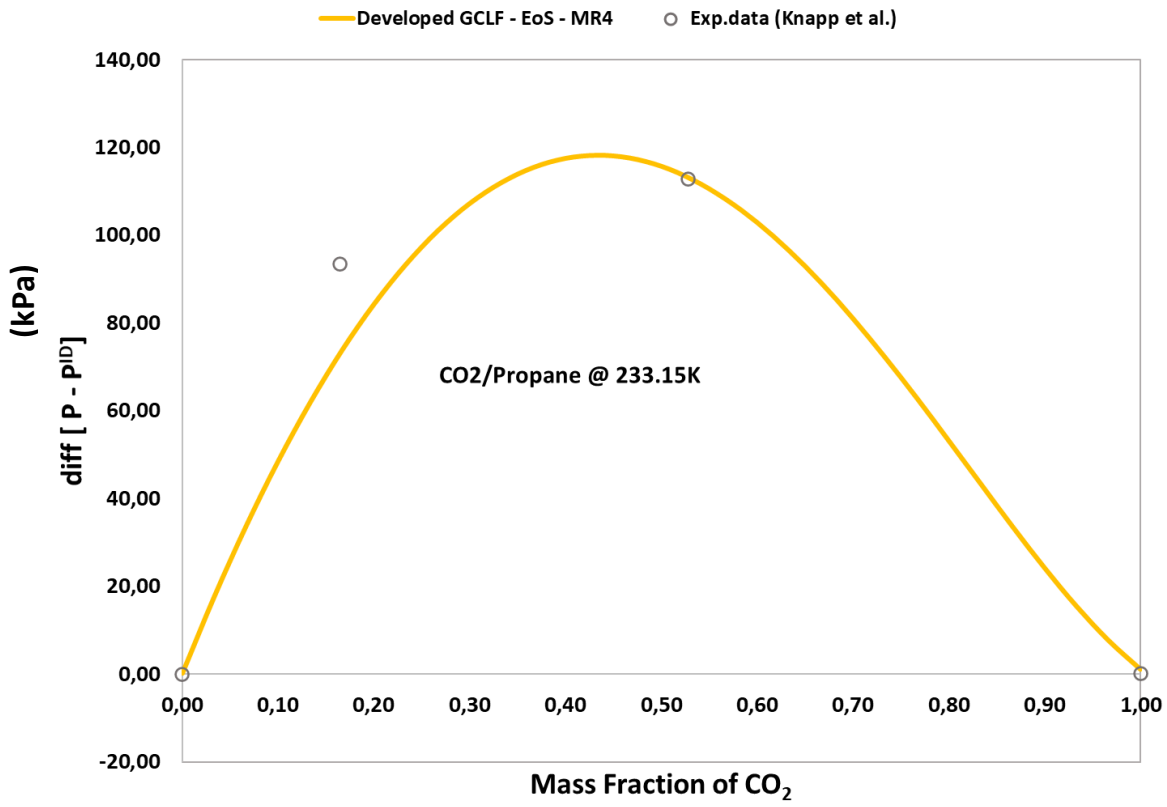

Fig. 8.6.1. VLE of CO2/Propane at 233.15 K: experimental data from ref 54 and predictions given by the developed GCLF EoS.

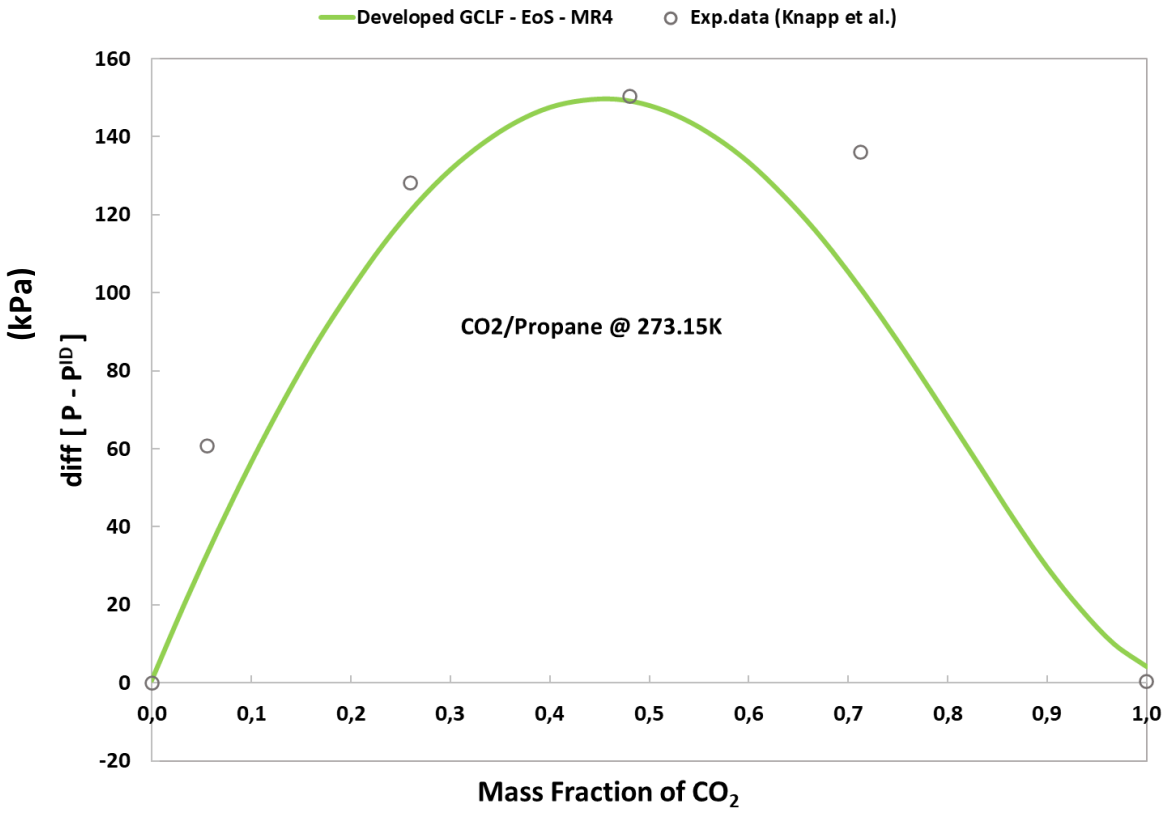

Fig. 8.6.2. VLE of CO2/Propane at 273.15 K: experimental data from ref 54 and predictions given by the developed GCLF EoS.

8.2.7. Prediction of the Molecular Reference Volume of CH3COO, Enthalpic Interaction Energy and Entropic Interaction Energy Parameters of CH3COO CH3COO, CH3 CH3COO Using the Properties of Vapor/Liquid Equilibria of Ethane/Methyl Acetate:

Fig 8.7.1 represents the prediction of the vapor pressure, P* at 298.15 K that was examined by studying the phase behaviour of vapor and liquid equilibria of ethane and methyl acetate. As it can be seen in Fig 8.7.1, the difference between the predicted vapor pressure by GCLF-EoS and the idea one with regard to the mass fraction of ethane showed high and low trendline compared to the DECHEMA experimental data [54]. Similarly to previous cases for a mixture, MR4 is applied for predicting the parameters of molecular reference volume of CH3COO, R^0_{CH3COO}, enthalpic interaction energy between like groups CH3COO and CH3COO, $e_{CH3COO\ CH3COO_h}$, entropic interaction energy between like groups CH3COO and CH3COO, $e_{CH3COO\ CH3COO_s}$, enthalpic interaction energy between unlike groups CH3 and CH3COO, $e_{CH3\ CH3COO_h}$, and entropic interaction energy between unlike groups CH3 and CH3COO, $e_{CH3\ CH3COO_s}$, [parameters, see Table 8.1-2]. As it was clarified in the previous cases that the objective function had been used for achieving the best estimation, [see, Eq.8.4.2].

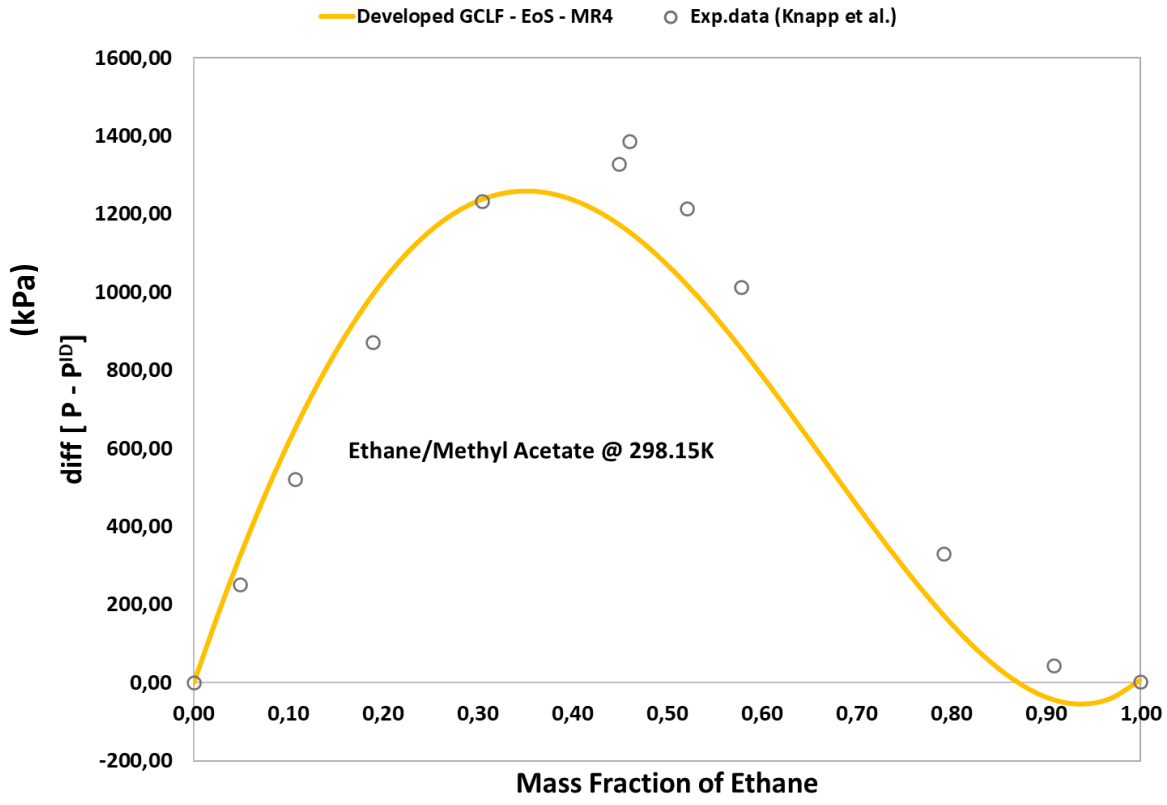

Fig. 8.7.1. VLE of Ethane/Methyl Acetate at 233.15 K: experimental data from ref 54 and predictions given by the developed GCLF EoS.

Fig 8.7.2 illustrates the prediction of the logarithmic of vapor pressure, P* and liquid density,ρ_{liq} at the temperature range of 175.15 to 425K. The predicted results by GCLF-EoS for the logarithmic of vapor pressure match perfectly to the Daubert and Danner experimental data [34]. Whereas, the predicted results by GCLF-EoS for the liquid density,ρ_{liq} do not show a satisfactory result. Nevertheless, the liquid density does not affect this work compared to the predicted vapor pressure, P*. Likewise previous cases, It has been used MR3 for predicting the pure component parameters of molecular reference volume of CH3COO, R^0_{CH3COO}, enthalpic interaction energy between like groups CH3COO and CH3COO, $e_{CH3COO\,CH3COO_h}$, entropic interaction energy between like groups CH3COO and CH3COO, $e_{CH3COO\,CH3COO_s}$and enthalpic interaction energy between unlike groups CH3 and CH3COO, $e_{CH3-\,CH3COO_h}$, entropic interaction energy between unlike groups CH3 and CH3COO, $e_{CH3\,CH3COO_s}$. [parameters, see Table 8.1-3]. It could be noted that the surface area constant of CH3COO, Q_{CH3COO} was retrieved from Fredenslund et al. book [32] which is equivalent to 0.880.

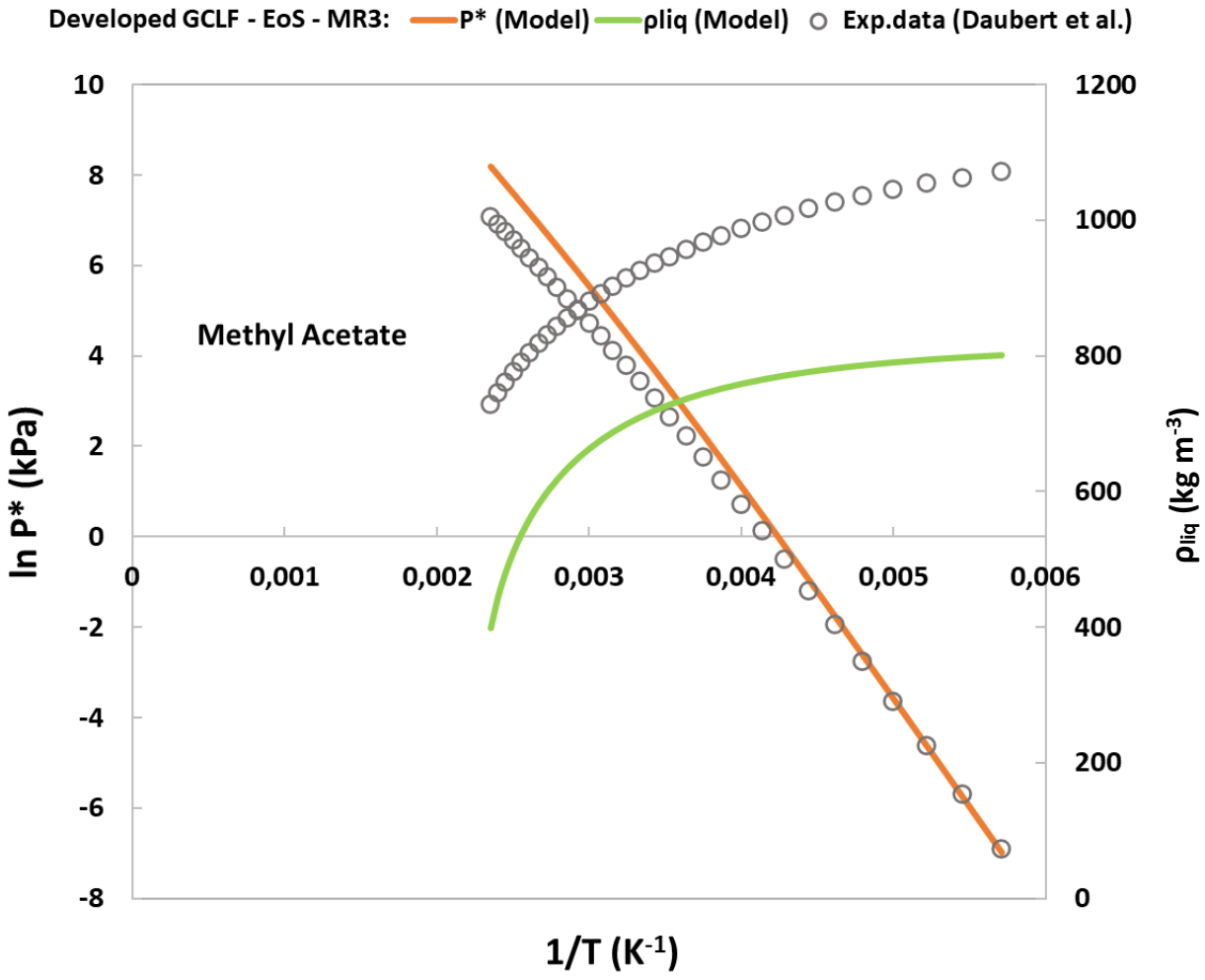

Fig. 8.7.2. Logarithmic vapor pressure and liquid density of methyl acetate: experimental data from ref 34 and predictions given by the developed GCLF-EoS.

8.2.8. Prediction of the Molecular Enthalpic Interaction Energy and Entropic Interaction Energy Parameters of CH2 CH3COO Using the Properties of Vapor/Liquid Equilibria of Methyl Acetate/Dodecane:

Figs 8.8.1 illustrates the prediction of the vapor pressure, P* at 323.15 K that was examined by analyzing the phase behaviour of vapor and liquid equilibria of methyl acetate and dodecane. The difference between the predicted results of the vapor pressure by GCLF-EoS and the ideal one is fitted to the DECHEMA experimental data [53] at the high concentration of methyl acetate. Parallelly to the previous cases for a mixture, MR4 is applied for predicting the parameters of molecular enthalpic interaction energy between unlike groups CH2 and CH3COO, $e_{CH2\ CH3COO_h}$, entropic interaction energy between unlike groups CH2 and CH3COO, $e_{CH2\ CH3COO_s}$,[parameters, see Table 8.1-2]. As it was stated in the previous cases that the objective function had been applied for obtaining the best estimation, [see, Eq.8.4.2].

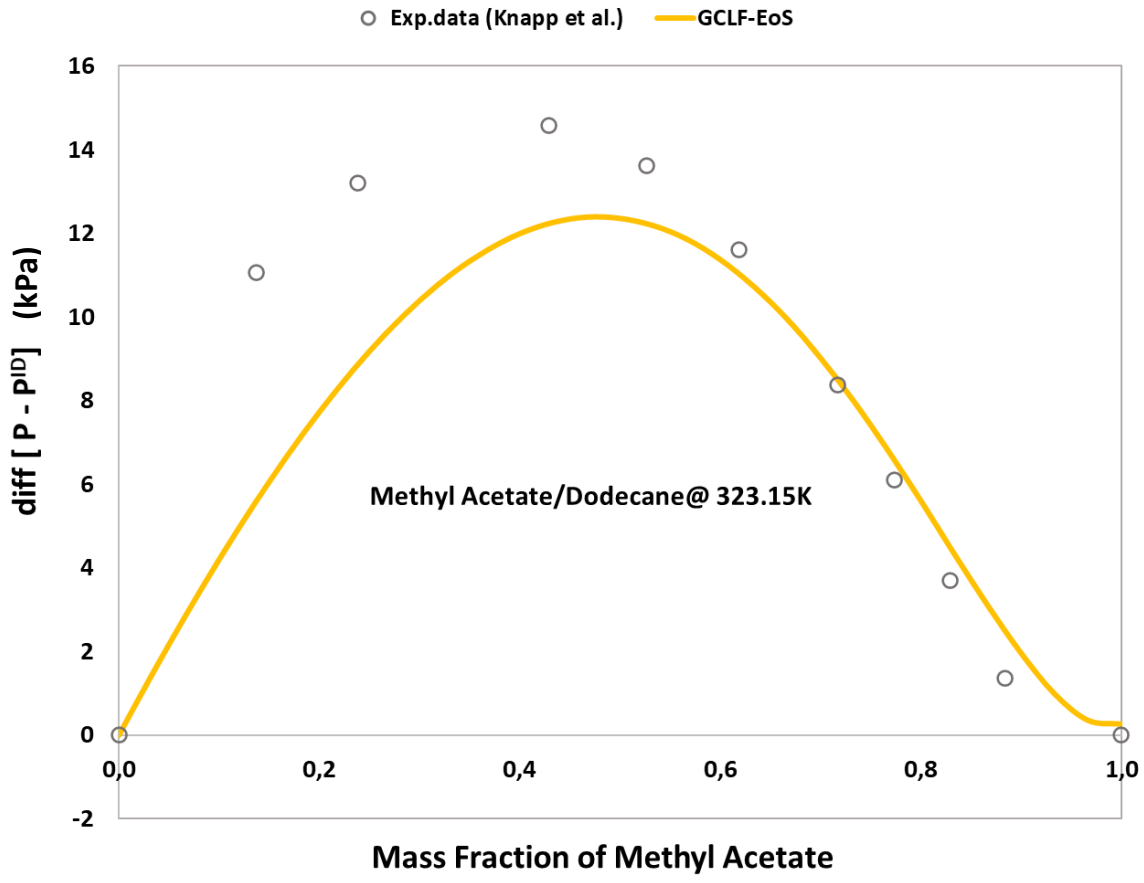

Fig. 8.8.1. VLE of Methyl Acetate/Dodecane at 323.15 K: experimental data from ref 53 and predictions given by the GCLF EoS.

Fig. 8.8.2 illustrates the prediction of the logarithmic of vapor pressure, P* and liquid density,ρ_{liq} at the temperature range of 187.35 to 490K. The predicted results by GCLF-EoS for the vapor pressure lay well on the Daubert and Danner experimental data [34]. Whereas, the predicted results of liquid density,ρ_{liq} do not demonstrate a convenient result. However, the liquid density does not influence this work in contrast to the predicted vapor pressure, P*. Similar to previous cases for a pure component, MR3 is applied for predicting the parameters of molecular enthalpic interaction energy between unlike groups CH2 and CH3COO, $e_{CH2\ CH3COO_h}$, and entropic interaction energy between unlike groups CH2 and CH3COO, $e_{CH2\ CH3COO_s}$,[parameters, see Table 8.1-2].

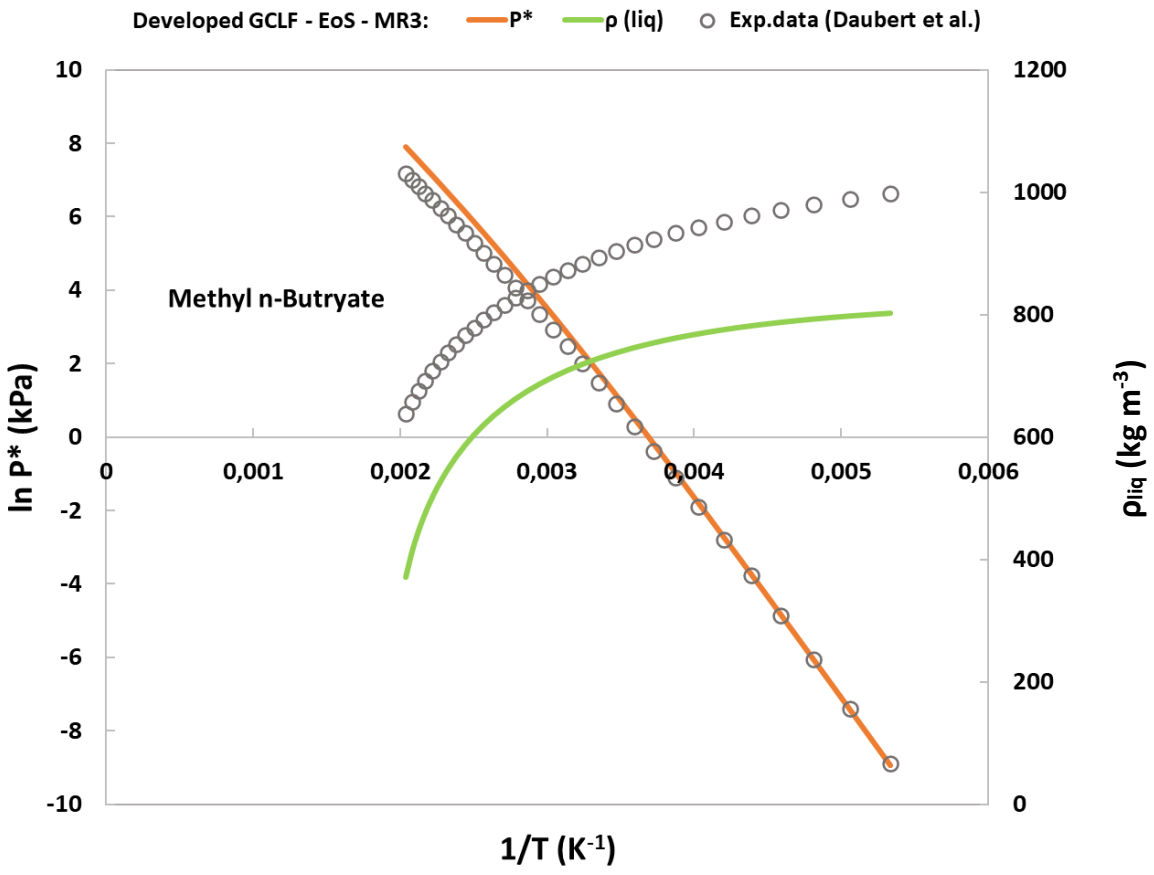

Fig. 8.8.2. Logarithmic of vapor pressure and liquid density of methyl n-butryate: experimental data from ref 34 and predictions given by the developed GCLF-EoS.

Fig. 8.8.3 represents the prediction of the logarithmic of vapor pressure, P* and liquid density,ρ_{liq} at the temperature range of 185.65 to 460K. The predicted results by GCLF-EoS for the vapor pressure fit appropriately to the Daubert and Danner experimental data [34]. Whereas, the predicted results of liquid density,ρ_{liq} do not show a reasonable result. However, the predicted liquid density does not affect this work contrary to the predicted vapor pressure, P*. Likewise previous cases for a pure component, MR3 is used for predicting the parameters of molecular enthalpic interaction energy between unlike groups CH2 and CH3COO, $e_{CH2\ CH3COO_h}$, and entropic interaction energy between unlike groups CH2 and CH3COO,$e_{CH2\ CH3COO_s}$, [parameters, see Table 8.1-2].

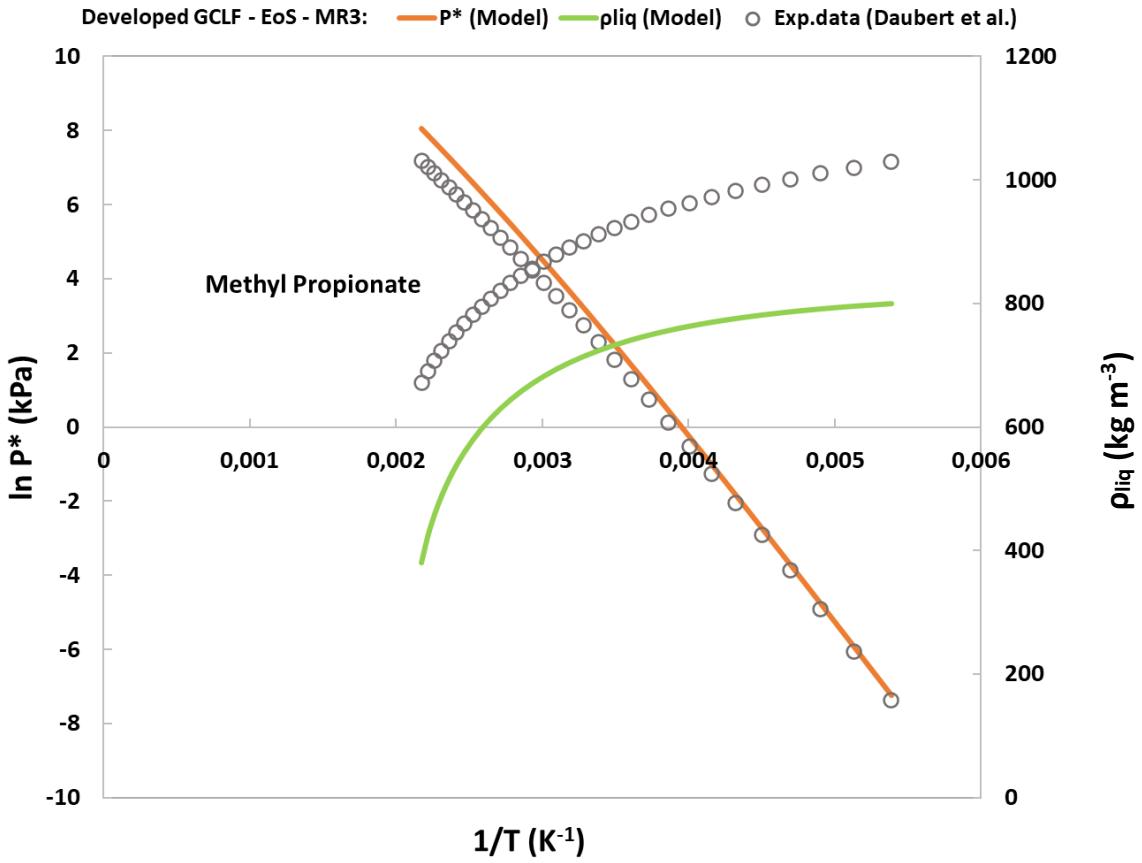

Fig. 8.8.3. Logarithmic of vapor pressure and liquid density of methyl propionate: experimental data from ref 34 and predictions given by the developed GCLF-EoS .

Figs. 8.9.1-2 illustrate the prediction of the vapor pressure, P* at two different temperatures 298.15 and 313.15 K that was analyzed by investigating the phase behaviour of vapor and liquid equilibria of carbon dioxide and methyl acetate. The difference of the predicted results by GCLF-EoS for the vapor pressure with respect to the mass fraction of CO2 showed high and low trends compared to the DECHEMA experimental data [54]. Similar to the previous cases for a mixture, MR4 is applied for predicting the parameters of molecular reference enthalpic interaction energy between unlike groups CO2 and CH3COO, $e_{CO2\ CH3COO_h}$, [parameters, see Table 8.1-2]. In addition, it has been calculated the molecular entropic interaction between unlike groups CO2 and CH3COO, $e_{CO2\ CH3COO_s}$ by interpolating the molecular enthalpic interaction energy linearly with taking into consideration the maximum temperature and minimum one, ultimately the interaction energy between unlike groups can be calculated at the temperature of interest, [see Eq. 8.1.1.1-2]. As it was mentioned in the previous cases that the objective function had been applied for attaining the best estimation, [see, Eq.8.4.2].

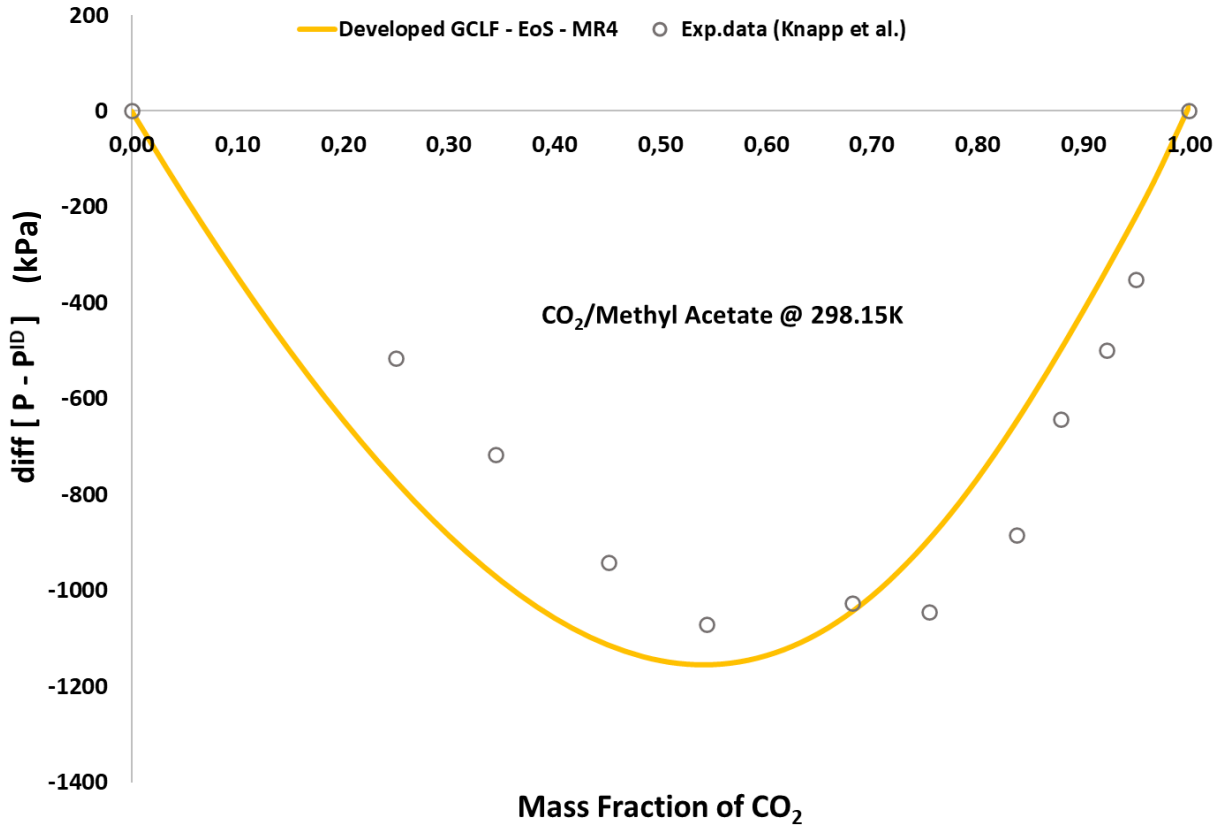

Fig. 8.9.1. VLE of CO2/Methyl Acetate at 298.15 K: experimental data from ref 54 and predictions given by the developed GCLF-EoS.

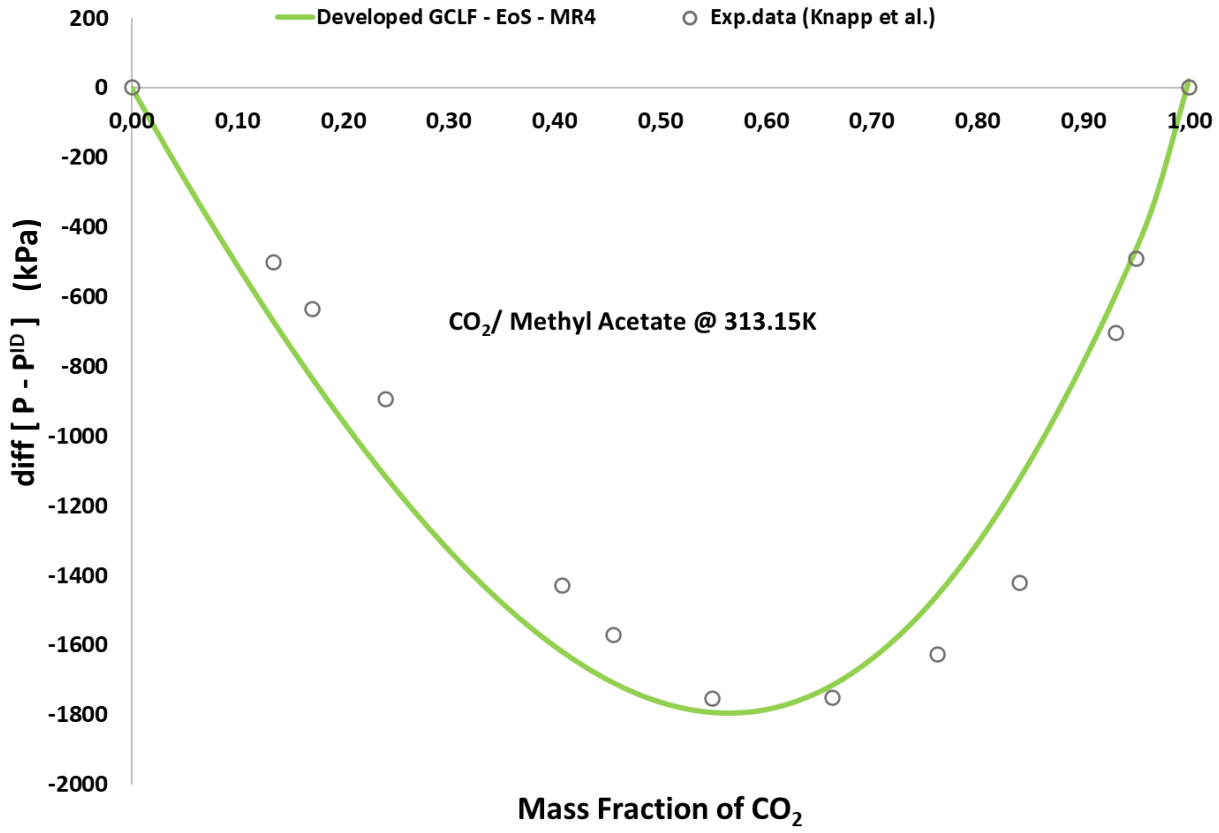

Fig. 8.9.2. VLE of CO2/Methyl Acetate at 313.15 K: experimental data from ref 54 and predictions given by the developed GCLF EoS.

8.3. Solubility Prediction in Poly (methyl methacrylate) + CO2 system:

It is worthful to mention that it has been used the same properties that already presented in [chap.7, sec. 7.3.1]. The PMMA molecular weight and its glass transition temperature were retrieved from Koros et. al. paper [44] which is equivalent to 599,000 g/mole and [120°C, see Table 7.1], respectively. Whereas, the compressibility parameter, χ, was retrieved from Minelli and Doghieri paper [49]. As it was mentioned that it had been applied (Eqs.7.1.1-2) for estimating the thermal expansion coefficient, which was equivalent to 0.45 [Zoller] [42].

Fig 8.10 exhibits the prediction of the carbon dioxide (CO2) solubility in poly(methyl methacrylate) (PMMA) at various pressures for different temperatures. The developed NE-GCLF EoS model that was examined by MR4 has shown unsatisfactory result contrasted to Koros's experimental data. Nonetheless, it can be said that the model has been launched properly in general term.

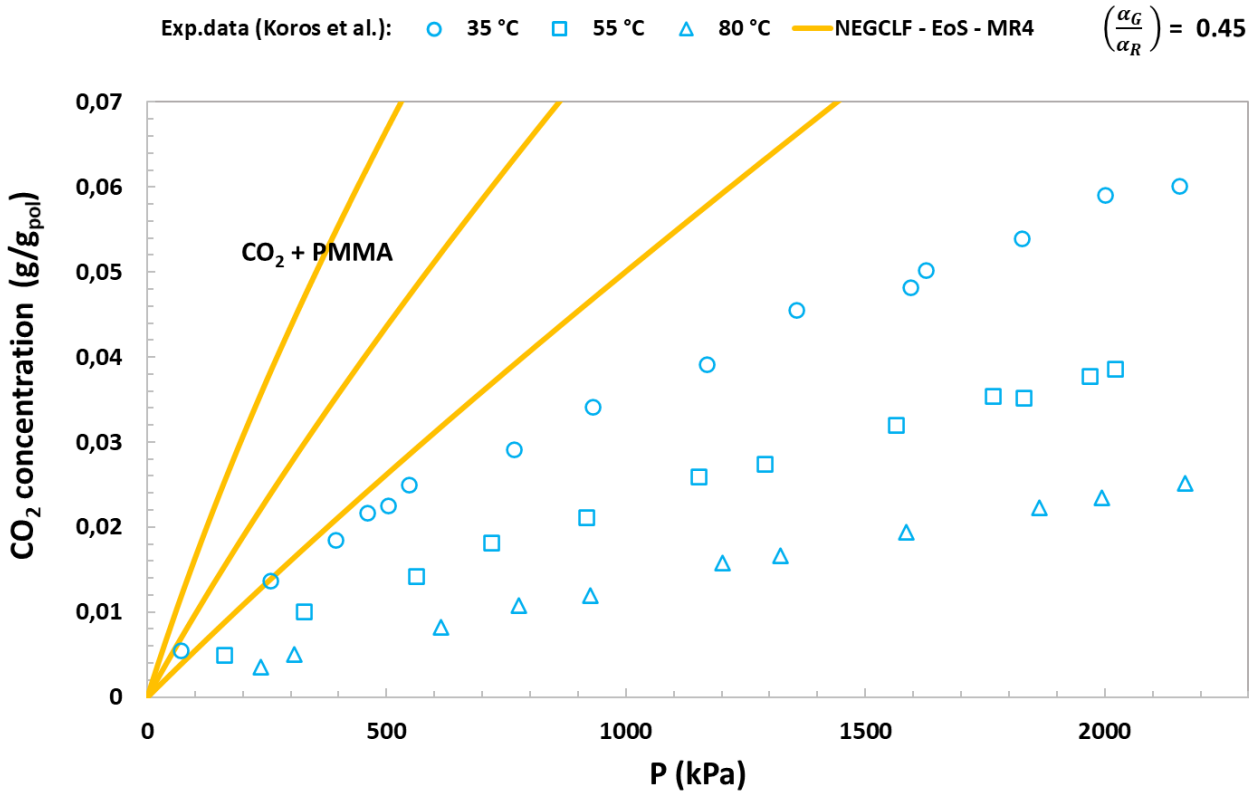

Fig. 8.10. Solubility isotherm of CO2 in PMMA at 35, 55 and 80°C: experimental data from ref 44 and predictions given by the developed GCLF EoS and NELF model.

8.4. Test and Consistency of the Developed GCLF - EoS:

For obtaining a perfect estimation to the developed GCLF-EoS model, the model must be examined by setting a mathematical expression for calculating the molecular interaction energy between groups.

Thus, it has been selected an arbitrary temperature which is equal to 300 K for this examination.

Table 8.4 represents the interaction energy between group m and n at 300 K.

Table 8.4

Interaction Energy between group m and n

e_{mn}	**Estimated Energy (kJ/kmol) [300K]**
$e_{CH_2\ CH_3COO}$	879
$e_{CH_3\ CH_3COO}$	661
$e_{CH_3COO\ CH_3COO}$	1048
$e_{CH_2\ CH_2}$	896.20
$e_{CH_3\ CH_3}$	625.87
$e_{CH_2\ CH_3}$	763.00
$e_{CO_2\ CO_2}$	705.40
$e_{CO_2\ CH_3COO}$	878.23

An interaction energy parameter is expressed to analyze the energy between like groups or unlike ones, as follows:

$$k_{mn} = 1 - \frac{e_{mn}}{\sqrt{e_{mm}e_{nn}}} \quad (8.4.1)$$

Table 8.5 shows an optimal result for the interaction energy parameter between groups CH2 and CH3 ~~in~~ which demonstrates that the carbon dioxide (CO2) is dissolved perfectly in the polymer that is composed of a group (CH3COO).

Table 8.5

Interaction Energy Parameter between group m and n

k_{mn}	Interaction Energy Parameter
$k_{CH2\ CH3COO}$	0.09
$k_{CH3\ CH3COO}$	0.18
$k_{CH2\ CH3}$	-0.0187
$k_{CO2\ CH3COO}$	-0.021

For approaching an optimal convergence to the program, an objective function is given by:

$$OF = \sum \frac{[(P^{Exp} - P^{IM}) - (P^{Calc} - P^{IM})]}{[(P^{Exp} - P^{IM}) + (P^{Calc} - P^{IM})]} \quad (8.4.2)$$

8.5. Conclusions of Solubility Part II:

A revision of the mixing rule was considered to optimize the prediction of gas solubility in glassy polymers, together with a specific activity to retrieve pertinent energy parameter for a limited list of functional group. Preliminary results obtained in this attempt do not appear to be self-consistent and suggest the use of a wider set of experimental data to retrieve the carboxylate ester group contribution parameters,

Chapter 9

ANALYSIS OF PERMEABILITY IN COMPOSITE MATERIALS

9.1. Introduction and aim:

The evaluation is here addressed of effective gas permeability properties of a composite material obtained through the dispersion of domains of phase “A” into a continuous matrix of phase “B”. Both type of domains are assumed to be isotropic and their gas permeability will be identified as P_A and P_B, for dispersed and continuous phase respectively. Even for this simple case, however, the permeability of the corresponding composite material may have a tensorial nature, depending on shape, as well as orientation and arrangement of dispersed domains. In general terms, for isothermal and low-pressure gradients processes, three different scalar permeability value would be necessary to characterize the steady state gas transport properties in the system, pertinent to the different principal directions of the structure:

$P_{i,mix} \quad i = 1,2,3$

The enhancement in gas permeability, $\left(P_{i,mix} - P_B\right)/P_B$ for the i-th principal direction in the composite material with respect to the matrix, is expected to increase, in the general case, with both the volume fraction of the dispersed phase ϕ (indicated as “loading”, in what follows) and the permeability ratio $\alpha = P_A / P_B$ (the enhancement vanishing, of course, for the case $\alpha \to 1$). In this respect, it may be interesting to represent the permeability enhancement coefficient K_i, for the i-th principal direction, defined as follows:

$$K_i \equiv \frac{\left(P_{i,mix} - P_B\right)/P_B}{\phi\left(\alpha - 1\right)}; \qquad i = 1,2,3 \tag{9.1.1}$$

and to discuss its dependence on orientation and space arrangement of dispersed domains, as well as on permeability ratio.

The simplest case, in this respect, is that of a planar multilayer composite material, in which orientation of principal directions can be easily recognized as the direction perpendicular to layers plane (corresponding permeability hereafter indicated as $P_\perp$) and any direction parallel to layers plane (corresponding permeability hereafter indicated as $P_\parallel$).

For multilayer materials, the following relations can be simply derived for the series combination of mass flow resistance ($P_\perp$) or of mass flow conductance ($P_\parallel$):

$$\begin{cases} \dfrac{1}{P_\perp} &= \dfrac{1}{P_B}\left[1+\phi\left(\dfrac{1}{\alpha}-1\right)\right] \\ P_\parallel &= P_B\left[1+\phi(\alpha-1)\right] \end{cases} \qquad (9.1.2)$$

which ultimately bring to the following relations for enhancement permeability coefficient:

$$\begin{cases} \dfrac{1}{K_\perp} = & 1+(1-\phi)(\alpha-1) \\ K_\parallel &= 1 \end{cases} \qquad (9.1.3)$$

so that a simple result can be drawn for the combination of permeability enhancement coefficient along principal directions in a layered composite:

$$\sum_{i=1}^{3}\left(\frac{1}{K_i}-1\right) = (1-\phi)(\alpha-1) \qquad (9.1.4)$$

It is interesting to observe that the latter relation works also for the case of dilute dispersion of spheres, in which the well-known Maxwell [55] relation holds:

$$\frac{1}{K_i} = 1+\frac{(1-\phi)(\alpha-1)}{3} \qquad i=1,2,3 \qquad (9.1.5)$$

It is useful to stress here that the above relation results from the exact solution of the mass transport problem in a composite material obtained through the dispersion of spherical domains in a matrix, for the case of arbitrary permeability ratio ($0<\alpha<\infty$), in the limit of vanishing loading ($\phi \to 0$).

The result in (Eq.9.1.4), in the same limits ($\phi \to 0\,; 0<\alpha<\infty$) can be also recognized from the exact solution of permeability problem in a composite material obtained through the dispersion of aligned spheroids (either oblate or prolate) [56], in which the coefficient along principal axes are generally different one from the other.

The same result also works for the case of dilute dispersion of aligned long circular section cylinders, for which the relation by Wiener [57] is known to hold:

$$\begin{cases} \dfrac{1}{K_\perp} = & 1+\dfrac{(1-\phi)(\alpha-1)}{2} \\ K_\parallel &= 1 \end{cases} \qquad (9.1.6)$$

where $K_{\perp}$ indicates the permeability enhancement coefficient in direction perpendicular to the axis of dispersed cylinders, while $K_{\parallel}$ refers to the same property evaluated in direction parallel to the same axis. It is useful to remember here, once more, that the above relation holds for vanishing loading, irrespective of the value of permeability ratio.

Results mentioned above are those for which a simple close form or the exact solution of the permeability problem is known. When you move away from the dilute dispersion of aligned spheroids (ultimately, the case of an isolated long cylinder is a limiting condition in the same set), only approximate results are found in the literature, which in turn have great relevance and are widely used. Among the latter, the Nielsen model [58] for diluted dispersion of infinitely long aligned ribbons (rectangular cross section cylinders) with cross section edges of length L_i in i-th direction (i =1,2), in which the following expressions of effective permeability in the principal directions of the composite are proposed:

$$\begin{cases} \dfrac{1}{K_1} = 1+\dfrac{(1-\phi)(\alpha-1)}{1+\dfrac{L_1}{L_2}} \\ \dfrac{1}{K_2} = 1+\dfrac{(1-\phi)(\alpha-1)}{1+\dfrac{L_2}{L_1}} \\ K_3 = 1 \end{cases} \tag{9.1.7}$$

It should finally be mentioned that relation in (Eq.9.1.4) is known to be obeyed by all composites materials in which domains of isotropic phase A are dispersed in a continuous isotropic phase B, in the limit of permeability ratio approaching unity ($\alpha \to 1$) [59]. It should however be kept in mind that condition represented in (E.9.1.4) does not have universal application and, indeed, the sum represented on the l.h.s. of the above equation, in the general case, depends on loading, shape, orientation and arrangement of dispersed domains, as well as o permeability ratio between dispersed and continuous phases. Several examples are offered in the literature of estimation of permeability in the principal direction of the composite material, from the numerical solution of the transport problem of traces of mobile components through a composite sample. Not many of them, however, were run with the accuracy needed to appreciate deviation from the simple rule represented in (Eq.9.1.4).

Aim of the activity described in the remaining of this section is the evaluation of deviations from results expressed in relation (Eq.9.1.4) for the case of composite geometries more complex than that of diluted dispersion of aligned spheroids. To represent these deviations in a compact and useful form, the coefficient Ψ is here introduced, defined as follows:

$$\Psi \equiv \frac{(\alpha+1)}{(\alpha-1)}\left\{\frac{\sum_{i=1}^{3}\left(\frac{1}{K_i}-1\right)}{(1-\phi)(\alpha-1)}-1\right\} \qquad (9.1.8)$$

Use of factor $\beta \equiv (\alpha-1)/(\alpha+1)$ in (Eq.9.1.8), to scale the deviations measured for a given composite structure from result in Eq.(9.1.4), is suggested both by the fact that variations are expected for term in brackets on r.h.s. of (Eq.9.1.8) of the same sign of $(\alpha-1)$ and by its limed range, as β increases from -1 to +1 when permeability ratio changes from 0 to ∞.

Effective permeability in the composite material of interest was estimated through the numerical solution of diffusive mass transport equation in a sample of the composite, for the case a fugacity jump was imposed at opposite faces of the sample. At this stage of the analysis, the attention was focused on the case of ordered dispersion of aligned domains o dispersed phase which could result in an overall isotropic composite material.

The exploration of permeability enhancement coefficient reached for a composite as effect of shape, orientation and arrangement of dispersed phase, as well as of the permeability ratio, are then discussed in terms of relation Ψ vs β, which directly expresses the deviation from value reached in ideal conditions represented in (Eq.9.1.4). As all structure considered are isotropic, the results of the comparison here performed can be seen as the analysis of deviation of actual effective permeability from prediction by the Maxwell model (Eq.9.1.5). Among composite structures considered in this work are rather peculiar shape of the dispersed domains, which were considered in order analyze the case of dispersed phase volume fraction in the full range, from zero to one. This will ultimately allow to test the validity of hypothesis formulated in the literature, according to which the Maxwell model well represents effective permeability in isotropic composite material also for the case of very large loading values [60].

Specific attention is given in this work to the evaluation of uncertainty of numerical output obtained, in order to validate the departure from Maxwell results discussed in the examples considered in this analysis.

9.2. Methods:

Permeability enhancement coefficient for composites resulting from ordered arrangement of dispersed domains of isotropic materials in a continuous isotropic matrix were calculated solving the corresponding mathematical steady state permeation problem in a convenient sample of the composite material. The problem is described by the Laplace equation for fugacity, distinctly considered for dispersed and continuous phase, together with continuity condition for gas fugacity value at the interphase between domains pertinent to different phases. The effective permeability of the composite is ultimately computes by evaluating the mass flow through the sample resulting for the case of assigned fugacity jump at opposite boundaries.

The problem is actually solved through the use of a CFD software (FLUENT) based on fine volume formulation of discretized transport equations [61]. By mean of the CFD software, a detailed representation is given of the geometry of the smallest portion (sample) of the material whose integral permeability coefficient is equivalent to the effective properties of the whole composite.

For each case considered, in term of geometry, loading and permeability ratio, several different fractionations of the calculation domain in discrete volumes (mesh) were considered and the results for the apparent effective permeability were examined as function of the number of volume elements in the mesh in order to identify, by extrapolation, the expected value for the case of infinite number of discrete volumes. The latter is indeed the effective permeability value used to evaluate the coefficient Ψ [see Eq. 9.1.8] shown in the following subsection, for all conditions examined. In addition to calculation for the case of finite value of permeability of the disperse phase, performed as just described, calculation were carried out for the case of null or infinite permeability value of the dispersed phase accounting for the solution of the Laplace equation in the continuous phase domain of the sample only, and imposing a zero-flux or iso-fugacity condition, respectively, at the boundary with the dispersed phase.

9.2.1. Laplace Equation for Fugacity:

The Laplace equation is considered as the prototypical elliptic partial differential equation (PDE):

$$\nabla^2 f = 0 \qquad (9.2.1.1)$$

Where ∇^2 is the Laplace operator, corresponding to the divergence of the gradient and f is the fugacity of the mobile species in the medium.

9.2.2. Discretization Method:

The discretization the differential equations is managed according to the method proposed by Patankar [61]. The numerical method treats as its fundamental unknowns the values of the dependent variable at a finite number of locations, namely the grid points in the calculation domain. The method includes the tasks of providing a set of algebraic equations for the unknown values and of prescribing an algorithm for solving the equations. The continuous information contained in the exact solution of the differential equation has been replaced with discrete values (values at grid points). The algebraic equations involving the unknown values of ϕ at selected grid points, are the discretization equations as derived from the differential equation governing ϕ. It is common to subdivide the calculation domain into a number of elements such as a separate profile assumption that can be associated with each subdomain. Hence, the value of ϕ at a grid point influences the distribution of ϕ only in its neighbourhood.

As the number of grid points becomes very large, the solution of the discretization equations is expected to approach the exact solution of the corresponding differential equation. Based on the consideration that, as the grid points get closer from each other, the change in ϕ between neighboring grid points becomes small, and then the actual details of the profile assumption become negligible. For a given differential equation, the required discretization equations can be derived in many ways. One of the ways is the control-volume formulation method.

9.2.3. Control-Volume Formulation Method:

The principle of the control-volume formulation is easy to understand and lends itself to direct physical interpretation. The calculation domain is divided into a number of non-overlapping control volumes such that there is one control volume surrounding each grid point. The differential equation is integrated over each control volume. Piecewise profiles expressing the variation of ϕ between the grid points in which are used to evaluate the required integrals. The outcome is the discretization equation containing the values of ϕ for a group of grid points. When the discretization equations are solved to obtain the grid-point values of the dependent variable, the result can be viewed in the finite-element method. In the finite-difference method, however, only the grid-point values of ϕ are considered to constitute the solution whereas in the control-volume approach, the solution seeks in the form of the grid-point values only. The interpolation formulas or the profiles will be regarded as supplementary relations needed to evaluate the required integrals in the formulation. Once the discretization equations are derived, the profile assumptions can be neglected.

9.2.4. Control-Volume-based Finite-Element Method:

At this work, it has been selected “tetrahedron” which takes the form of a triangular grid, that is based on the control volume and finite element methods. The triangular grids are dependent variables which can be calculated for grid points that lie at the vertices of the triangles. The discretization equations are set up by the control-volume method; i.e., the differential equation is integrated over the typical control volume illustrated in Fig. 9.1. The control volumes are created by joining the centroid of each triangle to the midpoints of the sides of that triangle. It can be seen from Fig. 9.1 that the triangular elements adjacent to the grid point P accommodate portions of the control volume and the corresponding control-volume faces. The discretization equation is formed by adding the contributions of these elements to the integral conservation for the control volume.

A shape function describing the variation of ϕ over an element is required to calculate the flux across the control-volume faces that fall within the element. The standard shape function for the triangular element is:

$$\phi = a + bx + cy \qquad (9.2.4.1)$$

Where the constants a, b, c are expressed in terms of the three grid-point values of ϕ.

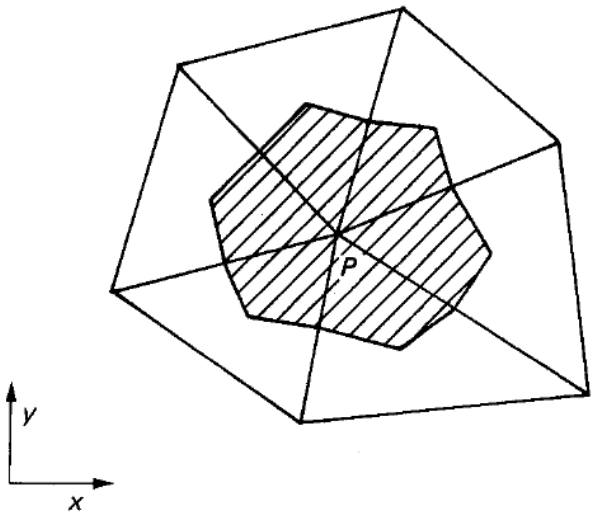

Fig. 9.1. Control volume for the triangular grid [61].

9.3. Prediction of the Effective Permeability along Principal Axis for the Case of Isotropic Composite Geometries:

At present work, it has been chosen several dispersed shaped such as octahedron, rhombic dodecahedron, truncated octahedron, spheres, and cubes. These dispersed shapes are common in isotropic condition, as they all have at least three distinct symmetry planes. On top of that, it should be mentioned that only ordered arrangements of dispersed phase which preserve the isotropic condition for the composite material. A portion is captured from the lattice to represent a repeated unit that can be minimized by slicing it to the smallest portion of the domain and then it can be brought to the calculation domain. It has been sorted different loading ratio from the smallest to the largest. It has been manipulated the highest possible loading ratio of the disperse to the matrix based on the dispersed shape with using the following permeability ratios: (0, 0.001, 0.01, 0.04, 0.1, 0.25, 0.5, 2,4, 10, 25, 100, 1000, ∞).

The effective permeability, P^{eff} is given by:

$$P^{eff} = \frac{(N_A\, L)}{(A\ \Delta f)} \tag{9.3.1}$$

Where N_A is the mass flux. L is the thickness of the membrane. A is the area of the membrane. Δf is the difference of the fugacity across the membrane.

The problem of searching for effective permeability of a composite medium to a mobile species at infinite dilution condition, from the know value of permeability of both dispersed and continuous phases, is indeed equivalent to the searching the corresponding effective thermal conductivity, from the pertinent known values for the constituent phases. The two enhancement coefficients result to be expressed by the same function of loading ratio, ϕ_D, and permeability/thermal conductivity ratio, α.

Thus,

at this work, it has been utilized the effective thermal conductivity, k^{eff} and its expression as follows:

$$k^{eff} = \frac{(Q\ L)}{(A\ \Delta T)} \tag{9.3.2}$$

Where Q is the heat flux. L is the thickness of the slab. A is the area of the slab. ΔT is the difference of the temperature between the inlet and outlet.

It could be noted that it has been predicted three heat flux values [1094.98, 1094.973,1094.971] with three different number of elements [9766510,4478523,3428567] considering the size of element mesh that were used in the calculation [0,009,0,0131,0,0148], as it has been observed that as the size of element mesh decreases as the total number of elements, N increases, Thus, it has been taken the intercept of the slope as infinity value as shown in Fig. 9.1.

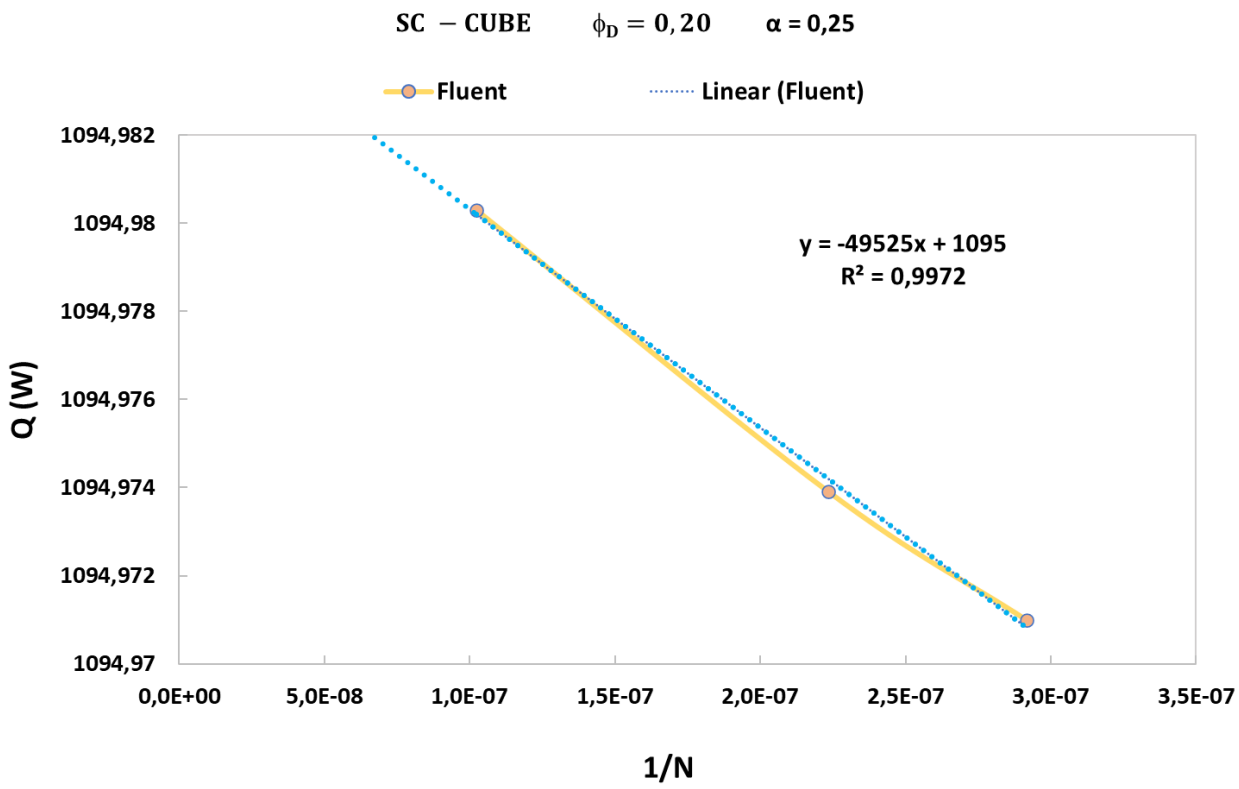

Fig. 9.2. Heat flux and mesh element size of simple cubic (SC) cubes: solids circles are three predicted heat flux values by Fluent and dashed line is the intercept.

The uncertainty error is calculated by taking the absolute difference between the average of three predicted heat flux values and the “y”intercept of the linear interpolation function, then dividing the difference result on the average of three predicted heat flux values.

After several solutions to multiple different cases, it has been found that 0.01% is the highest deviation measured this way, and this value has been assumed as uncertainty for effective permeability in all performed calculations. However, instead of predicting three heat flux values, the calculation can be

reduced to only one predicted value considering a total number of elements before this equal to the mid value of three originally examined, which is equal to an approximate five million element.

Table 9.1 represents the types of lattices and dispersed shapes: simple cubic (SC) lattice categorizes; octahedron, sphere, and cube. Face centered cubic (FCC) lattice classifies rhombic dodecahedron and sphere. Body centered cubic (BCC) lattice sorts truncated octahedron and sphere.

Table 9.1

Types of Lattices and Dispersed Shapes

Lattices	Dispersed Shapes
SC	Octahedron – Sphere - Cubes
FCC	Rhombic Dodecahedron - Sphere
BCC	Truncated Octahedron - Sphere

9.3.1. Prediction of the Effective Thermal Conductivity of Simple Cubic (SC) Octahedron:

Fig. 9.3.1 shows a simple cubic (SC) lattice for octahedron.

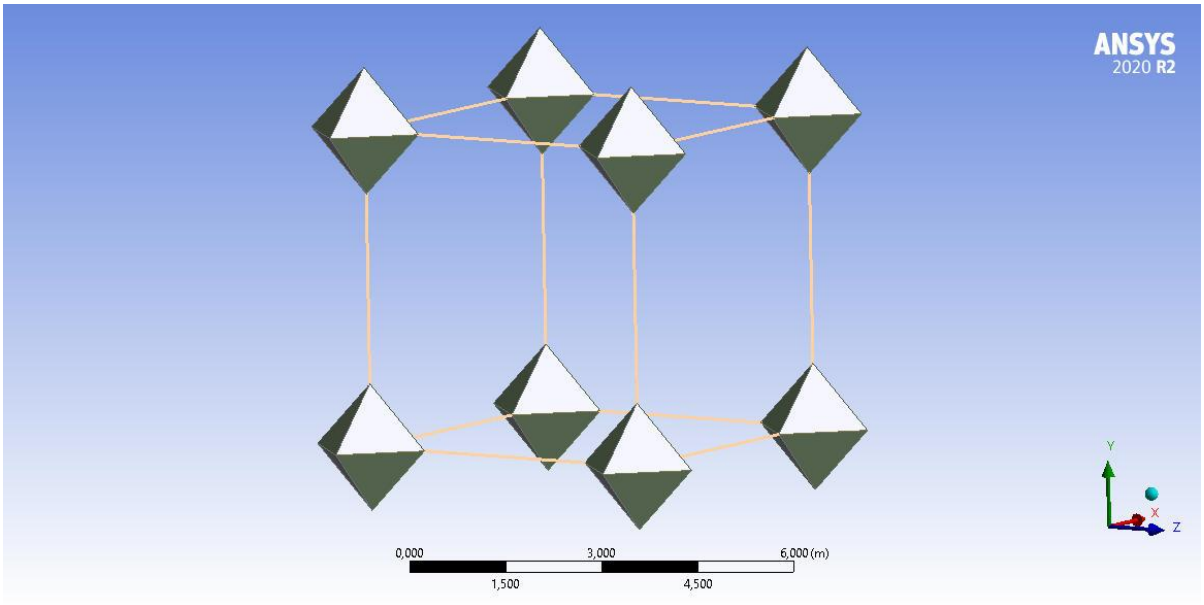

Fig. 9.3.1. Representation of simple cubic (SC) octahedron lattice.

Fig. 9.3.1. illustrates a captured unit cell for the simple cubic lattice of octahedron in which it remains eight portions of the domain.

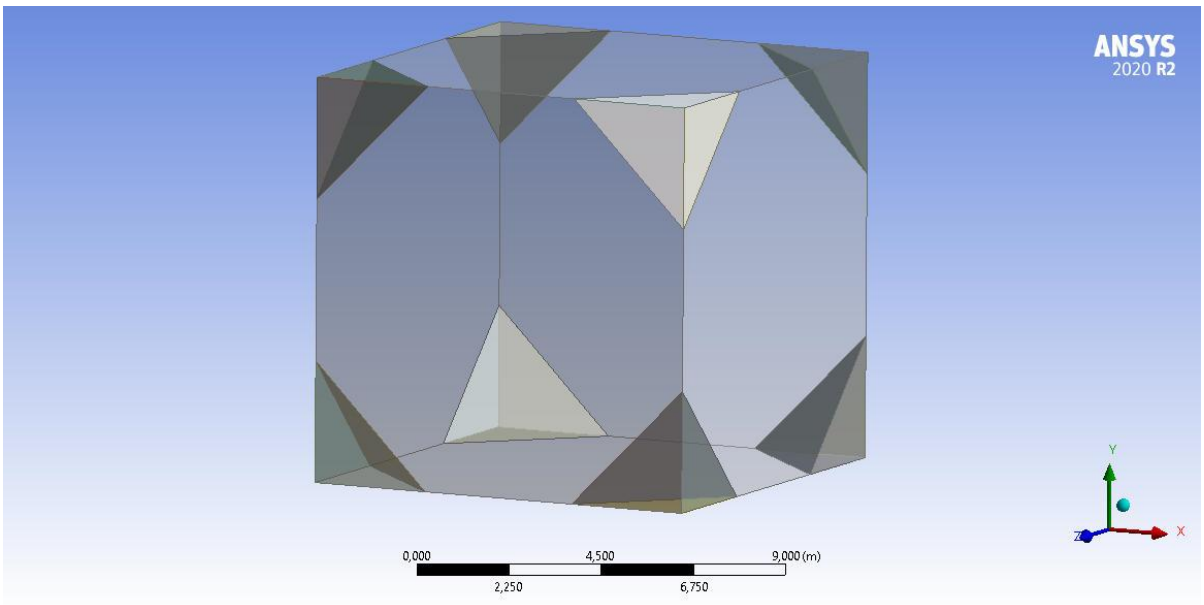

Fig. 9.3.2. Representation of simple cubic (SC) octahedron repeated unit.

The eight portions are similar to each other. Thus, the geometry has been sliced to the calculation domain for the ease of running the program and reaching an accurate result. An example of this work is the smallest loading ratio which equals to 0.00195 as shown in Fig. 9.3.3.

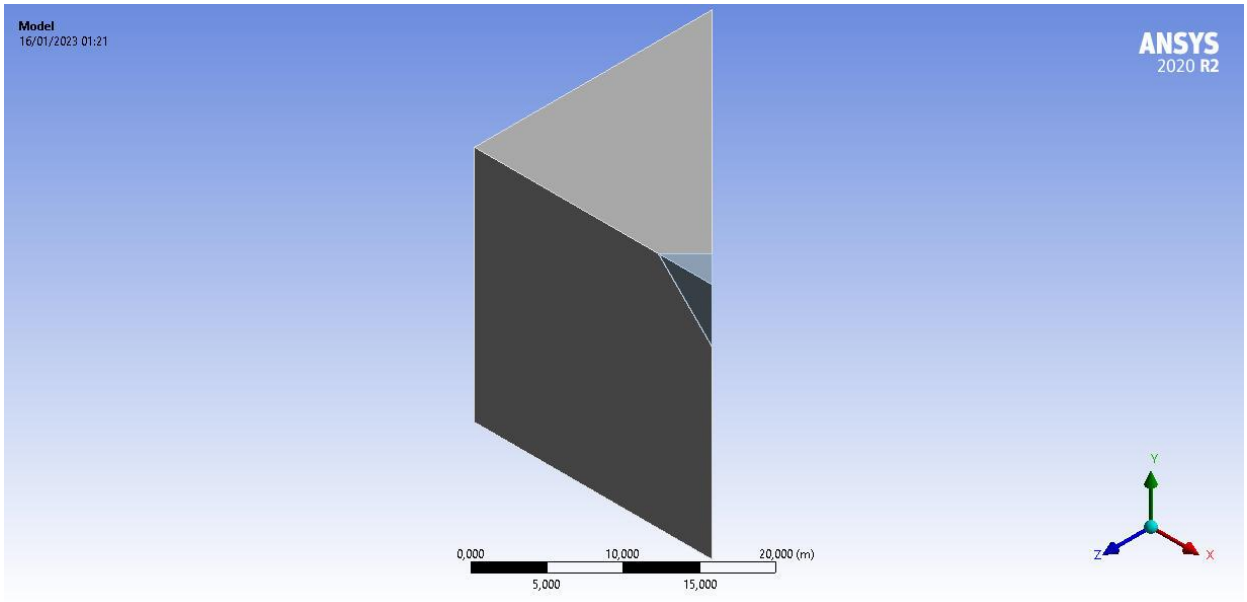

Fig 9.3.3 Representation of simple cubic (SC) octahedron of the calculation domain for the smallest loading ratio (0.00195).

Fig. 9.2.4 exhibits the mesh domain. The mesh is done by Fluent tool with choosing patch conforming tetrahedrons method.

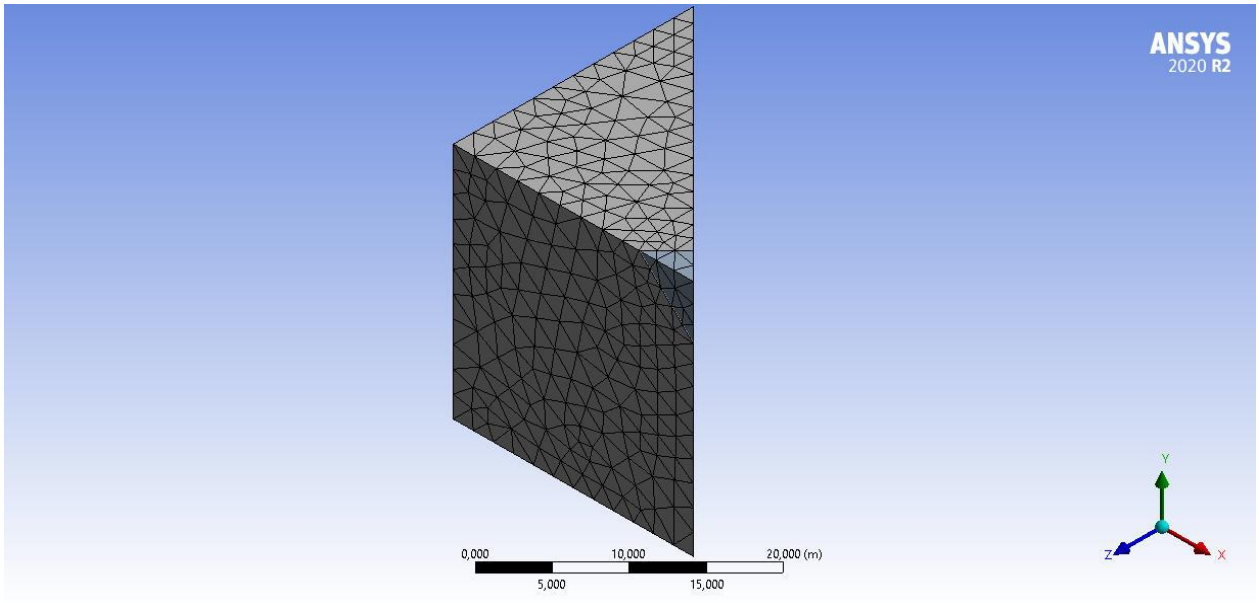

Fig 9.3.4 Representation of simple cubic (SC) octahedron mesh of the smallest loading ratio (0.00195).

Fig. 9.2.5 expresses a graph for the transport of the energy between disperse and matrix. At present work, it has been used the thermal conductivity property for calculating the permeability ratio. The graph in

Fig 9.3.5 demonstrates the process of the transport the energy from top with 400 K to bottom with 200 K whereas the heat flux is equal to zero from left to right or vice versa.

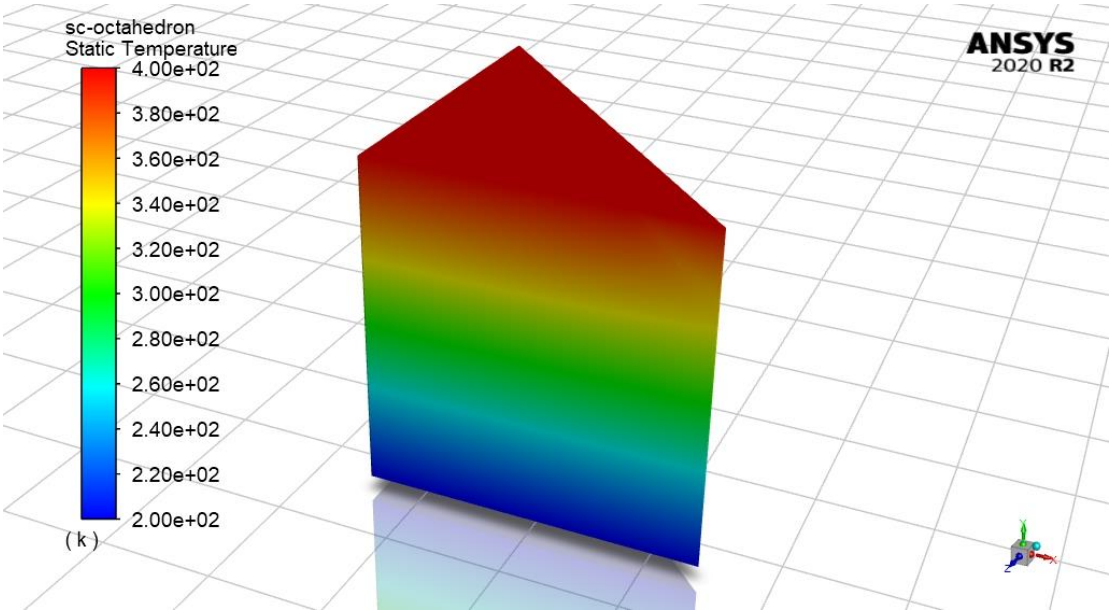

Fig. 9.3.5. Representation of simple cubic (SC) octahedron contour of the smallest loading ratio (0.00195) and lowest permeability ratio (0.001).

The same approach and data that were used in Fig 9.2.5 are utilized in Fig 9.3.6 except the permeability ratio is equal to 1000. The highest thermal conductivity of dispersed phase has shown an influence in the graph whereas in Fig. 9.3.5 the temperature is approximately equal to 350 K and in Fig. 9.3.6 the temperature in the region of dispersed phase equals nearly to 400K.

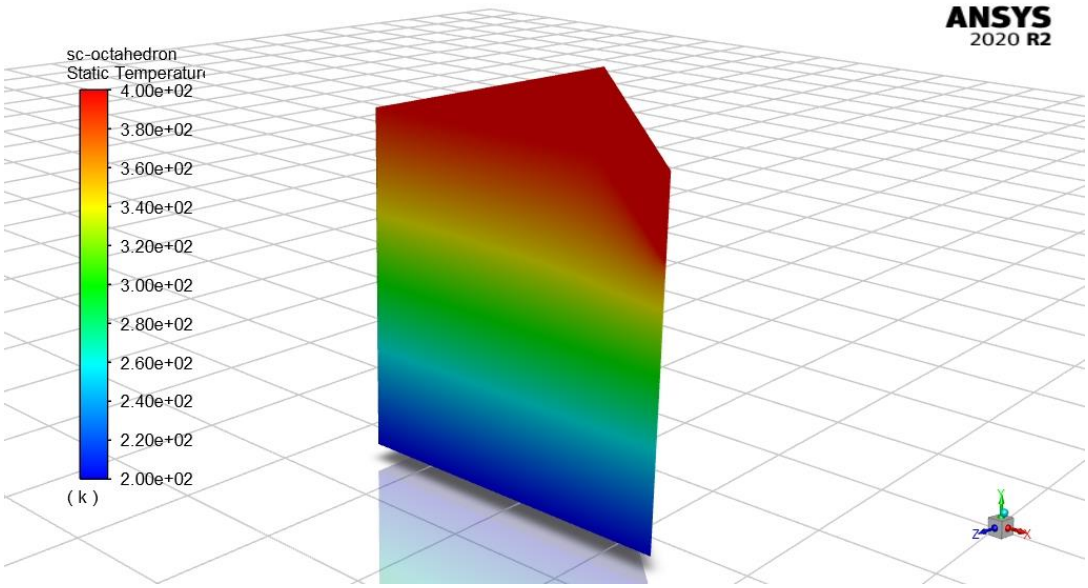

Fig 9.3.6 Representation of simple cubic (SC) octahedron contour of the smallest loading ratio (0.00195) and highest permeability ratio (1000).

Fig. 9.3.7 exhibits the same lattice and shape of the dispersed domain that was represented in Fig. 9.3.3 but with different loading ratio of dispersed phase regarding to the matrix phase which represents the largest loading ratio that is equal to 0.165.

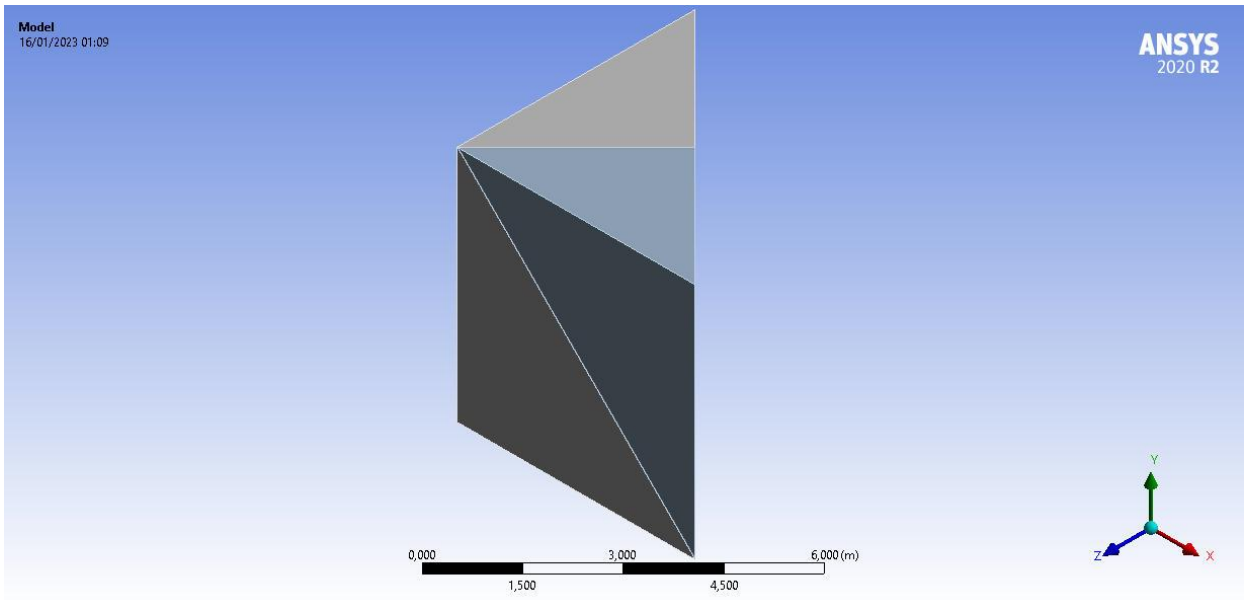

Fig. 9.3.7. Representation of simple cubic (SC) octahedron of the calculation domain of the highest loading ratio (0.165).

Fig. 9.3.8 expresses the same procedure that was followed in Fig. 9.3.4 for the type of method excluding the element size for the mesh.

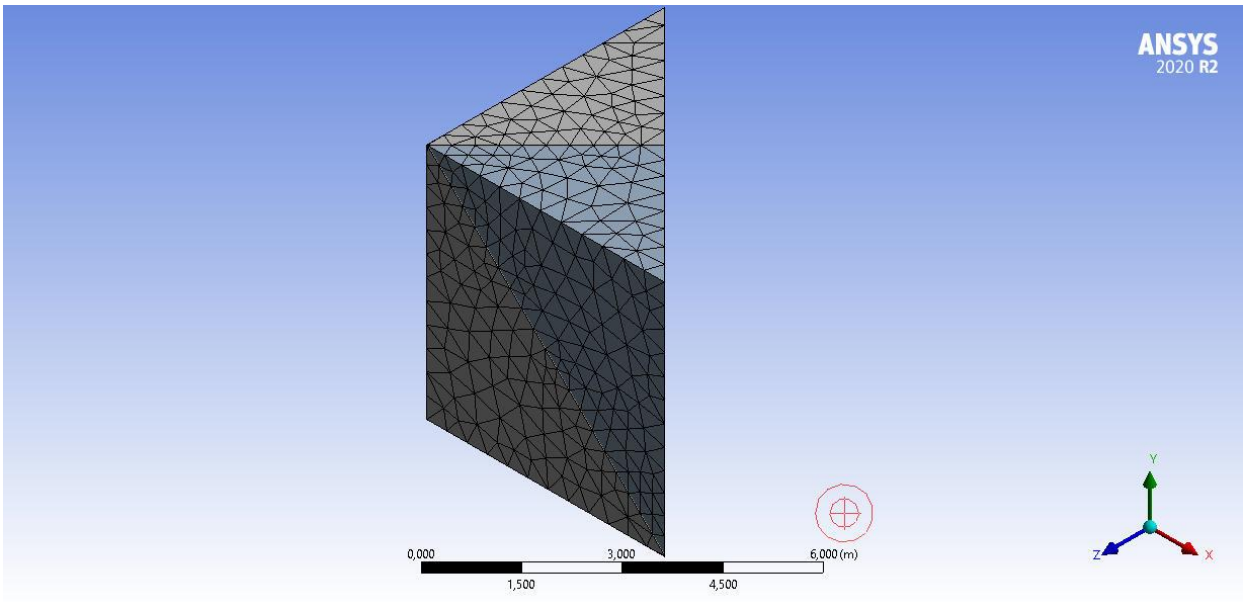

Fig 9.3.8 Representation of simple cubic (SC) octahedron mesh of the largest loading ratio (0.165).

Fig 9.3.9 represents a similar procedure that was done in Fig. 9.3.5 excludes the loading ratio which equals to 0.165.

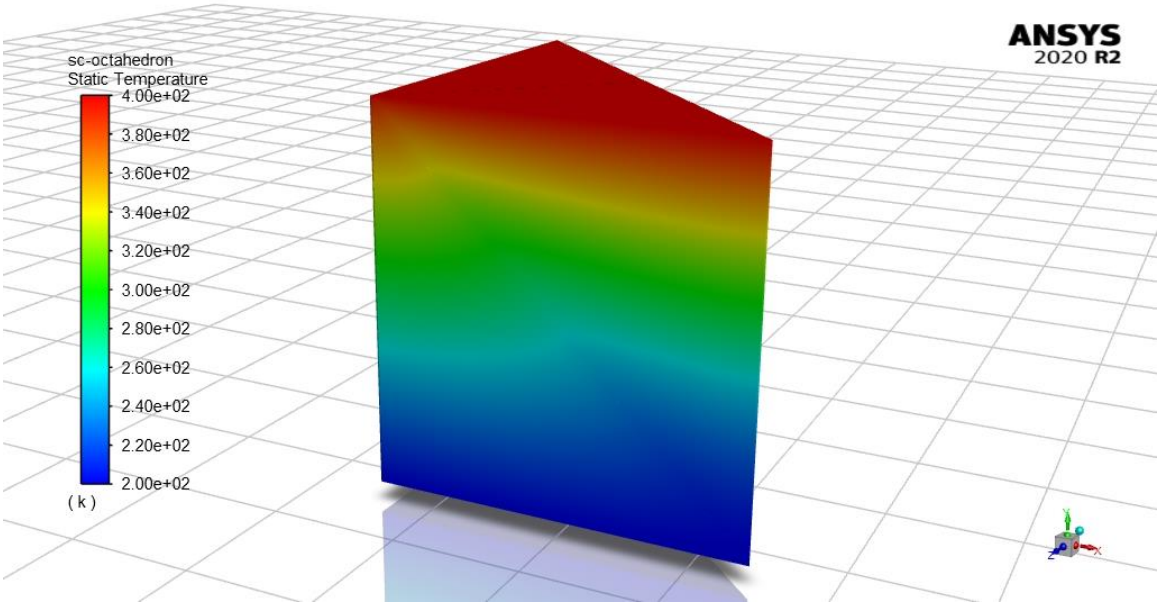

Fig 9.3.9. Representation of simple cubic (SC) octahedron contour of the largest loading ratio (0.165) and lowest permeability ratio (0.001).

Fig. 9.3.10 demonstrates an analogous approach that was accomplished in Fig. 9.3.6. As it has been indicated that higher thermal conductivity of the dispersed phase can affect the transport of energy

because of the conduction strength. As shown in Fig. 9.3.10, the largest zone has a red colour which is equal to 400 K.

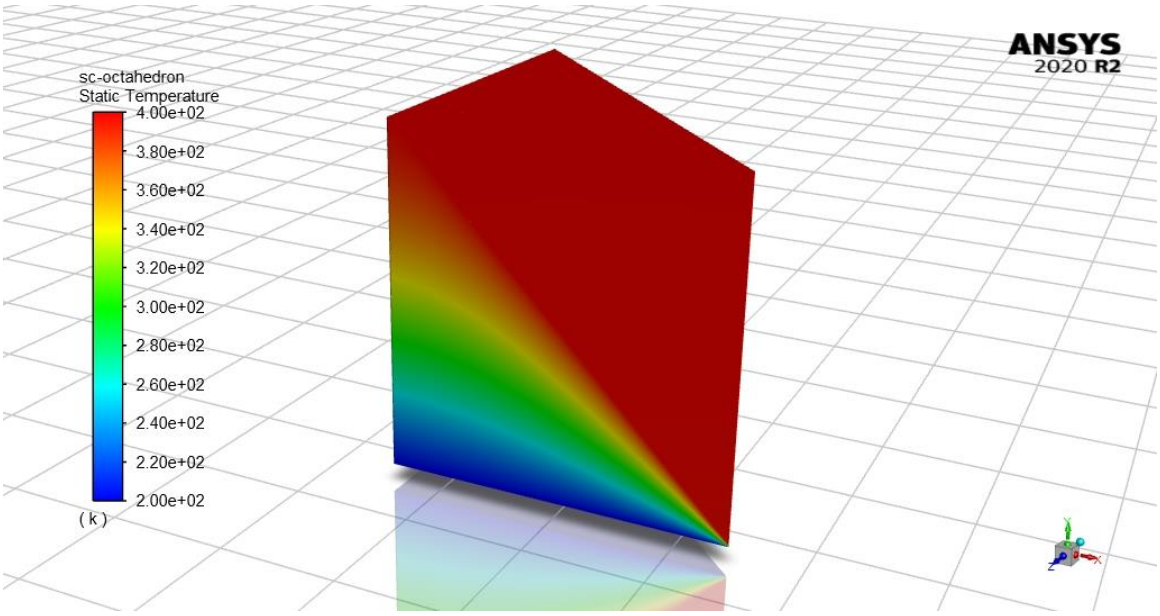

Fig 9.3.10. Representation of simple cubic (SC) octahedron contour of the largest loading ratio (0.00195) and highest permeability ratio (1000).

Figs. 9.3.11-13 show a matrix without its dispersed phase in which it has been extracted, then the heat flux has been calculated into two additional steps , first step when the permeability ratio is equal to zero in which the dispersed phase does not influence the matrix domain because the thermal conductivity of the dispersed phase is too low and vice versa for the second step, when the permeability ratio is equal to ∞ in which the extracted dispersed phase is conducted well due to its higher thermal conductivity. Thus, it could be said that the contact zone temperature equals to inlet or outlet temperature of the matrix. However, the value of ∞ cannot be added as input in the program. Thus, the dispersed phase has been removed phase from the domain. Moreover, these two steps can be employed as verified steps for the work.

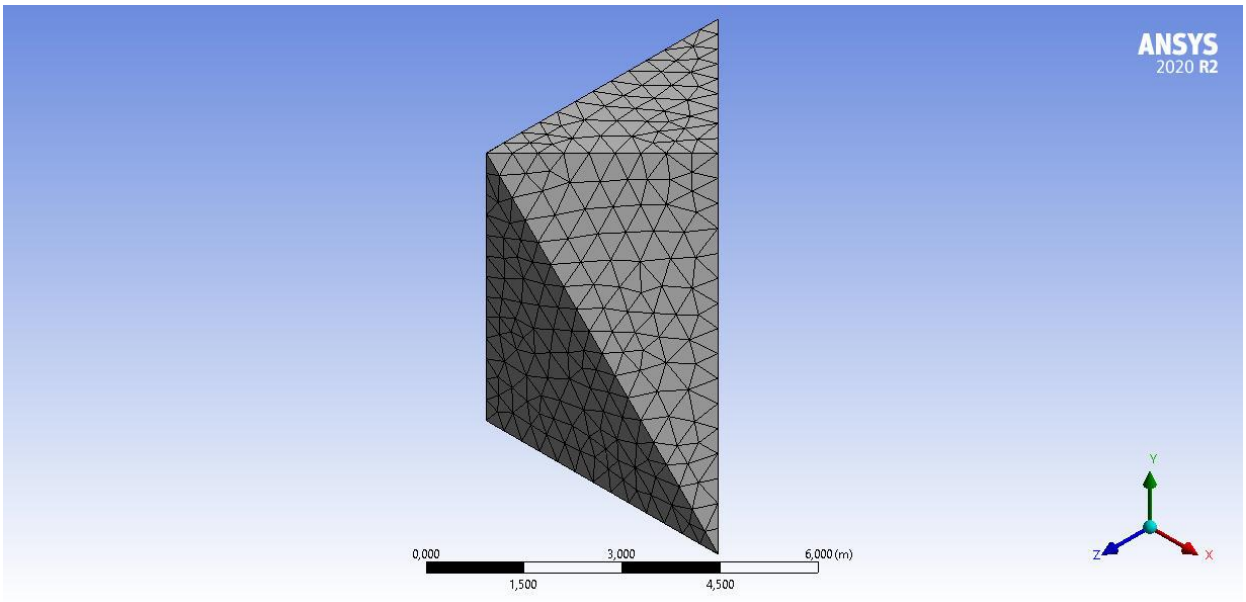

Fig 9.3.11 Representation of simple cubic (SC) octahedron mesh of the largest loading ratio (0.165) for the case of 0 & ∞ permeability ratios.

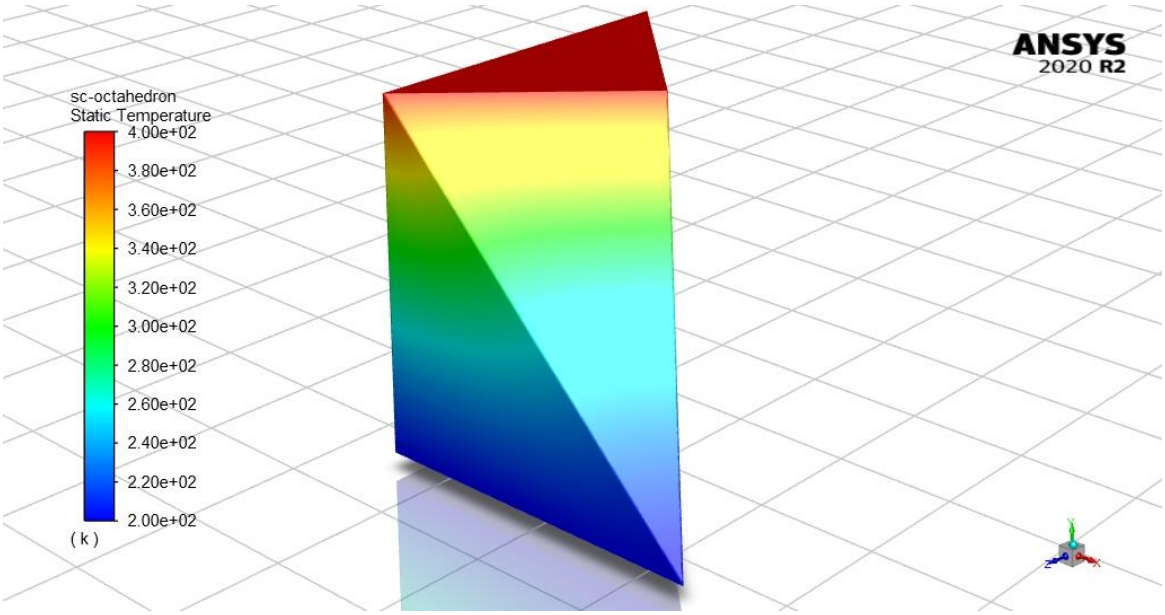

Fig. 9.3.12. Representation of simple cubic (SC) octahedron contour of (0) permeability ratio.

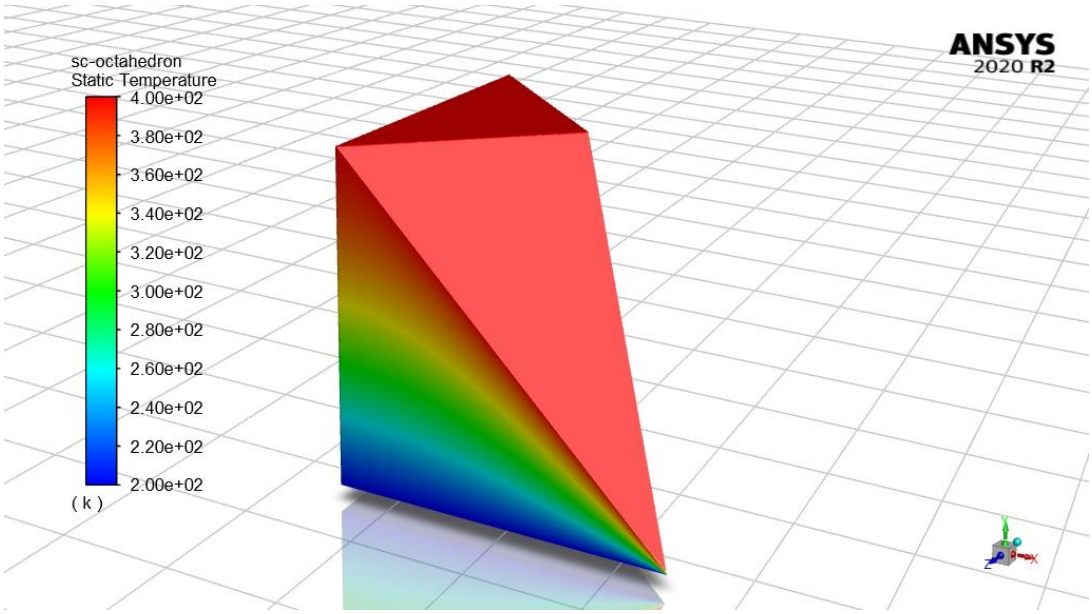

Fig. 9.3.13. Representation of simple cubic (SC) octahedron contour of (∞) permeability ratio.

9.3.2. Prediction of the Effective Thermal Conductivity of Face Centered Cubic (FCC) Rhombic Dodecahedron:

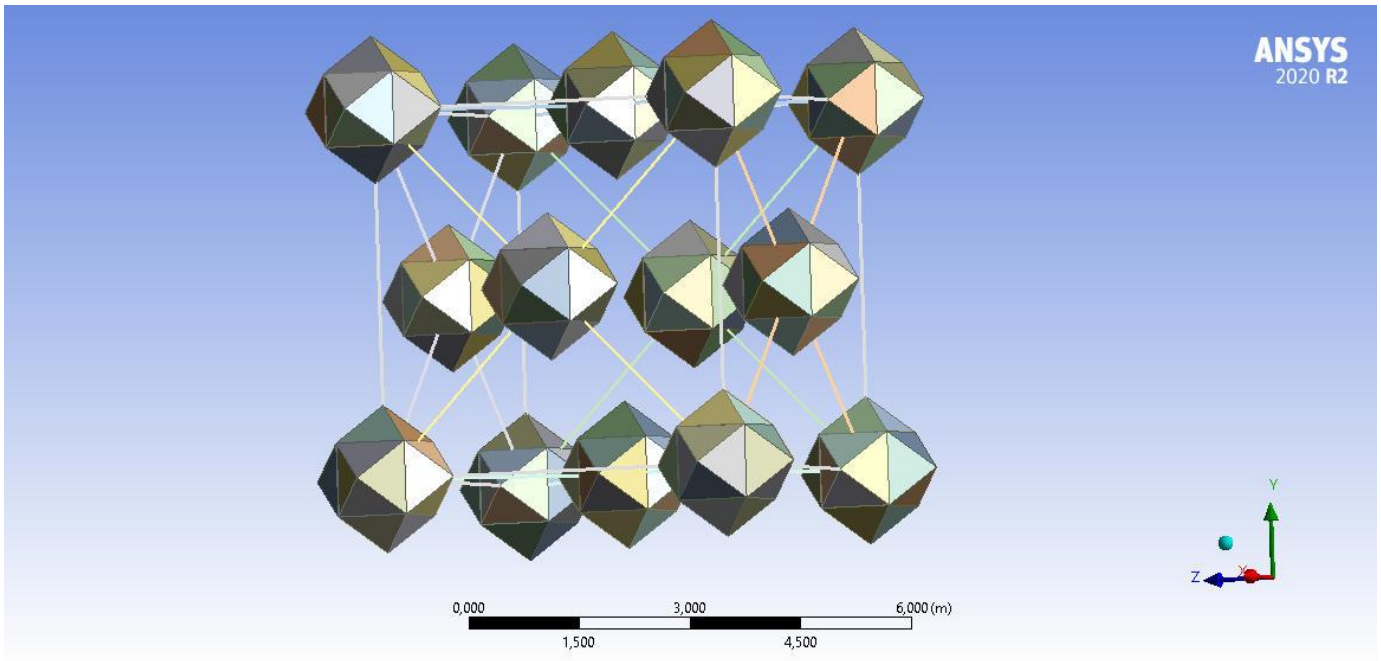

Fig. 9.4.1. Representation of face centered cubic (FCC) rhombic dodecahedron lattice.

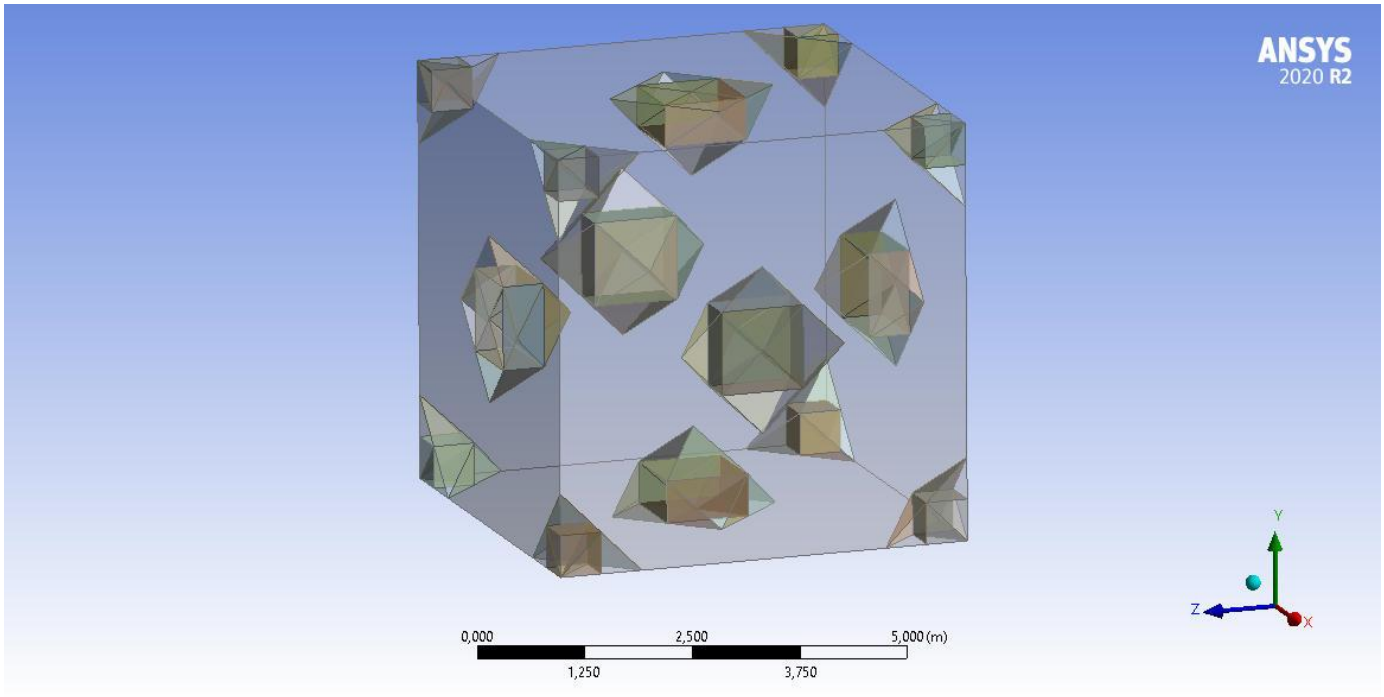

Fig. 9.4.2. Representation of face centered cubic (FCC) rhombic dodecahedron repeated unit.

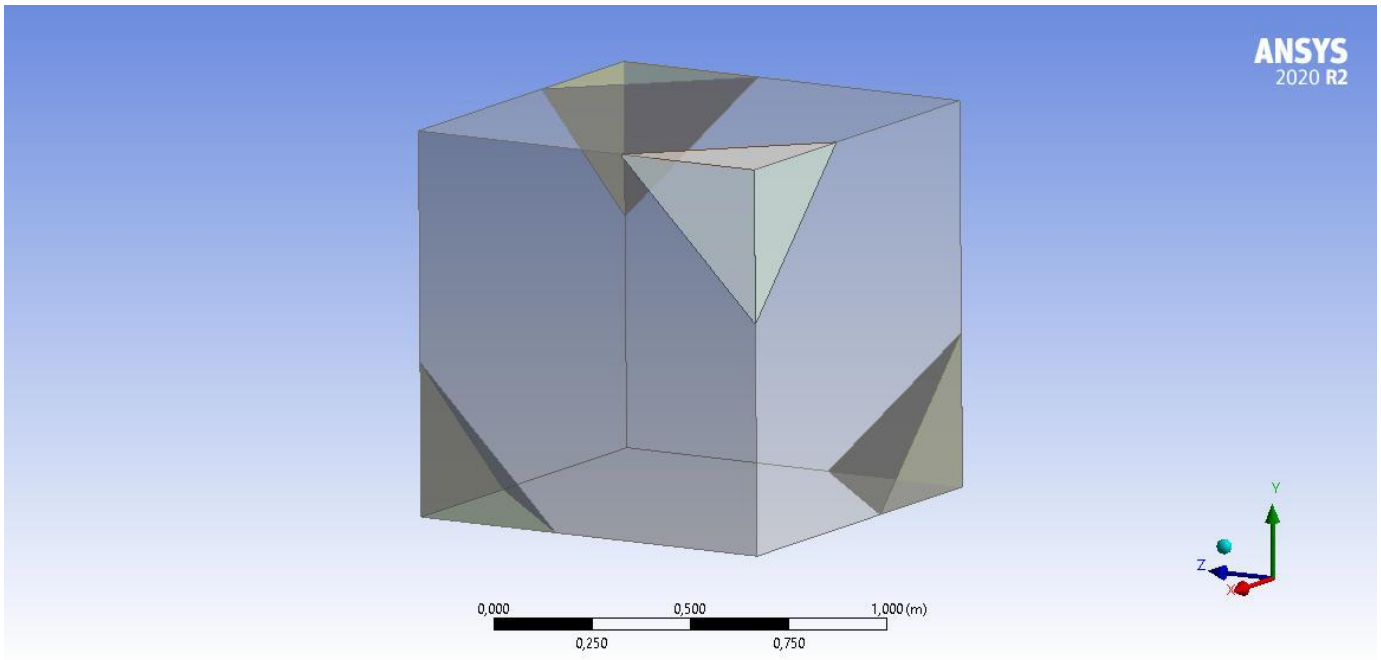

Fig. 9.4.3. Representation of face centered cubic (FCC) of the calculation domain rhombic dodecahedron.

9.3.3. Prediction of the Effective Thermal Conductivity of Body Centered Cubic (BCC) Truncated Octahedron:

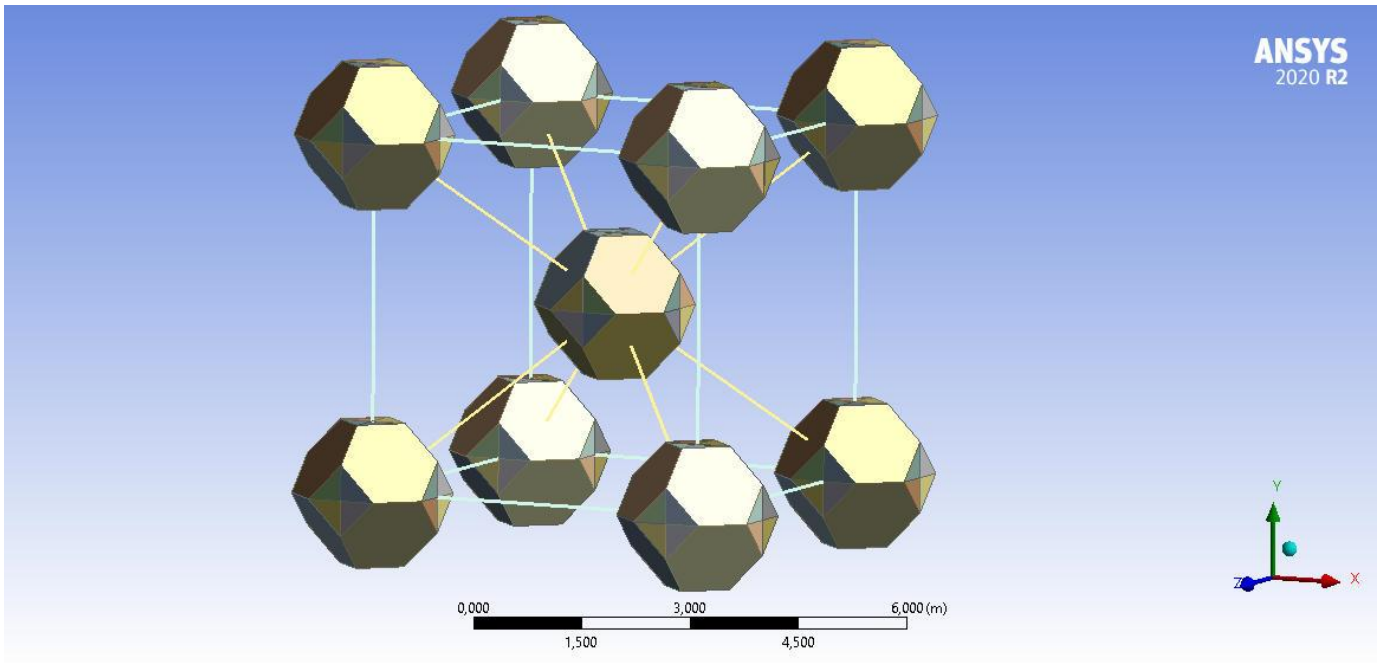

Fig. 9.5.1. Representation of body centered cubic (BCC) truncated octahedron lattice.

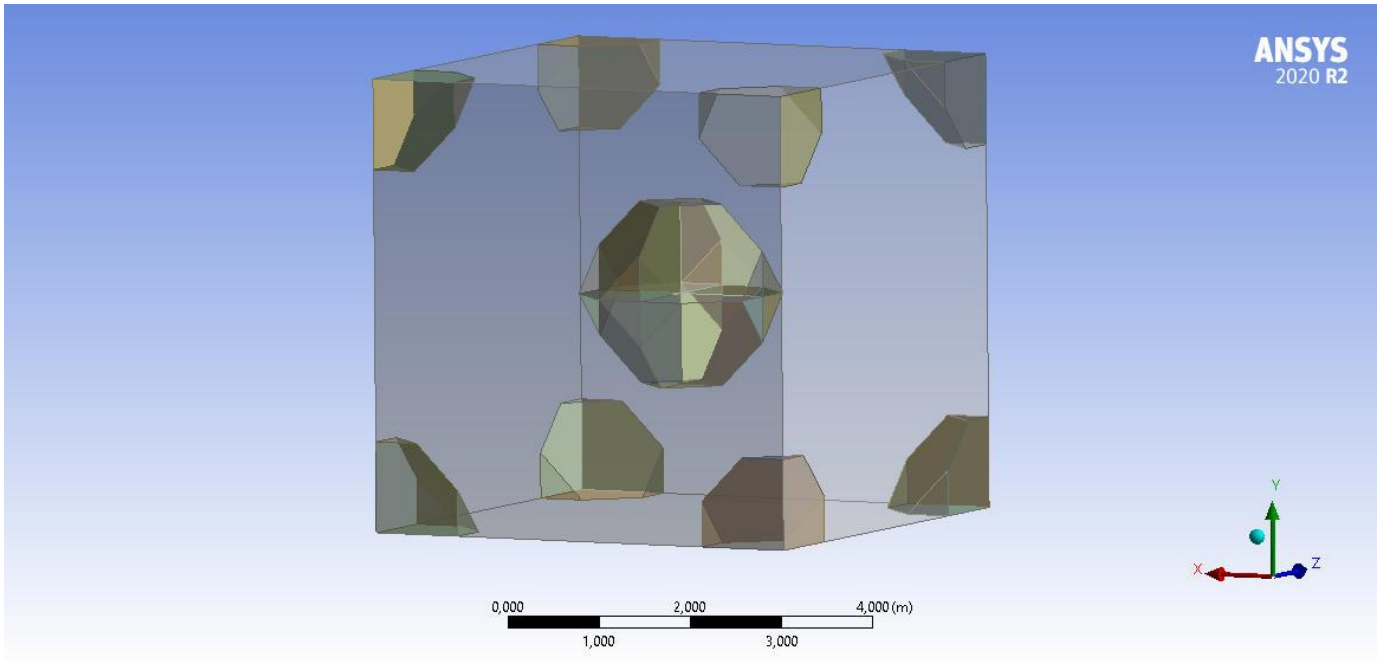

Fig. 9.5.2. Representation of body centered cubic (BCC) truncated octahedron repeated unit.

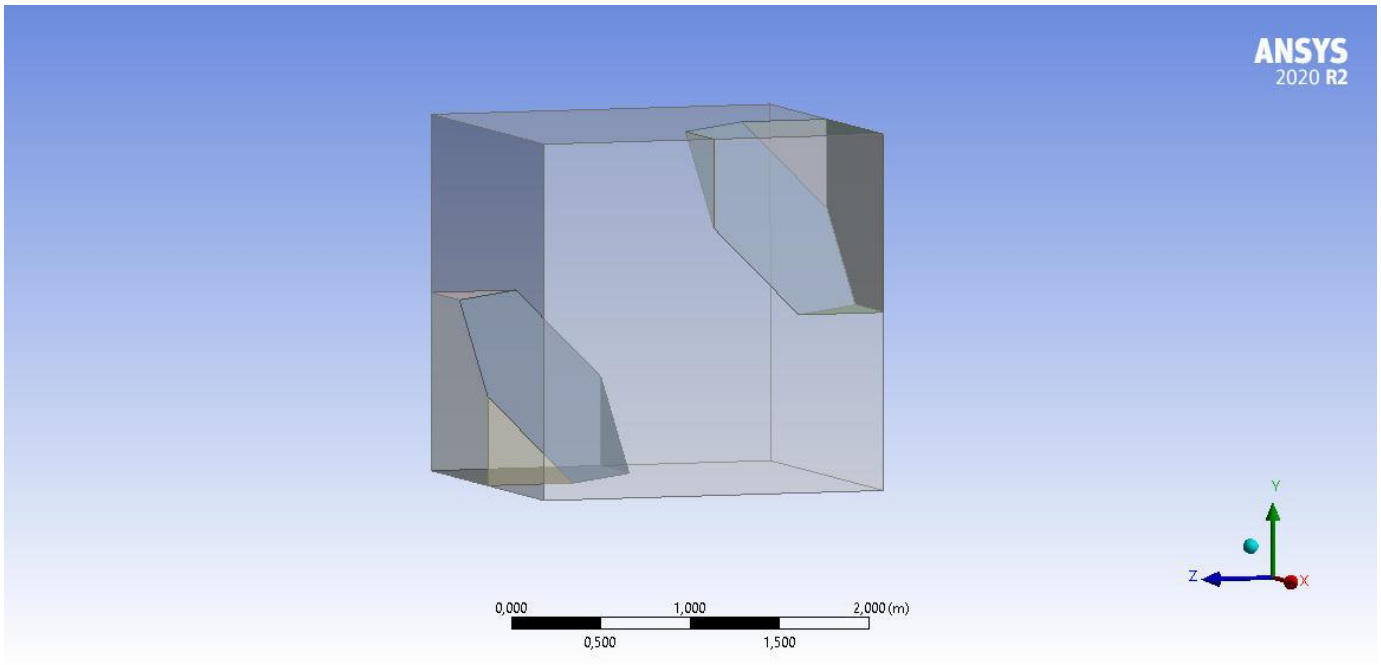

Fig. 9.5.3. Representation of body centered cubic (BCC) of the calculation domain truncated octahedron.

9.3.4. Prediction of the Effective Thermal Conductivity of Simple Cubic (SC) Cube:

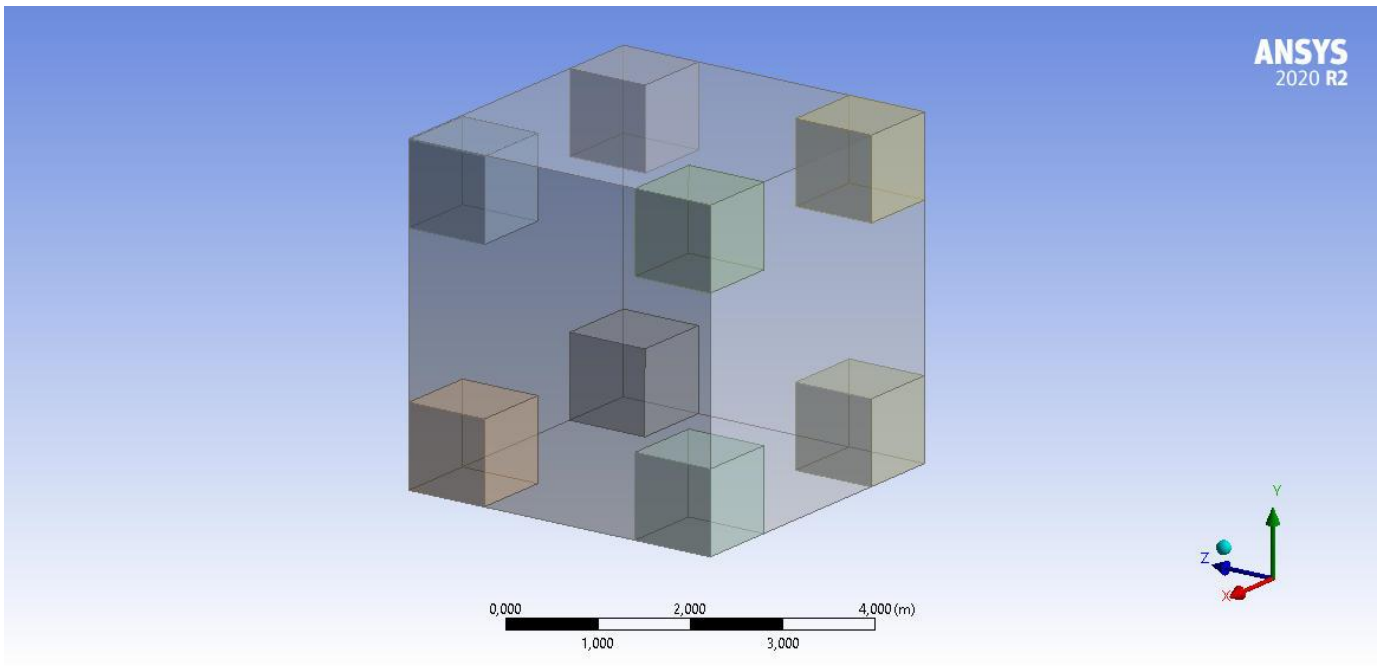

Fig. 9.6.1. Representation of simple cubic (SC) cube repeated unit.

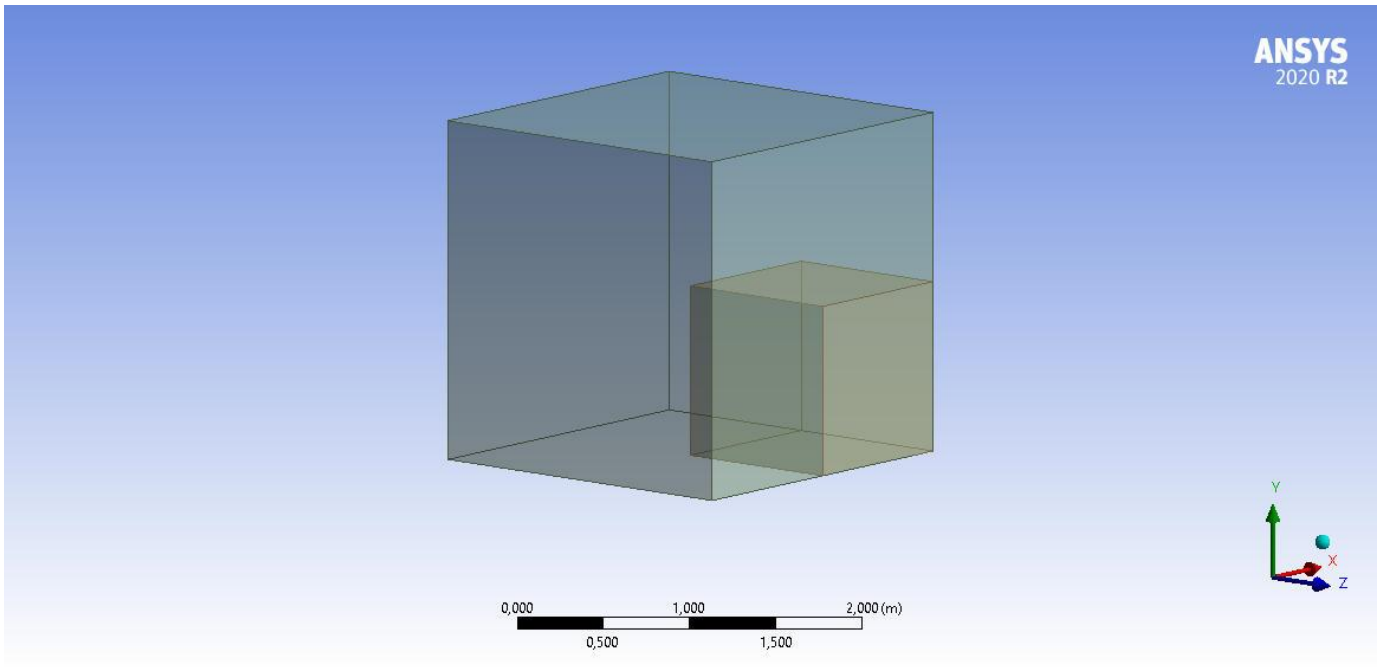

Fig. 9.6.2. Representation of simple cubic (SC) cube of the calculation domain.

9.3.5. Prediction of the Effective Thermal Conductivity of Body Centered Cubic (BCC) Sphere:

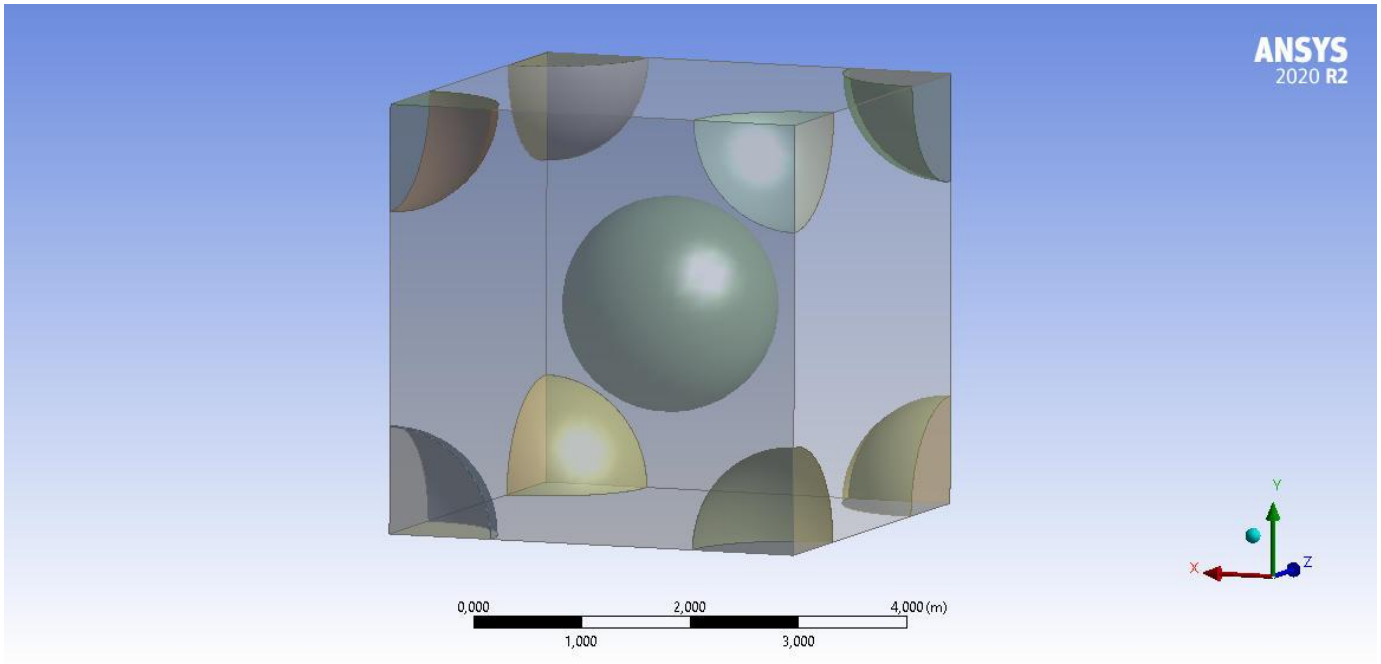

Fig. 9.7.1. Representation of body centered cubic (BCC) sphere repeated unit.

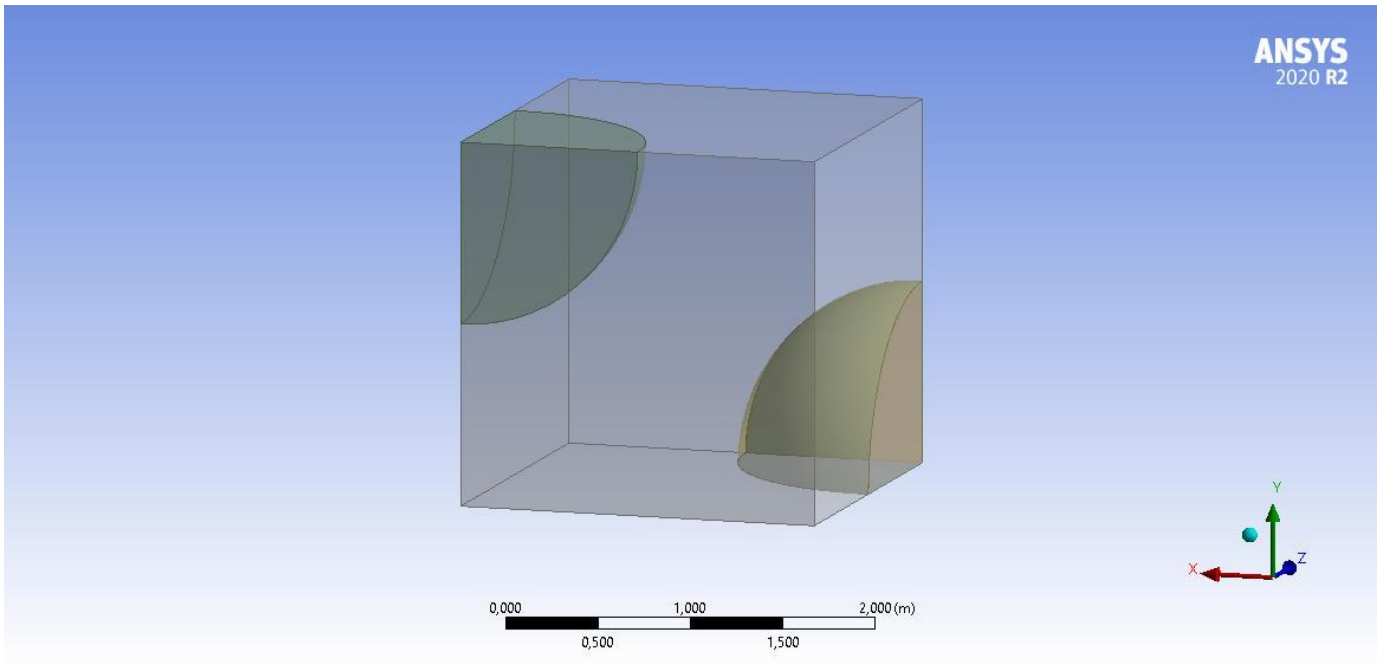

Fig. 9.7.2. Representation of body centered cubic (BCC) sphere of the calculation domain.

9.3.6. Prediction of the Effective Thermal Conductivity of Face Centered Cubic (FCC) Sphere:

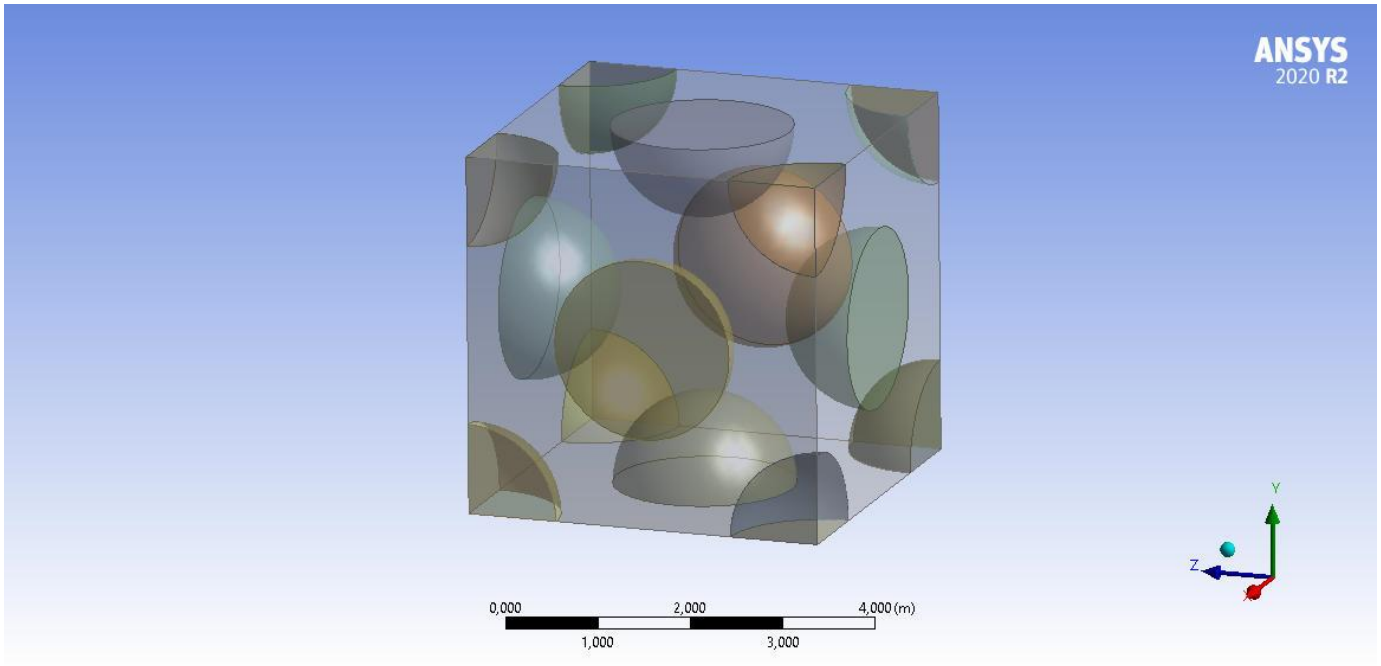

Fig. 9.8.1. Representation of face centered cubic (FCC) sphere repeated unit.

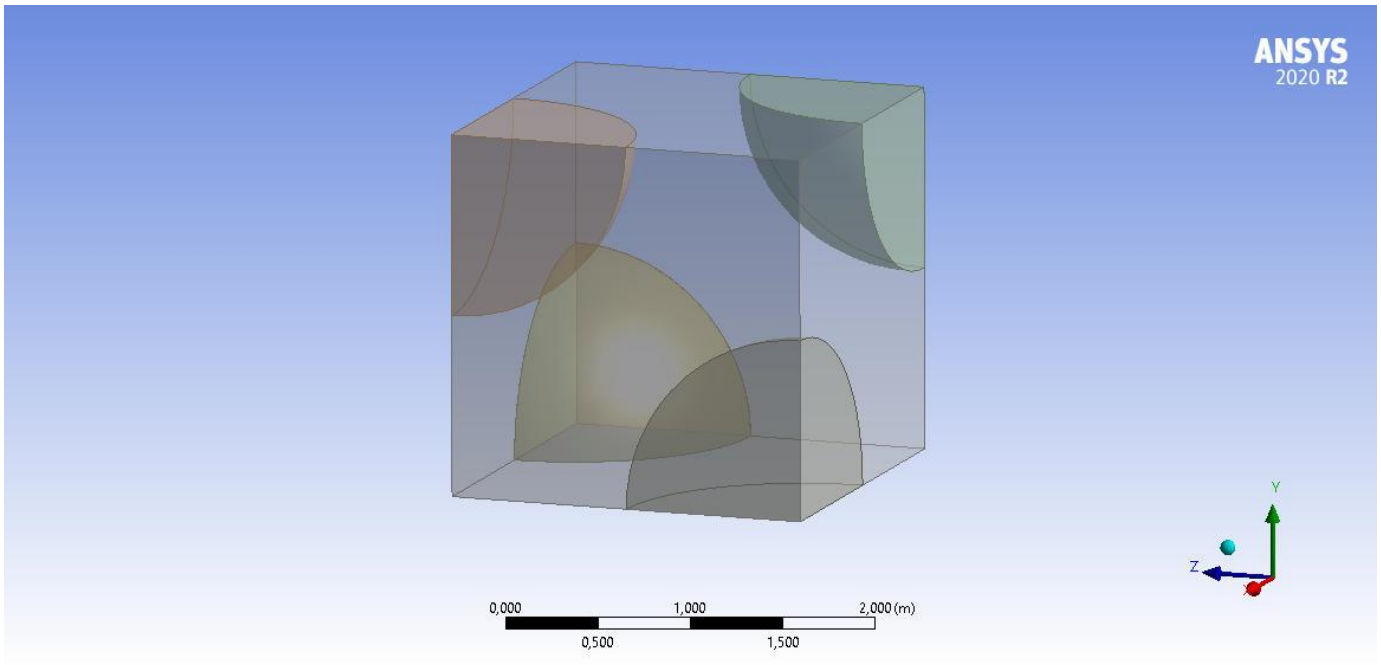

Fig. 9.8.2. Representation of face centered cubic (FCC) sphere of the calculation domain.

9.3.7. Prediction of the Effective Thermal Conductivity of Simple Cubic (SC) Sphere:

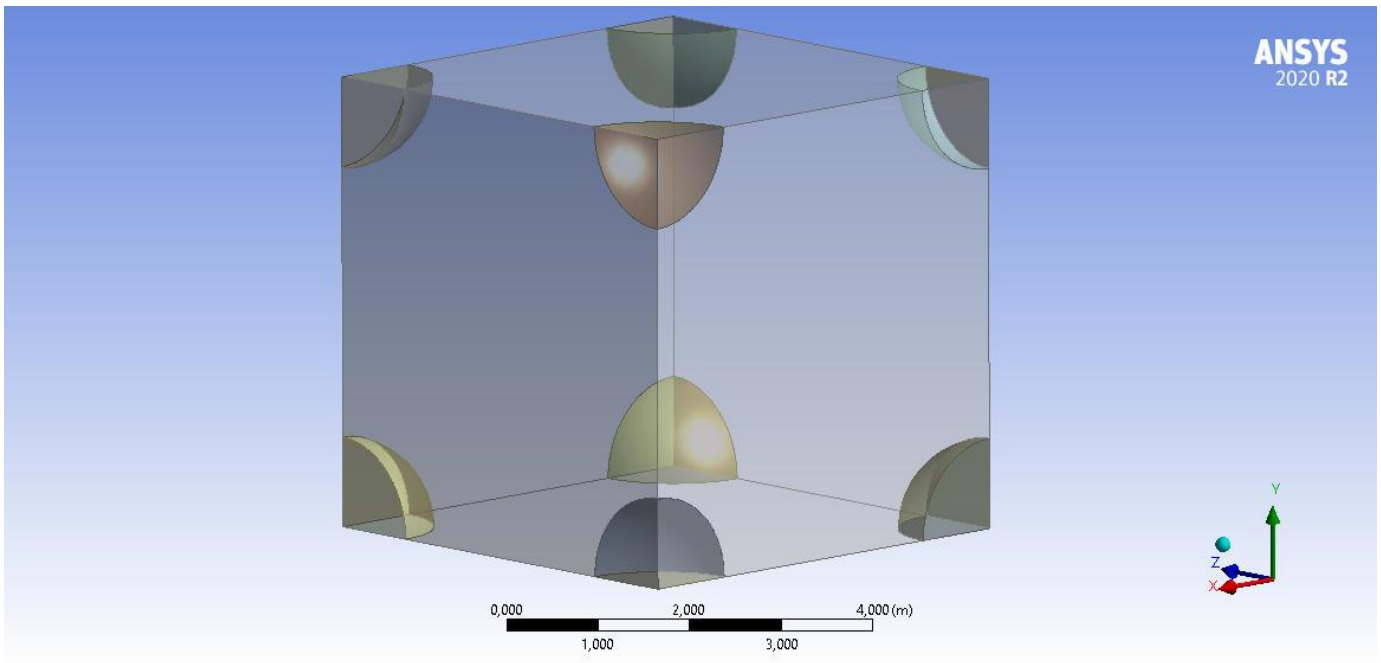

Fig. 9.9.1. Representation of simple cubic (SC) sphere repeated unit.

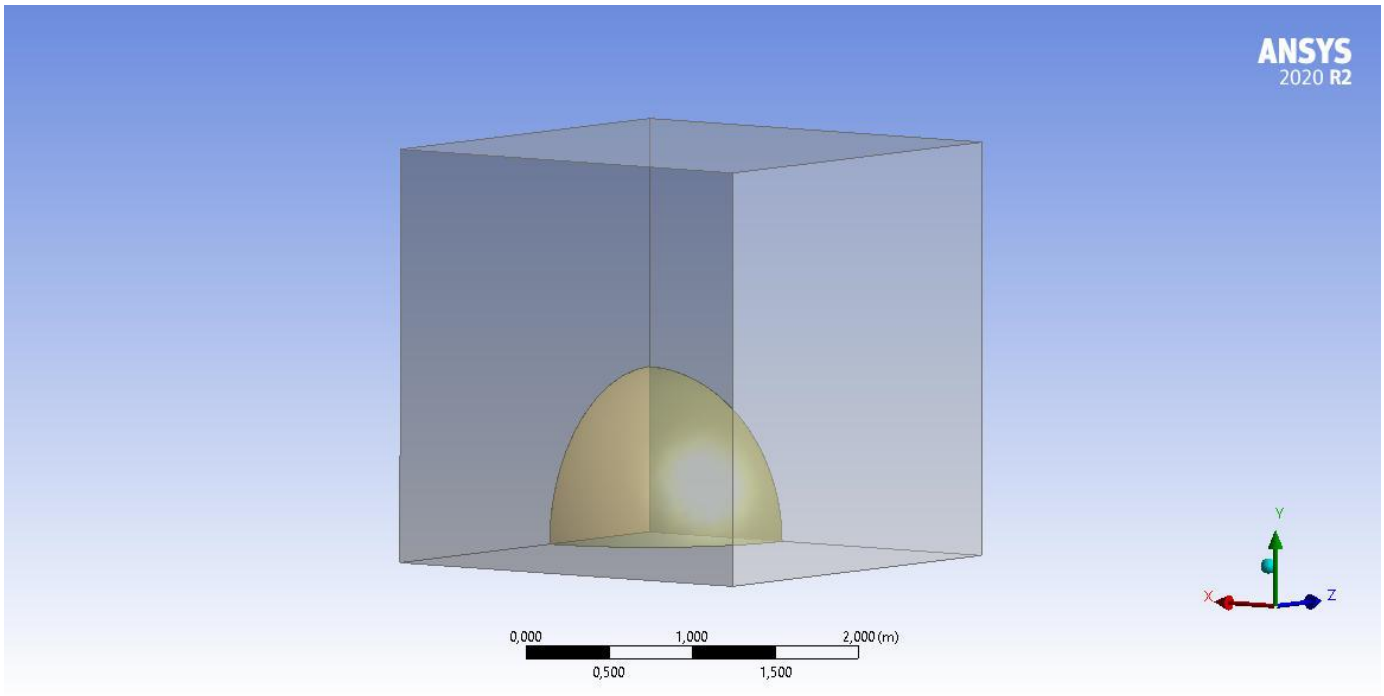

Fig. 9.9.2. Representation of simple cubic (SC) sphere of the calculation domain.

9.4. Results:

While more complex geometries are of interest in this study, only results for isotropic distribution of dispersed domains in the continuous phase are shown here. As all geometries considered result is isotropic transport properties of the composite material, we can ignore the specific direction of principal axes and refer to a single value of the permeability P and of the corresponding enhancement factor K, for which the expression of the coefficient Y can be simplified as indicated hereafter:

$$\Psi \equiv \frac{(\alpha+1)}{(\alpha-1)}\left\{\frac{3\left(\frac{1}{K}-1\right)}{(1-\phi)(\alpha-1)}-1\right\} \qquad (9.4.1)$$

which ultimately can be rearranged to express the permeability P in the composite material as:

$$\frac{P}{P_B} = 1+\frac{3\phi(\alpha-1)}{3+(1-\phi)(\alpha-1)\left[1+\Psi_{(\phi,\alpha)}\frac{(\alpha-1)}{(\alpha+1)}\right]} \qquad (9.4.2)$$

which, of course, resembles the Maxwell expression for the case of null value of coefficient Ψ.

(Eq.9.4.2) represent the main result in the preliminary analysis performed in this work as it allows to represent permeability data in a general isotropic composite medium though a Maxwell-type expression. Indeed, results reported in this section for coefficient Ψ can thus be seen as representation of deviation of actual permeability from Maxwell model, for the condition of interest. In this respect, it should also been considered that, as factor β= (α-1)/(α+1) is of order one for both high and low values of permeability ratio, the relevance of correction factor in (Eq.9.4.2) with respect to Maxwell relation can be identify from the order of coefficient Ψ.

The relative uncertainty ε_P for the value of effective permeability $\overline{P}$ estimated for the numerical procedure described above $P = \overline{P}\left(1 \pm \varepsilon_P\right)$ was estimated in the order of $\varepsilon_P \approx 10^{-4}$, from the exam of results obtained for the use of different mesh type and element size.

By means of the analysis of error propagation, from the expression of effective permeability P to that of deviation coefficient Ψ , through the representation of enhancement factor K, the following expression is obtained for the uncertainty affecting the estimate $\overline{\Psi}$ of the deviation coefficient :

$$\Psi = \overline{\Psi}\left(1 \pm \varepsilon_\Psi\right)$$

$$\varepsilon_\Psi = \varepsilon_P \left| 1 + \frac{\alpha + 1 + (1-\phi)\left(\alpha + 1 + \overline{\Psi}(\alpha - 1)\right)(\alpha - 1)}{\phi(\alpha - 1)(\alpha + 1)} \right| \left| 1 + \frac{\alpha + 1}{\left(\alpha + 1 + \overline{\Psi}(\alpha - 1)\right)(1-\phi)(\alpha - 1)} \right| \left| 1 + \frac{\alpha + 1}{\overline{\Psi}(\alpha - 1)} \right|$$

(9.1.11)

From the expression above, it can be calculated that the relative error for deviation coefficient Ψ computed through the above procedure is typically in the order of 1% for the case of limiting values of permeability ratio ($\alpha \to 0$ and $\alpha \to \infty$). On the other hand, it also results that uncertainty for the estimated deviation coefficient increases indefinitely when permeability ratio is close to 1. For this reason, the numerical results were not considered in the analysis for permeability ratio in the range $0.25 < \alpha < 4$, where relative uncertainty for Ψ exceeds 10%. It is also in evidence, in the above expression, that the uncertainty depends on the order of the same coefficient Ψ and it can be concluded that relative error for the deviation coefficient approaches 100% when the absolute value of calculated $\overline{\Psi}$ decreases below 10^{-3}.

For each case of geometry and loading considered in this work, coefficient Ψ has been calculated for the following list of values of permeability ratio α: {0, 0.001, 0.01, 0.1, 0.25, 0.5, 2, 4, 10, 100, 1000, ∞}. The results for Ψ are finally shown in plots as function of parameter β = (α-1)/(α+1). In all plots, trends

are highlighted separately for negative and positive β, respectively corresponding to values of a lower and higher than 1, because uncertainty for coefficient Ψ calculated for a higher than 0.5 but lower than 2.0 was considerably larger than that associated to points in the rest of the range for a and definitely not acceptable for the purpose of this work.

The first case here represented is that of isotropic ordered lattice of spheres. Three different types of cubic lattice were considered: “simple cubic” (SC) lattice, “body centered cubic” (BCC) lattice and “face centered cubic” (FCC) lattice. Results are shown in (Fig. 9.10), for the case of two different loading values for each type of lattice, always pointing at the largest admissible value of ϕ which is consistent with the geometry of interest.

It can be recognized that smooth variation of coefficient Ψ are estimated for variations of permeability ratio in the whole range from zero to infinity, while the value of the same coefficient decreases when the loading decreases, as expected in view of the Maxwell result for vanishing fraction of dispersed phase. It can be also appreciated, from data in the plot, that highest measured Ψ values (in the order of 30%) correspond to the arrangement of simple cubic lattice, high loading. Less than half the value of Ψ is obtained for the case of FCC loading and even lower level are registered for the case of BCC lattice.

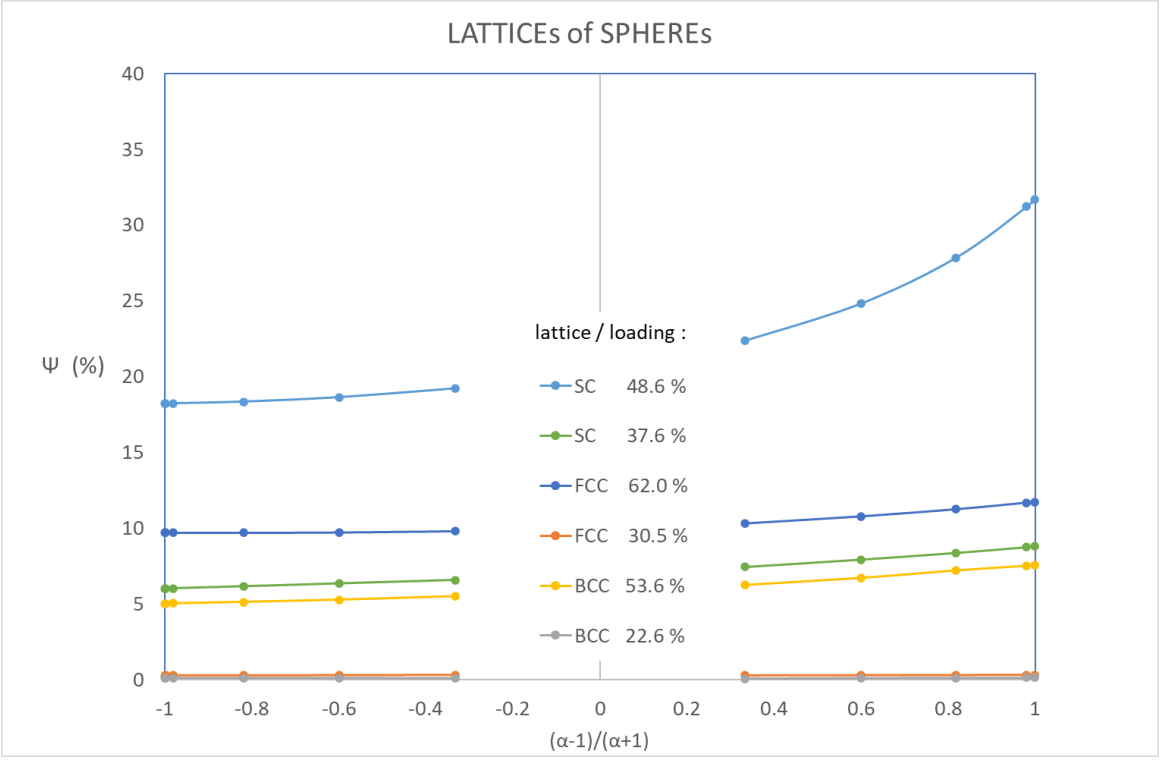

Fig. 9.10. Ψ coefficient calculated for regular cubic lattice of sphere, as function of loading and permeability ratio.

In (Fig.9.11) results are reported for the case of simple cubic lattice of cubes and it can be observed that the coefficient Ψ mainly depends on the loading, while only minor variation results from change in

permeability ratio. It can be also observed that the higher the loading the lower the value of Ψ. Indeed, a higher limit value, in the order of 17%, seems to be reached for vanishing loading, although results from calculation for value of ϕ lower than 1% are not reported, as they reveled to be not accurate enough to be compared with others.

Interestingly, at very high loading (for this geometry there is no limit to admissible value of ϕ), coefficient Ψ seems to vanish, although results from calculation for value of ϕ higher than 90% are not reported as they reveled to be not accurate enough to be compared with the remaining.

With reference to the same type of lattice (simple cubic), Fig.9.12 show the value of coeffiicent for the case of dispersed domain shaped in regular octaherdrons. It can be observed that, unlike the case of cubes, but similar to that of spheres, higher deviations for Maxwell results are observed for higher loading. Dependence of coefficient Ψ on permeability ratio is higher than in the case of cubes (the coefficient results higher for higher permeability ratio), although the dependece remains smooth, again similar to the case of spheres.

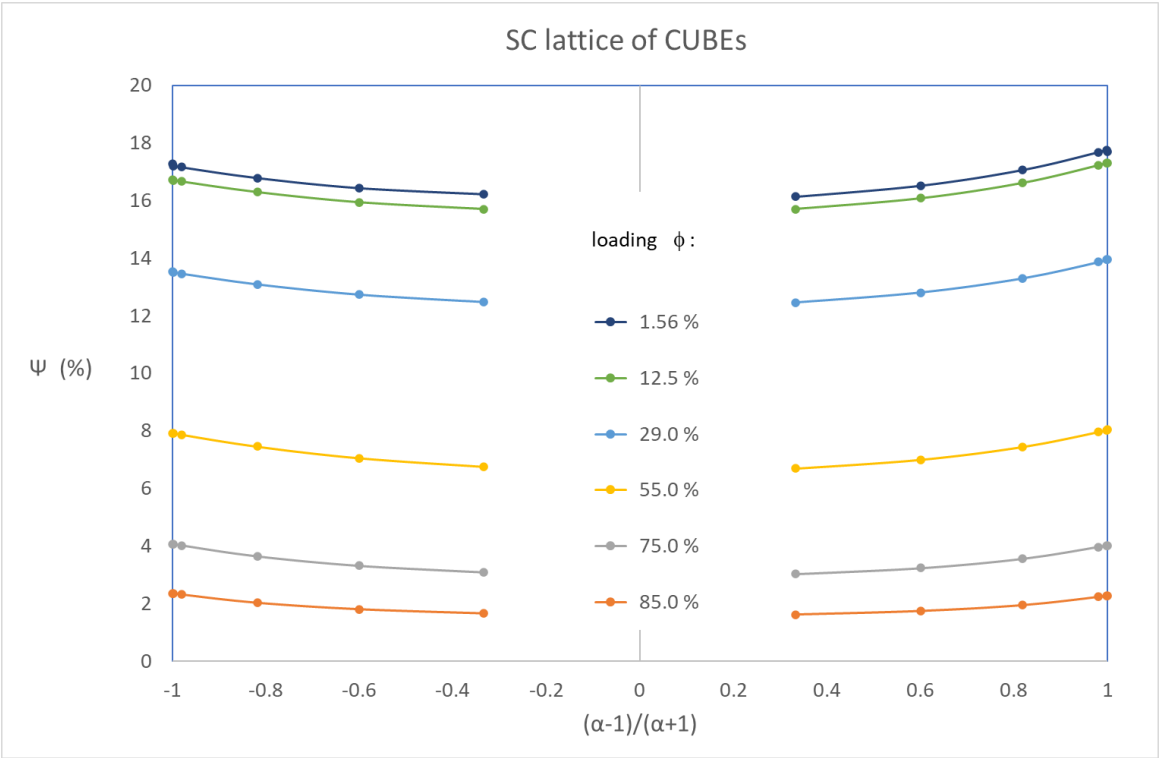

Fig. 9.11. Ψ coefficient calculated for regular simple cubic lattice of cubes, as function of loading and permeability ratio.

Last two figures in this section are pertinent to two different lattice type (FCC and BCC). For each type of lattice, domains are considered of that shape which allow to explore the whole range of loading values,

from null to unity, just as it happens for SC in the case of cubic inclusions. Corresponding solid are “rhombic dodecahedron” for FCC lattice and “truncated octahedron” for BCC.

Results are reported in (Fig.9.13) and (9.14), where coefficient Ψ is shown to change mostly with loading and only slightly with permeability ratio and in both cases they results be signifincantly lower (in the order of 7% maximum) than in the case of cubes. With repect to effect of loading, it clearly results that the coefficient generally decreases with loading and it appears to vanish for the case of $\phi \to 1$. In both cases, however, a maximum in the coefficient Ψ results for loading variation in the region of dilute dispersion.

The observation about order of deviation coefficient for higest loading, in all example considered, confirms the hypothesis stated in the mentioned paper by [Petropoulos,1985][60], about thenegligible deviation from Mawell relation for the case of isotropi structure at vey high loading of dispersed phase.

The exam is in order of non isotropic structures, both in terms of coefficient Ψ and of ratio of permeability coefficient in different principal directions.

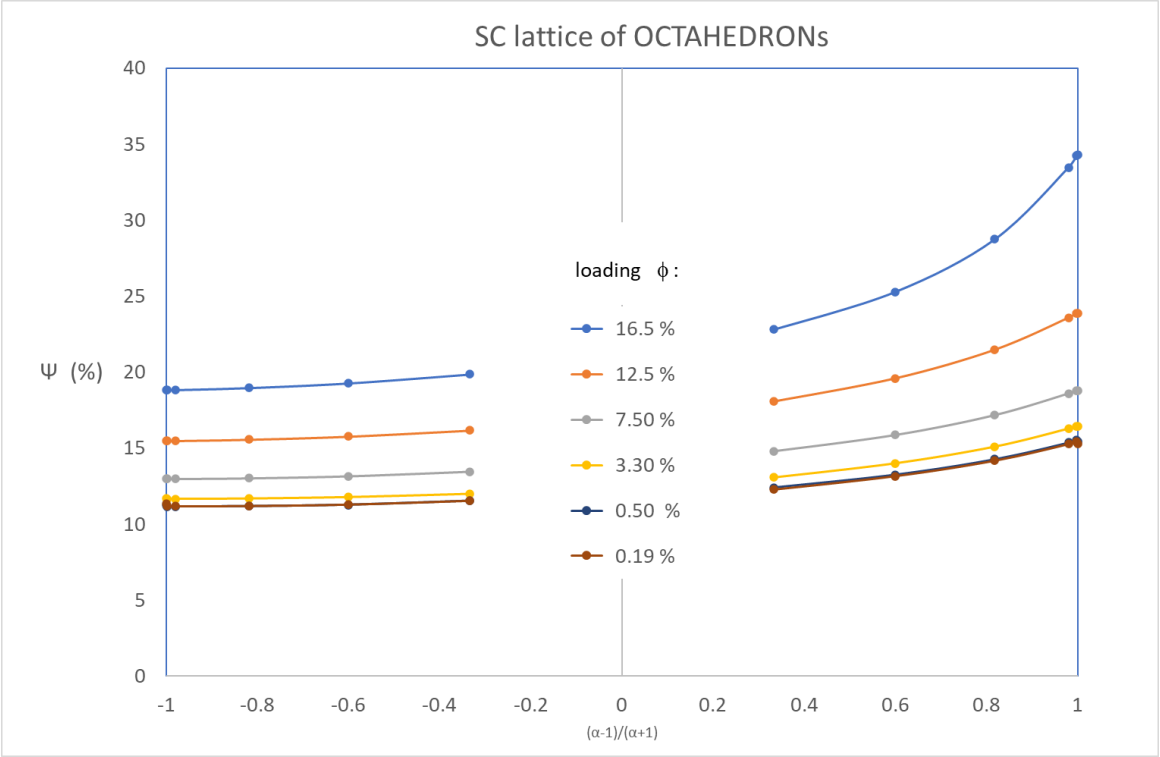

Fig. 9.12. Ψ coefficient calculated for regular simple cubic lattice of cubes, as function of loading and permeability ratio.

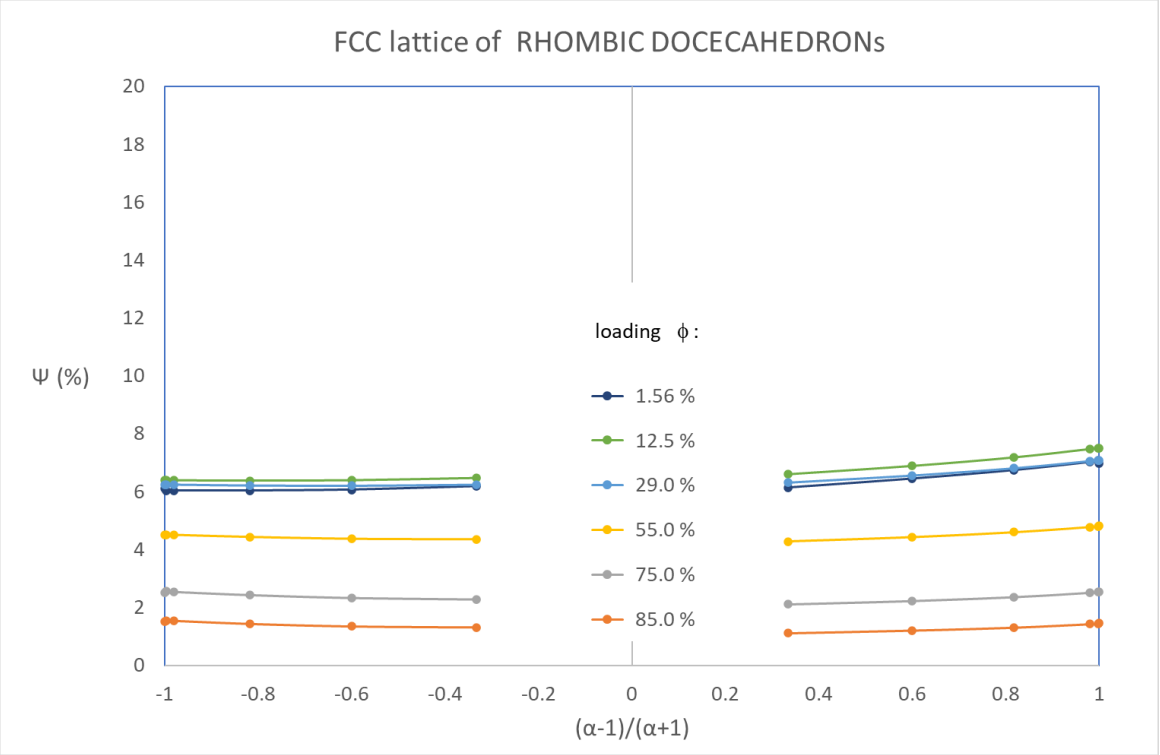

Fig. 9.13. Ψ coefficient calculated for regular face centered cubic lattice of rhombic dodecahedron, as function of loading and permeability ratio.

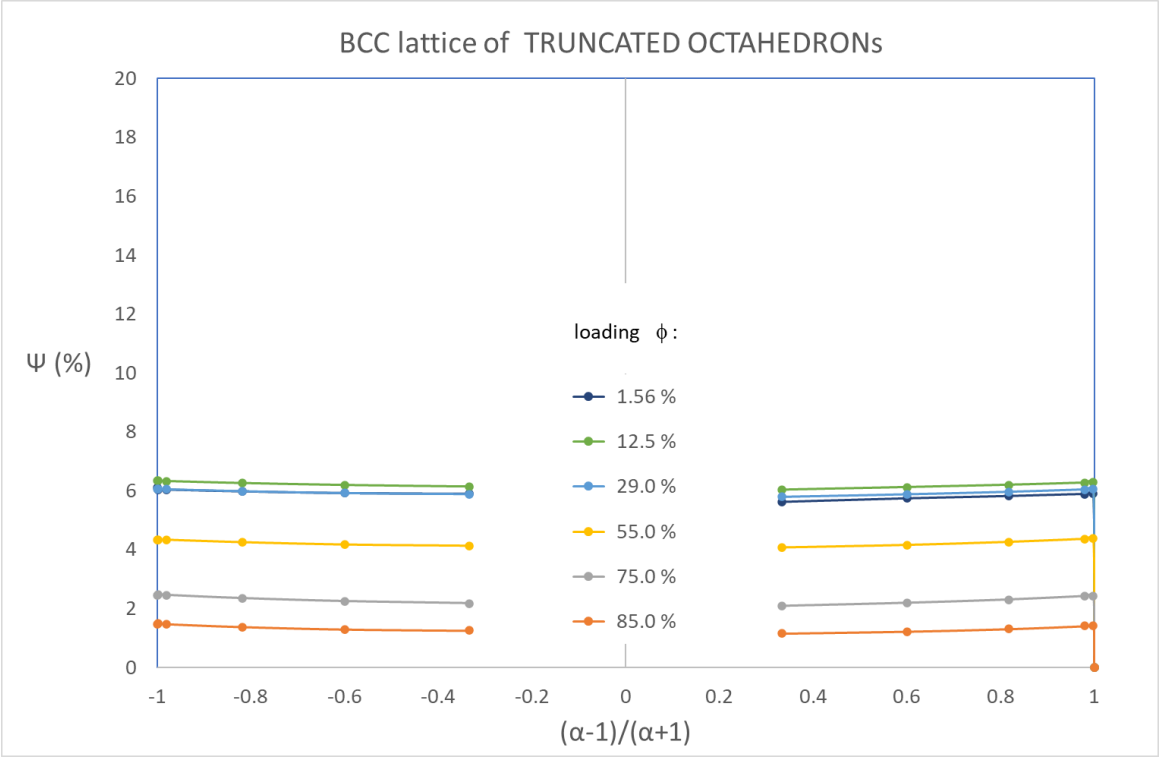

Fig. 9.14. Ψ coefficient calculated for regular body centered lattice of truncated octahedron, as function of loading and permeability ratio.

BIBLIOGRAPHY

[1] Fredenslund, A., Jones, R. and Prausnitz, J., "Group-Contribution Estimation of Activity Coefficients in Nonideal Liquid Mixtures", AIChE J., Vol. 21, 1086 (1975).

[2] Holten-Andersen, J., Rasmussen, P. and Fredenslund, Aa., "Phase Equilibria of Polymer Solutions by Group Contribution. 1. Vapor-Liquid Equilibria", Ind. Eng. Chem. Res., Vol. 26, 1382 (1987).

[3] Chen, F., Fredenslund, Aa. and Rasmussen, P., "Group-contribution Flory equation of state for vapor-liquid equilibria in mixtures with polymers", Ind. Eng. Chem. Res., Vol. 29, 875 (1990).

[4] Lee, B.C., "Prediction of Phase Equilibria in Polymer Solutions'', Ph.D. Dissertation, The Pennsylvania State Univ., University Park, PA (1995).

[5] Lee, B. C. and Danner, R. P., "Prediction of Polymer-Solvent Phase Equilibria by a Modified Group-Contribution EOS'', AIChE. J., Vol. 42, 3 (1996).

[6] Panayiotou, C. and Vera, J. H., "An Improved Lattice-Fluid Equation of State for Pure Component Polymeric Fluids", Polym. Eng. Sci., Vol. 22, 345 (1982).

[7] Panayiotou, C. and Vera, J. H., "Statistical Thermodynamics of r-Mer Fluids and Their Mixtures'', Polym. J., Vol. 14, 681 (1982).

[8] High, M.S. and Danner, R.P., "A Group Contribution Equation of State for Polymer Solutions", Fluid Phase Equilib., Vol. 53, 323 (1989).

[9] Danner, R.P., Hamedi, M. and Lee, B.C., "Applications of the Group-Contribution, Lattice-Fluid Equation of State", Fluid Phase Equilib., Vol.194, 619 (2002).

[10] Hamedi, M., Muralidharan, V., Lee, B.-C. and Danner, R.P., "Prediction of Carbon Dioxide Solubility in Polymers Based on a Group-Contribution Equation of State", Fluid Phase Equilib. 204, 41 (2003).

[11] Doghieri, F. and Sarti, G.C., “Nonequilibrium Lattice Fluids: A Predictive Model for the Solubility in Glassy Polymers”, Macromolecules, Vol. 29, 7885 (1996).

[12] Crank, J., and Park, G. S., “Diffusion in Polymers”, Academic Press, London (1968).

[13] Fick, A., “Fick's second law”, Ann. der Physik., Vol. 94, 59-86 (1855).

[14] High, M. S., “Prediction of Polymer-Solvent Equilibria with a Group Contribution Lattice-Fluid Equation of State”, Ph.D. Thesis, The Pennsylvania State Univ., University Park, PA (1990).

[15] Danner, R.P., and High, M. S., “Polymer Solution Thermodynamics”, AIChE, New York (1993).

[16] William, D., and Callister, J., “Materials Science and Engineering an Introduction”, John Wiley & Sons (2007).

[17] Matteucci, S., Yampolskii, Y., Freeman, B. D. and Pinnau, I., " Transport of Gases and Vapors in Glassy and Rubbery Polymers", Materials Science of Membranes for Gas and Vapor Separation, John Wiley & Sons, Ltd, 1- 48 (2006).

[18] Maxwell, J. C., “A Treatise on Electricity and Magnetism”, Dover Publications, New York (1954).

[19] O’Brien, K. C., Koros, W. J. and Barbari, T. A., “A New Technique for Measurement of Multicomponent Gas Transport Through Polymeric Films”, Vol. 29, 229-238 (1986).

[20] Zornoza, B., Tellez, C., Coronas, J., Gascon, J. and Kapteijn, F., "Metal Organic Framework Based Mixed Matrix Membranes: An Increasingly Important Field of Research with A Large Application Potential", Microporous and Mesoporous Mater., Vol. 166, 67-78 (2013).

[21] Pandey, P. and Chauhan, R. S., "Membranes for Gas Separation", Porg. Polym. Sci., Vol. 26, 853-893 (2001).

[22] Rezakazemi, M., Amooghin, A. E., Montazer-Rahmati, M. M., Ismail, A. F. and Matsuura, T., "State-of-the-Art Membrane Based CO2 Separation Using Mixed Matrix Membranes (MMMs): An Overview on Current Status and Future Directions", Prog. Polym. Sci., Vol. 39, 817-861 (2014).

[23] Bernardo, P., Drioli, E. and Golemme, G., "Membrane Gas Separation: A Review/State of the Art", Ind. Eng. Chem. Res., Vol. 48, 4638-4663 (2009).

[24] Javaid, A., "Membranes for Solubility-Based Gas Separation Applications", Chem. Eng. J., Vol. 112, 219-226 (2005).

[25] Flory, P. J., "Thermodynamics of High Polymer Solutions," J. Chem. Phys., Vol. 9, 660 (1941).

[26] Flory, P.J., Oriji, R.A. and Vrij, A., “Statistical Thermodynamics of Chain Molecule Liquids. I. An Equation of State for Normal Paraffin Hydrocarbons”, J. Am. Chem. Soc., Vol. 86, 3507 (1964).

[27] Sanchez, L.C. and Lacombe, R.H., “An Elementary Molecular Theory of Classical Fluids. Pure Fluids” J. Phys. Chem., Vol. 80, 2352 (1976).

[28] Sanchez, I. C. and Lacombe, R. H., "Statistical Thermodynamics of Polymer Solutions," Macromolecules H 1145 (1978).

[29] MacHugh, M.A. and Krukonis, V.J., “Supercritical Fluid Extraction: Principles and Practice”, 2nd Edition, H. Brenner, Boston (1993).

[30] West, B.L., Bush, D., Brandley, N.H., Vincent, M.F., Kazarian, S.G. and Eckert, C.A. Ind. Eng. Chem. Res., Vol. 37, 3305 (1998).

[31] Sanchez, I.C. and Panayiotou, C., "Equation-of-State Thermodynamics of Polymers and Related Solutions, in: Models for Thermodynamic and Phase Equilibria Calculations", Sandler, S.I., New York (1994).

[32] Fredenslund, Aa., Gmehling, J. and Rasmussen, P., "Vapor-Liquid Equilibria Using UNIFAC", ELSEVIER, New York (1977).

[33] Constantinou, L. and Gani, R., "New Group Contribution Method for Estimating Properties of Pure Compounds", AIChE J., Vol. 40, 1697 (1994).

[34] Daubert, T.E. and Danner, R.P., "Physical and Thermodynamic Properties of Pure Compounds: Data Compilation", Taylor and Francis, New York (extent 1993).

[35] Gmehling, J. and Onken, U., "Vapor-Liquid Equilibrium Data Collection", DECHEMA, Frankfurt, Vol. 1, Parts 1 (1977), 2a (1977).

[36] Gmehling, J., Onken, U. and Arlt, W., "Vapor-Liquid Equilibrium Data Collection", DECHEMA, Frankfurt, Vol. 1, Parts 1a (1981), 2b (1978), 2c (1982), 3 and 4 (1979), 6a (1980), 6b (1980), 7 (1980), 8 (1984).

[37] Gmehling, J., Onken, U. and Grenzheuzer, P., "Vapor-Liquid Equilibrium Data Collection", DECHEMA, Frankfurt, Vol.1 Part 5 (1982). Series, DECHEMA, Frankfurt, Vol. 1, Part 6c (1983).

[38] Gmehling, J., Onken, U. and Weidlich, U., "Vapor-Liquid Equilibrium Data Collection", DECHEMA, Frankfurt, Vol. 1, Part 2d (1982).

[39] Gmehling, J., Onken, U. and Kolbe, B., "Vapor-Liquid Equilibrium Data Collection", DECHEMA, Frankfurt, Vol. 1, Part 6c (1983).

[40] Gmehling, J., Onken, U. and Rarey-Nies, J. R., "Vapor-Liquid Equilibrium Data Collection", DECHEMA, Frankfurt, Vol.1, Parts 1b (1988), 2e (1988), 2f (1990), 3b (1993).

[41] Minelli, M. and Doghieri, F., "A Predictive Model for Vapor Solubility and Volume Dilation in Glassy Polymers" Ind. Eng. Chem. Res., Vol. 51,16505 (2012).

[42] Zoller, P., Walsh, D., “Standard Pressure−Volume−Temperature Data for Polymers”, Technomic, Lancaster, 1995.

[43] Kamiya, Y., Mizoguchi, K., Hirose, T. and Naito, Y., “Sorption and Dilation in Poly(Ethyl Methacrylate)−Carbon Dioxide System”, J. Polym. Sci. B: Polym. Phys. 27, 879 (1989).

[44] Koros, W.J., Smith, G.N. and V. Stannett, “High-Pressure Sorption of Carbon Dioxide in Solvent-Cast Poly(methyl methacrylate) and Poly(ethyl methacrylate) Films”, J. Appl. Polym. Sci., Vol. 26, 159 (1981).

[45] Chern, R.T., Jia, L., Shimoda, S. , and Hopfenberg, H.B., “A Note on the Effect of Monoand di-Bromination on the Transport Properties of Poly(2,6 dimethylphenylene oxide)”, J. Membr. Sci., Vol. 48, 333-341 (1990).

[46] Fleming, G. K., and Koros, W. J., “Dilation of Polymers by Sorption of Carbon Dioxide at Elevated Pressures. 1. Silicone Rubber and Unconditioned Polycarbonate”, Macromolecules. 19, 2285 (1986).

[47] Hwang, S., Kim, J. and Yoo, K.P., “Vapor Liquid Equilibrium Data of Binary Polymer Solutions by Vacuum Electromicrobalance”, J. Chem. Eng. Data., Vol. 43, 614 (1998).

[48] Tsutsui, K., Katsumata, T., Fukatsu, H., Yoshimizu, H.; Kinoshita, T. and Tsujita, Y., “The Isomer Effect on Complex Formation in Syndiotactic Polystyrene−Xylene system”, Polymer J., Vol. 31, 268 (1999).

[49] Minelli, M. and Doghieri, F., “Predictive Model for Gas and Vapor Solubility and Swelling in Glassy Polymers I: Application to Different Polymer/Penetrant Systems”, Fluid Phase Equilib. 381, 1 (2014).

[50] Kamiya, Y., Mizoguchi, K., Naito Y. and Hirose, T., “Gas Sorption in Poly(Vinyl Benzoate)”, J. Polym. Sci. Polym. Phys. Ed., Vol. 24, 535 (1986).

[51] Kamiya, Y., Mizoguchi, K., Naito, Y. and Hirose, T., “Gravimetric Study of High-Pressure Sorption of Gases in Polymers”, J. Polym. Sci. Polym. Phys. Ed., Vol. 24, 1525 (1986).

[52] Minelli, M. and Sarti, G.C., "Thermodynamic Model for the Permeability of Light Gases in Glassy Polymers", AIChE J., Vol. 61, 2776 (2015).

[53] Gmehling, J. and Onken, U., Vapor-Liquid Equilibrium Data Collection, DECHEMA, Frankfurt, Vol. I, Part 5b (2002).

[54] Knapp, H., Doring, R., Oellrich, L., Plocker U., and Prausnitz, J. M., "Vapor-Liquid Equilibria for Mixtures of Low Boiling Substances", DECHEMA, Frankfurt, Vol. VI (1982).

[55] Maxwell, J.C., "A Treatise on Electricity and Magnetism", third ed. Vol 1, Academic Reprints, Stanford, CA (1831)

[56] Giordano, S., "Order and Disorder in Heterogeneous Material Microstructure: Electric and Elastic Characterization of Dispersions of Pseudo-Oriented Spheroids", International J. Eng. Sci., Vol. 43, 1033 (2005).

[57] Wiener, O., "Die theorie des Mischkorpers fur das Feld der Statonären Stromüng," Abh. Math. Phys. sach Wiess, Vol. 32, 509-604 (1912).

[58] Nielsen, L.E., "The Thermal and Electrical Conductivity of Two-Phase Systems", Ind. Eng. Chem. Fundam., Vol. 13, 17–20 (1974).

[59] Mejdoubi, A. and Brosseau, C. "Finite-Element Simulation of the Depolarization Factor of Arbitrarily Shaped Inclusions", Physical Review E., Vol. 74, 031405 (2006).

[60] Petropoulos, J. H., "A Comparative Study of Approaches Applied to the Permeability of Binary Composite Polymeric Materials", J. Polym. Sci. Polym. Phys. Ed., Vol. 23, 1309-1324 (1985).

[61] Patankar, S.V., "Numerical Heat Transfer and Fluid Flow", McGraw-Hill (1980).

APPENDIX A

ALGORITHM LOOP FOR SOLVING PURE COMPONENT EOS

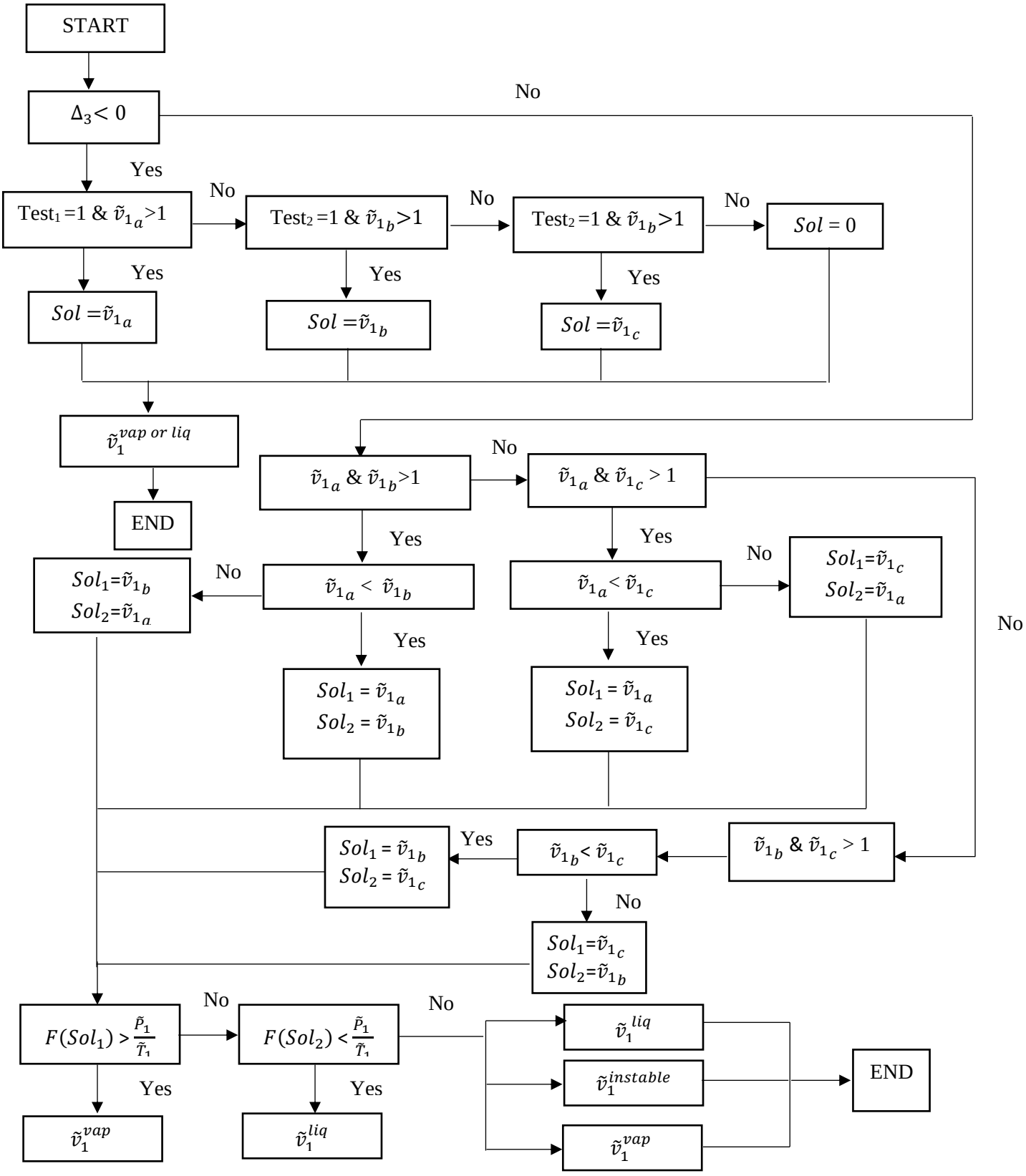

APPENDIX B

ALGORITHM LOOP FOR SEARCHING PURE COMPONENT REDUCED VOLUME OF LIQUID OR VAPOR IN EOS

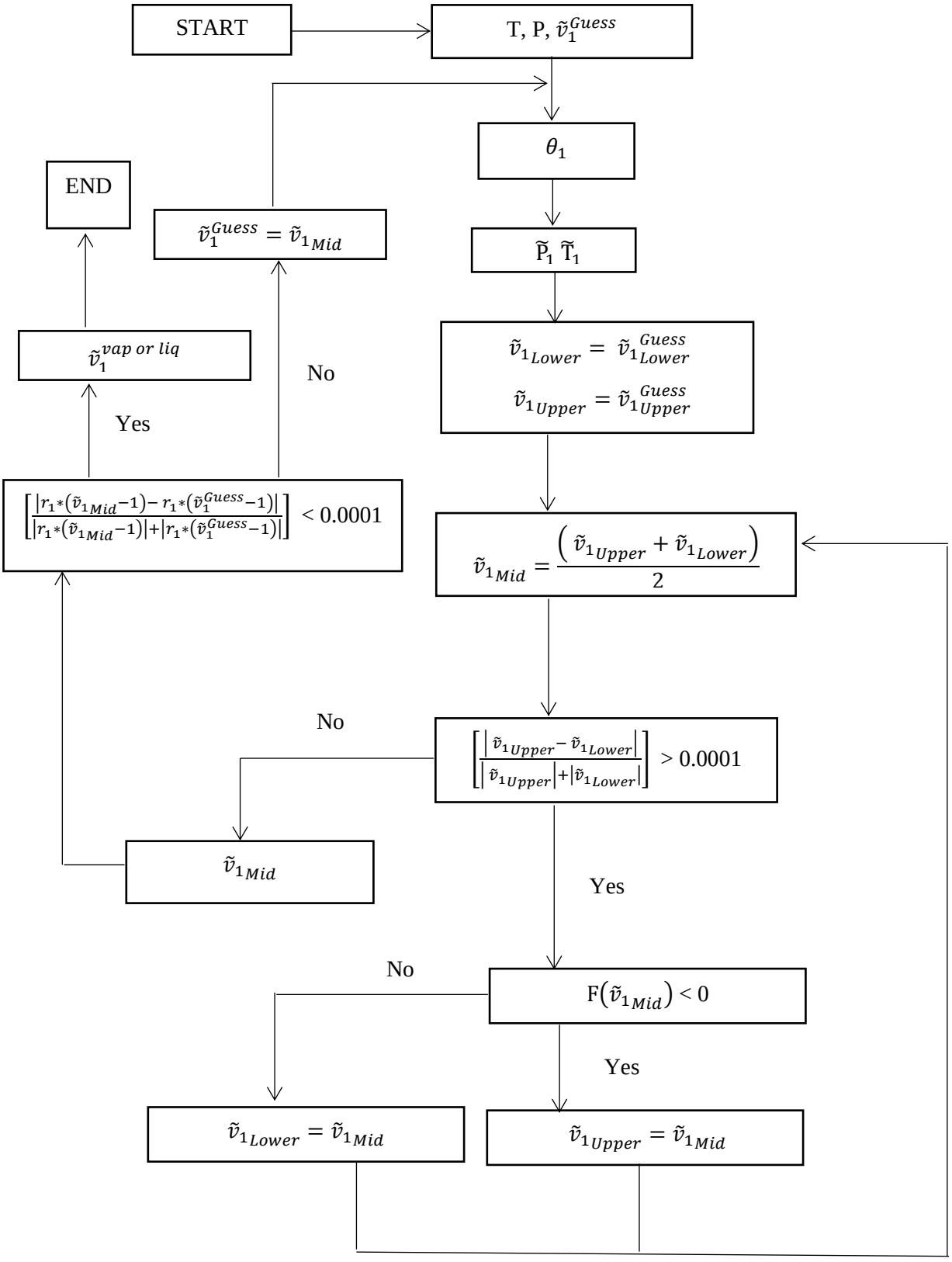

APPENDIX C

CALCULATION OF THE EQUILIBRIUM CONCENTRATION ω_1^{Eq}

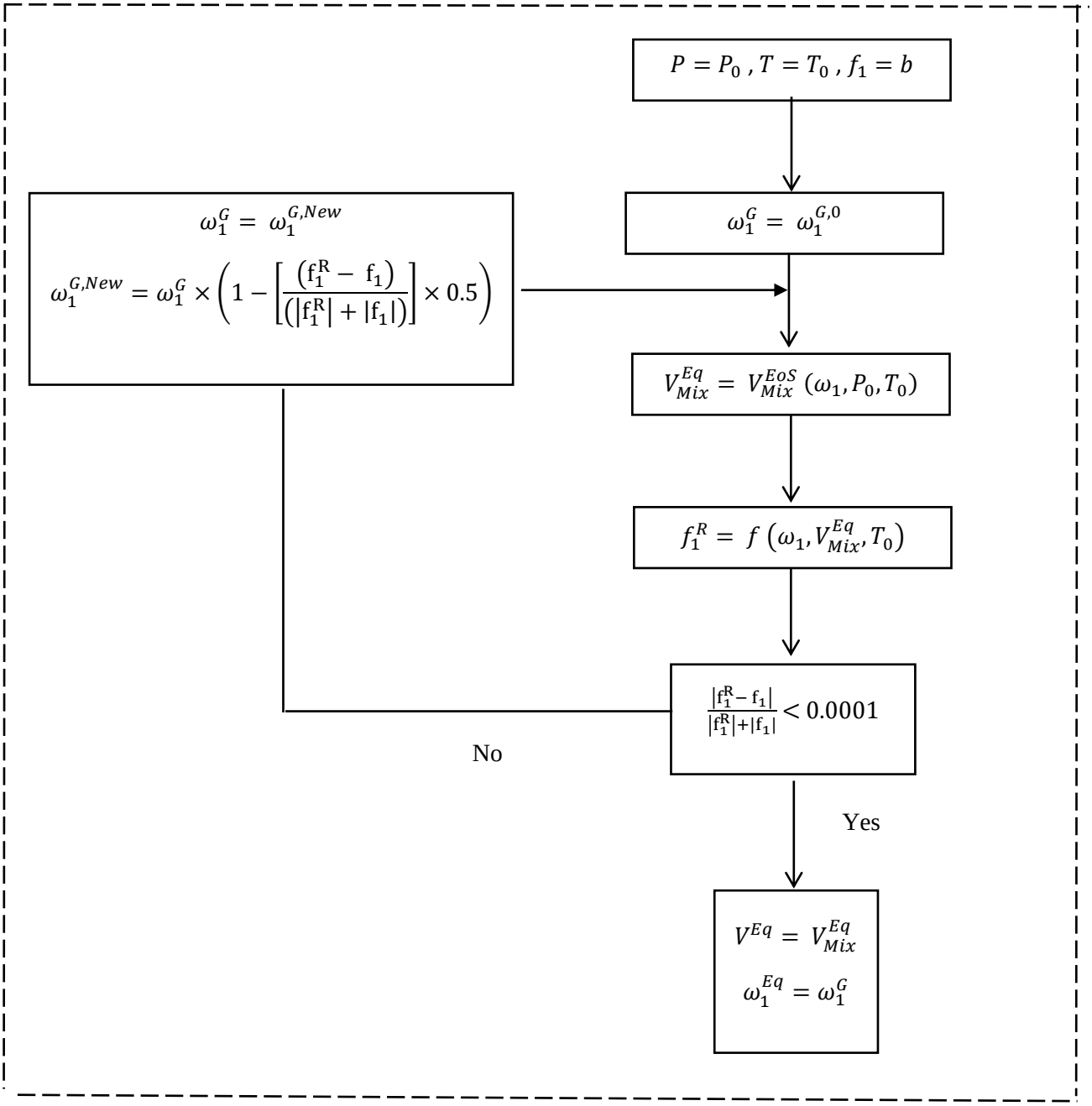

APPENDIX D

CALCULATION OF THE NON-EQUILIBRIUM CONCENTRATION ω_1^{NE}